BILIVERDIN REDUCTASE IN CARDIOVASCULAR INFLAMMATION

By Jason Sangha

A Thesis submitted to The University of Birmingham for the degree of MASTER of PHILOSOPHY

Centre for Cardiovascular Science
School of Clinical and Experimental Medicine
College of Medical and Dental Sciences
The University of Birmingham

September 2010

ABSTRACT

Abstract

Biliverdin Reductase (BVR) functions downstream of Heme Oxygenase 1 (HO-1) in the process of heme degradation and catalyses the reduction of biliverdin to bilirubin. For over thirty years, BVR was regarded as rather a trivial enzyme whose only known function was to aid heme disposal. Over the last decade however, it has become increasingly clear that BVR is pleiotropic in function and for example, functions as a dual-specificity protein kinase and also as a transcription factor. The bile pigment bilirubin is now known to possess potent anti-inflammatory and antioxidant effects, and this finding is underscored clinically by the observation that mild hyperbilirubinemia, due to Gilbert's syndrome, protects patients against cardiovascular diseases associated with atherosclerosis. However a number of studies have suggested that BVR, aside from its bilirubin generating capacity, is pro-inflammatory. In the present study, we show that BVR acts in an anti-inflammatory manner in the endothelium; by increasing eNOS activation and nitric oxide release, inducing HO-1 protein expression and by inhibiting TNFα-induced leukocyte-endothelium interaction. These highly novel findings give credence to future therapeutic strategies aiming to modulate BVR activity *in vivo* in the fight against chronic inflammatory diseases such as atherosclerosis.

ACKNOWLEDGEMENTS

Acknowledgements

I would like to thank Prof Asif Ahmed for allowing me to work in his lab for the year on a highly novel avenue of research, and also for generally putting up with me! I would also like to thank Dr Shakil Ahmad for his expert knowledge and guidance during the course of the project. Dr Stuart Egginton, Dr Takeshi Fujisawa, Dr Kequing Wang, Dr Meng Cai, Dr Melissa Cudmore and Dr Peter Hewett were also extremely helpful and always made time for intellectual discussion and technical assistance. I thank Prof Libor Vitek (Charles University, Czech Republic) for kindly agreeing to analyse samples for intracellular unconjugated bilirubin using HPLC (Figure 3.5).

CONTENTS

ABBREVIATIONS

Abbreviations

BVR – Biliverdin Reductase

CMV – Cytomegalovirus

SnPP – Tin Protoporphyrin

PI3K – PhosphatidylInositol 3-kinase

PKC – Protein Kinase C

TBST – Tris-Buffered Saline Tween-20

IKK – IκB Kinase

Ad – Adenovirus

ICAM-1 – Inter-Cellular Adhesion Molecule 1

VCAM-1 – Vascular Cell Adhesion Molecule 1

PBMC – Peripheral Blood Mononuclear Cell

HUVEC – Human Umbilical Vascular Endothelial Cell

PAEC – Porcine Aortic Endothelial Cell

HAEC – Human Aortic Endothelial Cell

VSMC – Vascular Smooth Muscle Cell

PIP_3 – Phosphatidylinositol (3, 4, 5)-trisphosphate

LDL – Low-Density Lipoprotein

ELISA – Enzyme-Linked Immunosorbent Assay

MOI – Multiplicity of Infection

DMSO – Dimethyl Sulfoxide

SDS-PAGE – Sodium Dodecyl Sulfate Polyacrylamide Gel Electrophoresis

SDS-PAG – Sodium Dodecyl Sulfate Polyacrylamide Gel

UCB – Unconjugated Bilirubin

FACS – Fluorescence Activated Cell Sorter

UGT1A1 – Uridine Diphosphoglucuronate-Glucuronosyltransferase 1

UDP – Uridine Diphosphate

Ox-LDL – Oxidised LDL

VEGF – Vascular Endothelial Growth Factor

TNFα – Tumour Necrosis Factor-α

HRP – Horseradish Peroxidase

ECL – Enzymatic Chemiluminescence

TMB – 3,3’,5,5’-Tetramethylbenzidine

MTT – 3-(4,5-Dimethylthiazol-2-yl)-2,5-diphenyltetrazolium bromide

BSA – Bovine Serum Albumin

PVDF – Polyvinylidene Fluoride

TEMED – Tetramethylethylenediamine

APS – Ammonium Persulfate

CVD – Cardiovascular Disease

HO – Heme Oxygenase

PBS – Phosphate Buffered Saline

TBS – Tris Buffered Saline

NFκB - Nuclear Factor κ-light-chain-enhancer of activated B cells

MCP-1 – Monocyte Chemotactic Protein-1

PFA – Paraformaldehyde

ERK – Extracellular-signal-Regulated Kinase

MAPK – Mitogen-Activated Protein Kinase

FCS – Fetal Calf Serum

eNOS – endothelial Nitric Oxide Synthase

iNOS – inducible Nitric Oxide Synthase

NOX – NADPH Oxidase

INTRODUCTION

Introduction

Inflammation is the complex reaction of the microcirculation to insult or injury, in which leukocytes and various serum proteins transcend the endothelium to the extravascular space (Lawrence and Gilroy, 2007). Inflammation can be defined as acute or chronic, and it is chronic inflammation that drives the pathophysiology of numerous diseases, from rheumatoid arthritis to atherosclerosis. Acute inflammation consists of the recruitment of circulating leukocytes and, following successful elimination of the stimulus (e.g. infection); the response subsides via a process broadly termed as resolution. However chronic non-resolving inflammation, in which tissue damage occurs, ensues if the initiating stimulus is not neutralised (Lawrence and Gilroy, 2007).

Biliverdin reductase (BVR) is a component of the HO-1/BVR pathway and it catalyses the reduction of biliverdin to bilirubin. Over the last decade, it has become increasingly clear that BVR is pleiotropic in function, acting for example as a dual specificity kinase and a transcription factor. The bile pigments, biliverdin and bilirubin, have potent anti-inflammatory and antioxidant effects, and their therapeutic potential has been demonstrated in a number of *in vivo* animal models. Furthermore Gilbert's syndrome patients, who experience mild hyperbilirubinemia, are protected from cardiovascular diseases such as atherosclerosis (Schwertner *et al*, 1994). On the other hand, the non-canonical activities of BVR are largely pro-inflammatory. For example via its dual-specificity kinase activity, BVR potentiates TNFα-induced NFκB activation (Kapitulnik and Maines, 2009).

The function of the non-canonical activities of BVR and the interplay of these with its established reductase activity in disease processes has not yet been evaluated, not least because the pleiotropic functions of the enzyme were realised only very recently. In this regard, no published study has yet evaluated the role of this enzyme in atherosclerosis – the leading cause of mortality in most developed nations (Beckman *et al*, 2002).

History of BVR

The reduction of biliverdin to bilirubin in animal tissues was first described at the start of the 20th century, at a time when BVR was yet to be identified (Lemberg and Wyndham, 1936). Little was known about the oxidation and reduction of bile pigments and even the premise that bilirubin arose from the reduction of the primary product of haem breakdown, biliverdin, was dubious. Lemberg and Wyndham showed that most guinea pig tissues could reduce biliverdin to bilirubin, in a manner which would suggest that biliverdin was in fact the primary product of heme breakdown. Although the corresponding enzyme system was yet to be identified (i.e. the HO-1-BVR axis), this study provided a basis for Laster and Singleton to identify the enzymatic reducing activity responsible for biliverdin reduction nearly three decades later (Laster and Singleton, 1965). Laster and Singleton purified the enzyme some 15-fold from guinea pig liver homogenate and showed that NADH or NADP was in fact required for the biliverdin reduction.

Further characterisation of BVR was hampered for over a decade until the enzyme was eventually purified sufficiently for accurate analyses. Using a partially purified BVR preparation from pig spleen, Noguchi *et al* demonstrated for the first time that the enzyme had markedly different pH optima for the NADH- and NADPH-dependent reactions – the

reductase activity is NADH-dependent at acidic pH however, NADPH-dependent at basic pH (Noguchi *et al*, 1979). A couple of years later, BVR was purified to homogeneity from rat liver cytosol and further characterised – including relevant K_m values and pH optima (Kutty and Maines, 1981). During this time, BVR was regarded as rather a trivial enzyme whose only known physiological function was purported to be the *in utero* facilitation of foetal-maternal biliverdin placental transfer via reduction of water-soluble biliverdin to the lipophilic, cell-membrane permeable bilirubin (McDonagh *et al*, 1981). The human form of BVR was first purified from liver tissue in 1993 (Maines and Trakshel, 1993) and this allowed further characterisation.

Amongst the first indications that BVR may be pleiotropic was the observation that BVR was an evolutionarily conserved protein found in many non-placental organisms from unicellular red algae to puffer fish (Beale and Cornejo, 1984). Furthermore it was later shown that bilirubin could in fact function as a physiologically relevant antioxidant (Stocker *et al*, 1987). The recently realised pleiotropic nature of BVR is reflected by a growth in the literature (Figure 1.1).

The first published study (Breimer *et al*, 1995) to link serum bilirubin levels to cardiovascular disease showed that low serum bilirubin levels were predictive of increased ischemic heart disease (IHD). This relationship was later conclusively clarified in a study that demonstrated low prevalence of IHD in Gilbert's syndrome patients due to increased serum antioxidant capacity (Vitek *et al*, 2002).

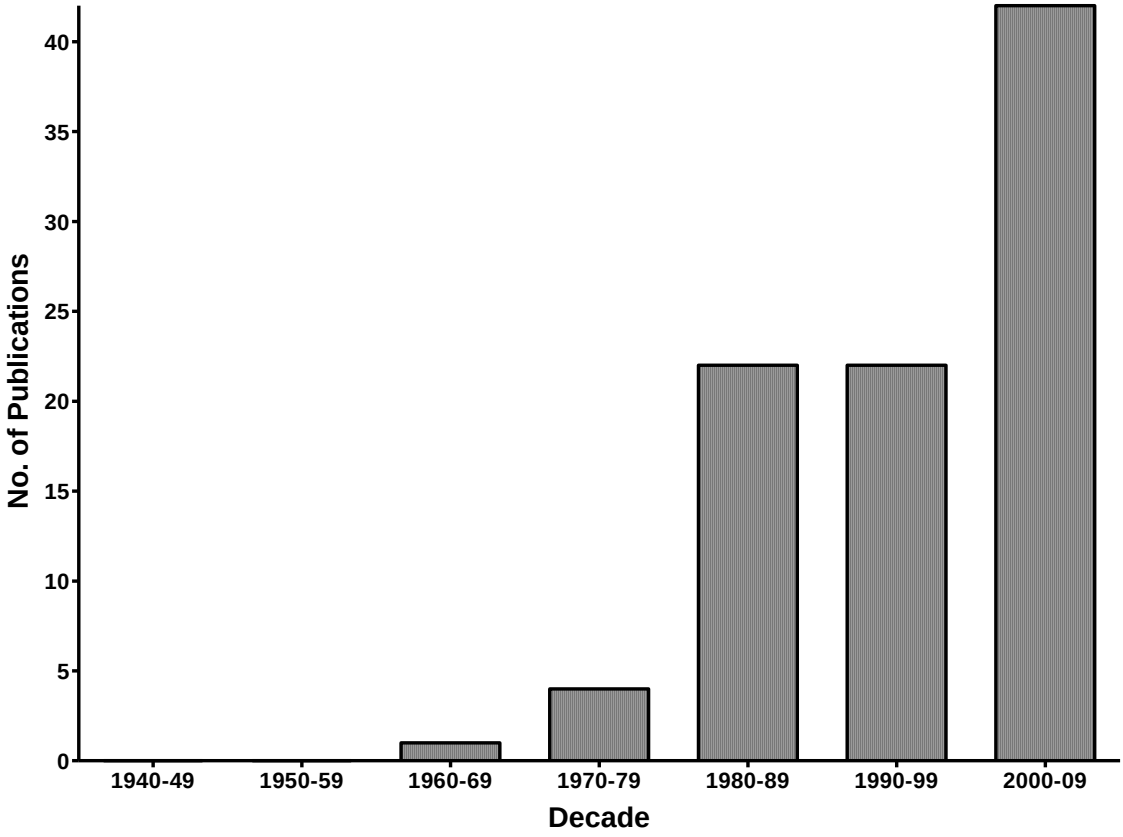

Figure 1.1 ***Interest in BVR doubled from the '90s to the '00s***. Number of publications with a PubMed ID that contain the phrase 'biliverdin reductase' in the title by decade. There have been 4 such publications in the first 6 months of 2010, and hence a projection of nearly 80 publications by the end of the decade is reasonable.

Structure of BVR

Human adult BVR is a 296-residue polypeptide (Yamaguchi *et al*, 1994). There are actually two different forms of human BVR with differing molecular weights; BVR-IXα (isozymes I and II) and BVR-IXβ (isozymes III and IV). The reason for the two different forms of BVR is due to differences in the isoforms of bile pigments present in foetal and adult life. Adult human bile is composed of 95-97% bilirubin-IXα and 3-5% bilirubin-IXβ (Yamaguchi *et al*, 1994). At 20 weeks of gestation however, foetal bile is composed of approximately 6% bilirubin-IXα and

87% bilirubin-IXβ. BVR-IXβ does not reduce biliverdin-IXα at all whereas BVR-IXα can reduce biliverdin-IXβ to a small extent. BVR-IXα has a molecular weight of 34kDa (296 amino acids) whereas BVR-IXβ (206 amino acids) has a molecular weight of 21kDa. Human BVR-IXα is encoded by single copy gene with five exons and four introns (Florczyk *et al*, 2008).

Biliverdin Isomer/Cofactor	**BVR Isozyme K_m**			
	BVR-IXβ		**BVR-IXα**	
	I	**II**	**III**	**IV**
Biliverdin-IXα (μM)	-	-	1.0	0.8
Biliverdin-IXβ (μM)	0.3	0.3	50.0	43.0
NADPH (μM)	35.9	13.1	10.9	34.1
NADH (mM)	5.6	8.2	7.9	23.4

Table 1.1 ***K_m values of BVR isozymes for biliverdin substrates and cofactors***.

BVR is a monomeric protein and consists of two structural domains (Whitby *et al*, 2002), the N-terminal 'catalytic domain' and the C-terminal 'regulatory domain', which form a cleft in the middle of the protein that constitutes the active site (Figure 1.2). The N-terminal domain consists of an α/β Rossmann-fold (dinucleotide-binding motif) in which six α-helices (turquoise) surround a central parallel β-sheet (pink). The C-terminal domain consists of a relatively flat parallel β-sheet (orange) which presents polar/charged residues to solvent at one side. On the other side, the β-sheet is flanked by six α-helices (green) which form the rest of the C-terminal domain. The majority of these helices interact with the N-terminal domain and some also contain residues which form the active site cleft.

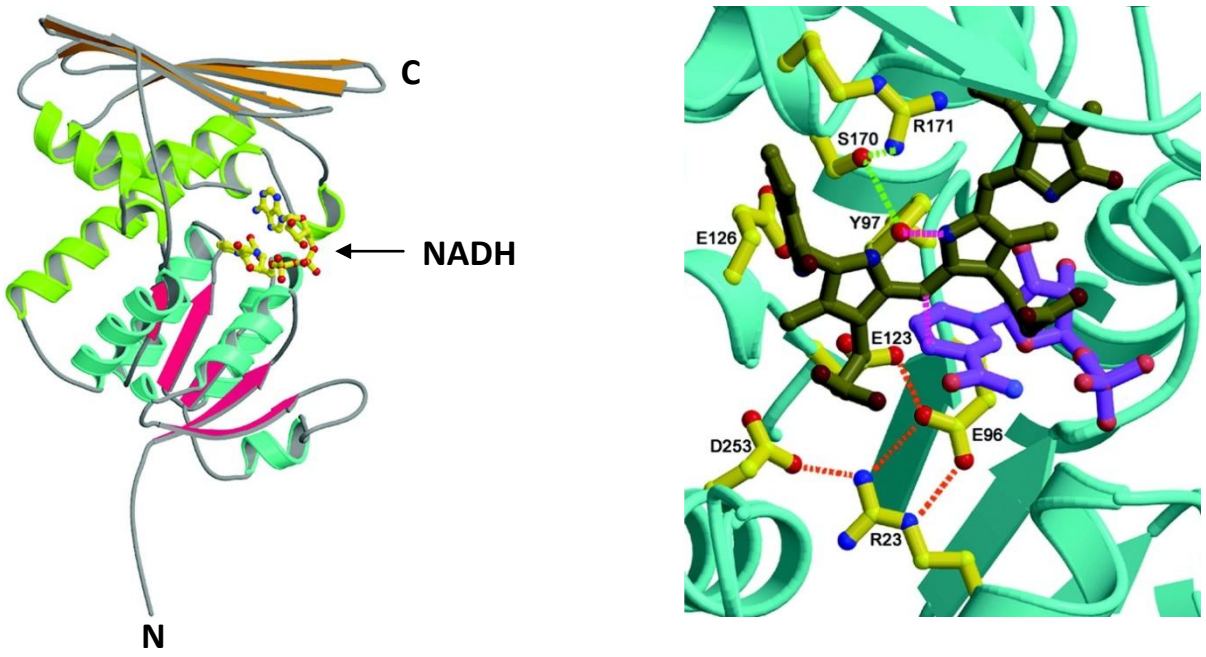

Figure 1.2 (***Left) Ribbon diagram of rat BVR with NADH cofactor at the active site***. N-terminal domain helices and strands are coloured in turquoise and pink respectively whereas C-terminal helices and strands are coloured bright green and orange respectively. The NADH cofactor is shown in ball-and-stick form (coloured by atom type – Carbon; yellow, Oxygen; red, Nitrogen; blue) and is sitting in the active site, interacting with a number of important highly conserved residues. (***Right***) ***Ribbon diagram showing BVR active site (turquoise) with NADH cofactor (bright purple bonds) and biliverdin (dark green bonds) shown in ball-and-stick form (coloured by atom type)***. The adenine part of the cofactor is omitted for clarity. Highly conserved residues in sidechains of the BVR protein active site residues are shown with yellow bonds (coloured by atom) in ball-and-stick form. Adapted from Whitby *et al*, 2002.

The organisational structure of BVR is generally similar to that of the PKC isozymes (Newton, 2001). The greatest (tertiary) structural similarity however is with the periplasmic, homotetrameric enzyme Glucose-Fructose Oxidoreductase (GFOR) from *Zymomonas mobilis* (Kingston *et al*, 1996). The primary structure of BVR (Figure 1.3) is similar to the primary structures of the kinase domains of the Insulin Receptor (IR) and Insulin Receptor Substrate (IRS) proteins (Lerner-Marmarosh *et al*, 2005).

The non-canonical activities of BVR – i.e. its ability to function as a dual specificity kinase and also as a leucine zipper (bZip) transcription factor – are primarily conferred by the C-terminal domain, which contains various consensus signalling motifs consistent with the pleiotropic functions of the protein. The N-terminal domain however is primarily involved in catalysis. The C-terminal β-sheet is the putative site for protein-protein interactions. This contains two Src Homology 2 (SH2)-binding motifs. Indeed, tyrosine residues (Y^{198}MKM and Y^{228}LSF) contained in these two SH2-binding motifs are phosphorylation targets of Insulin Receptor Kinase (IRK). The β-sheet also contains a C-box and a D-box, F^{162}GFP and K^{275}KRILHCLGL respectively, both of which are consensus MAPK docking motifs. The C- and D-boxes are sites for ERK interaction and therefore crucial for BVR-mediated ERK activation (Lerner-Marmarosh *et al*, 2008). The C-box has high affinity for kinases in the MAPK pathway whilst the D-box has low affinity (Myers *et al*, 1996). A leucine-rich motif, L176VSLFGELSL, is a characteristic of nuclear export signal (NES) and is also found in the C-terminal β-sheet. BVR also has a nuclear localisation sequence (NLS). Both the NES and NLS are involved in the BVR-facilitated transport of ERK and heme to the nucleus (Maines *et al*, 2001 and Ahmad *et al*, 2002).

The N-terminal G^{15}XGXXG motif is characteristic of protein kinases and ATP-binding domains. In BVR, this motif binds NADH/NADP (for reductase activity) and ATP (for kinase activity). Adjacent to this motif is a cluster of four valine residues (V4) which are essentially (due to the sidechain) hydrophobic and such a motif is generally found in proteins that interact with cell membranes. The Ser/Thr kinase consensus motif, G^{148}(T/S)XX(Y/F)XAPQ, is found within the bZip motif (Hunter and Cooper, 1985). The bZip motif interacts with DNA, binding to 7/9-BP AP-1 sites, and is found in stress-activated transcription factors such as c-Jun (Ahmad

et al, 2002). Furthermore, BVR contains a structure similar to the conserved Pleckstrin Homology (PH) domain (Lerner-Marmarosh *et al*, 2005). This would suggest a possible scaffolding role for BVR. The cysteine-rich sequence (CC-box) located at the C-terminus of BVR is involved in Zn^{2+} binding (Kapitulnik and Maines, 2009).

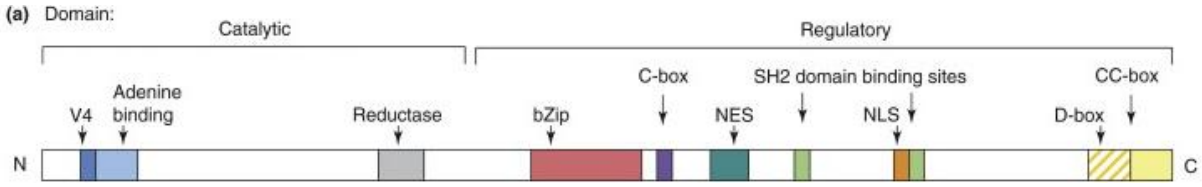

Figure 1.3 ***Primary structure of BVR showing various conserved regulatory and catalytic motifs implicated in the canonical and non-canonical activities of BVR***. Adapted from Kapitulnik and Maines, 2009.

Atherosclerosis

Atherosclerosis is regarded as a chronic inflammatory condition affecting mainly large and medium-sized arterial blood vessels. Its downstream complication, cardiovascular disease (CVD), represents the leading cause of mortality in most industrialised nations (Beckman *et al*, 2002). As recently as three decades ago, atherosclerosis was widely regarded as a mere arterial proliferative disorder, in which passive lipid deposition on the artery wall results in atheroma formation (Ross and Glomset, 1976). Recent studies have elucidated the molecular processes underlying the pathophysiology of atherosclerosis and in so doing, the importance of inflammation in the conception, progression and eventually rupture of atherosclerotic plaques has been demonstrated. More recently, inflammatory processes

have been identified as a link between the numerous risk factors of atherosclerosis and the numerous cardiovascular complications associated with the disease (Corrado *et al*, 2010).

Atherosclerosis is characterised by the formation and progression of atherosclerotic plaques, which consist of lipid regions, calcified regions, necrotic cores and foam cells, all in an inflammatory milieu. Atherosclerosis is a progressive condition, and early forms of atherosclerotic plaques, termed 'fatty streaks', are evident in young children (Mallika *et al*, 2007). Fatty streaks progress to form *bona fide* atherosclerotic plaques, which then generally clinically manifest themselves in middle to late adulthood. The appearance of fatty streaks – yellow/white sub-endothelial discoloration – reflects the accumulation of foam cells, macrophages which have endocytosed oxidised LDL.

Fatty streaks progress to atherosclerotic plaques as a result of three fundamental driving processes; **1**, proliferation and consequent accumulation of intimal smooth muscle cells (and also accumulation of macrophages and T cells), **2**, secretion, by the smooth muscle cell population, of connective tissue matrix and **3**, accumulation of intracellular lipids (and also extracellularly in the connective tissue). The acute perils of atherosclerotic plaques are associated with the degree of arterial stenosis, and also thrombogenic potential (Libby *et al*, 2010). Inflammation is an essential process that governs the progression of atherosclerosis, from initial endothelial dysfunction to plaque rupture and thrombosis (Corrado *et al*, 2010).

On a molecular level, the process of atherosclerosis begins with activation of the endothelium, in response to cardiovascular risk factors such as hypertension or obesity. This is an early, initiating event that is often termed 'endothelial dysfunction'. The endothelial cells then begin to express adhesion molecules (e.g. ICAM-1, VCAM-1 or E-selectin) on their apical surfaces which function to recruit specific leukocytes (Figure 1.4). This recruitment is

facilitated by the secretion of chemokines into the arterial lumen. Circulating monocytes are the most abundant of the infiltrating leukocytes that populate the forming plaque. Indeed, there are two distinct populations of circulating monocytes; $Gr1^{+}/Ly6C^{high}$ monocytes and $Gr1^{-}/Ly6C^{low}$ (Woollard and Geissmann, 2010). The monocytes are recruited into the intima and sub-intima and, via their scavenger receptors, they internalise oxidised LDL (ox-LDL). The monocytes are then activated (to macrophages) and they begin to accumulate. Macrophages progressively become foam cells, characterised by a microscopic 'frothy' appearance due to intracellular accumulation of lipids in cytoplasmic vesicles. This results in the formation of 'fatty streaks', which progressively develop to form atherosclerotic plaques (Libby *et al*, 2010).

Ox-LDL has a key role in both the initiation and progression of atherosclerosis. The ox-LDL hypothesis of atherosclerosis, in which LDL penetrates the arterial endothelial wall, is oxidised, and promotes the formation of lipid-rich foam cells, was originally proposed by Steinberg over twenty years ago (Steinberg, 1989). Macrophages and vascular smooth muscle cells (VSMCs) are primarily responsible for producing the reactive oxygen species (ROS) that oxidise the LDL (Antoniades *et al*, 2007).

It is now known that macrophages express several scavenger receptors, responsible for ox-LDL uptake. A seminal study by Sawamura *et al* also identified the first endothelial ox-LDL receptor, LOX-1 (Sawamura *et al*, 1997). Ox-LDL is cytotoxic to the vascular endothelium and therefore contributes to endothelial dysfunction (Balla *et al*, 1991).

The atherosclerotic plaque further develops via accumulation of inflammatory cells and extracellular lipid. Arterial stenosis arises because cells in the developing plaque secrete cytokines (e.g. TNFα), chemokines (e.g. MCP-1), growth factors, and smooth muscle cells

secrete extracellular matrix. This causes smooth muscle cell proliferation and further recruitment of inflammatory cells. The central core of the atherosclerotic plaque becomes necrotic and consequently, pro-angiogenic mediators are released which leads to neovascularisation. The secretion of enzymes that degrade the extracellular matrix, such as matrix metalloproteinases (MMPs), may eventually cause plaque rupture. The plaque contains pro-thrombotic material and the ensuing thrombus may occlude the lumen of the artery, resulting in for example myocardial infarction (Libby *et al*, 2010).

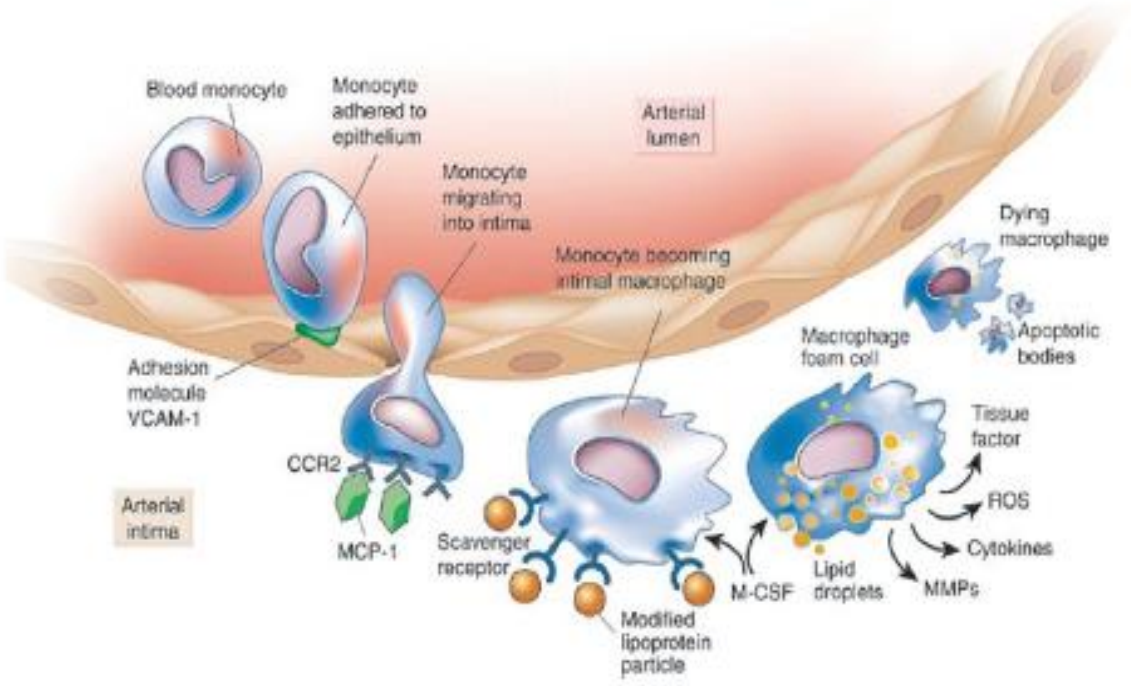

Figure 1.4 ***Role of monocyte-endothelial interactions in atherosclerosis***. Endothelial dysfunction, due to smoking, diabetes, etc, results in the activation of endothelial cells. Hence, the endothelial cells begin to express adhesion molecules which function to recruit inflammatory cells. Monocytes migrate into the intima and this process is driven, at least in part, by the chemokine monocyte chemotactic protein-1 (MCP-1). Monocytes differentiate into macrophages, which express scavenger receptors. This differentiation may be driven by the cytokine macrophage-colony stimulating factor (M-CSF). The macrophages become engorged with lipids thus becoming foam cells. The foam cells contribute to the inflammatory process but eventually undergo apoptosis. Taken from Libby *et al*, 2010.

HO-1/BVR Axis in Atherosclerosis

Heme Oxygenase (HO) is the rate-limiting enzyme in the degradation of heme, producing the bile pigment biliverdin, carbon monoxide (CO) and iron (Fe^{2+}) in an NADPH-dependent manner (Figure 1.5). There are three known isoforms of HO, HO-1, HO-2 and the catalytically-inactive HO-3. HO-1 is inducible and responds to stress whereas HO-2 is constitutively active. Biliverdin is reduced to bilirubin by the functionally pleiotropic BVR. HO-1 is a key vasoprotective mediator and this is largely thought to be conferred by the three end-products of the HO-1/BVR axis; CO and the two bile pigments, biliverdin and bilirubin. These molecules exhibit anti-inflammatory, antioxidant, anti-mutagenic and anti-apoptotic effects (Ollinger *et al*, 2007). The significance of these properties, in terms of CVD, is reflected in individuals with Gilbert's syndrome.

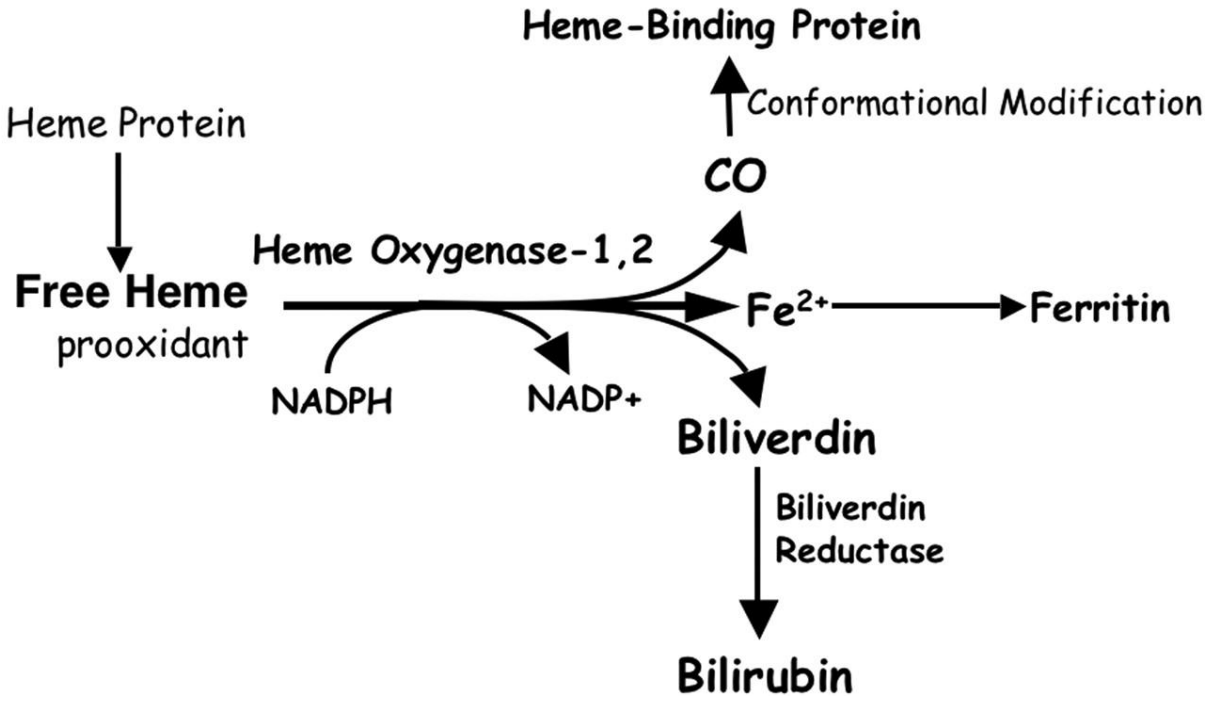

Figure 1.5 ***The HO-1/BVR axis***. HO degrades free heme in an NADPH-dependent manner, yielding CO, Fe^{2+} and biliverdin. Fe^{2+}, which is cytotoxic, is stored by ferritin. Biliverdin reductase reduces biliverdin to bilirubin in an NADPH-dependent manner. Taken from Morita, 2005.

Induction of the HO-1/BVR axis with pharmacological mediators and gene delivery approaches is therefore likely to be beneficial in atherosclerosis. Numerous studies have already evaluated the therapeutic potential of administration of the three end-products of the HO-1/BVR axis, in animal models of inflammatory diseases.

HO-1 degrades heme and this is beneficial, in terms of atherosclerosis, *per se*. This is because heme is both pro-oxidant and cytotoxic, and can catalyse protein peroxidation. Jeney *et al* showed that heme can catalyse LDL oxidation (Jeney *et al*, 2002). Endothelial cells upregulate HO-1 in response to ox-LDL, suggesting that the HO-1/BVR axis is a defence-mechanism against ox-LDL. Heme also induces the expression of ICAM-1, VCAM-1 and E-selectin adhesion molecules in endothelial cells (Wagener *et al*, 1997).

A study by Nakayama *et al* showed that HO-1 mRNA and protein is increased in endothelial and foam cells, from atherosclerotic plaques, in hypercholesterolemic rabbits (Nakayama *et al*, 2001). Bilirubin was also found to be accumulated in foam cells. Several *in vivo* studies have shown that inhibition of endogenous HO-1 activity, with metalloporphyrins (i.e. tin protoporphyrin), exacerbates atherosclerotic lesion formation. For example, Ishikawa *et al* showed that the number of atherosclerotic lesions in HO-1-inhibited hyperlipidemic rabbits was elevated compared to controls (Ishikawa *et al*, 2001). Togane *et al* showed that endothelial denudation resulted in upregulation of HO-1 in a rat model of balloon injury. Importantly, HO-1 inhibition in this system promoted neointimal formation whereas a HO-1 inducer (hemin) had the opposite effect (Togane *et al*, 2000).

In summary, hundreds of studies have examined the effect and/or therapeutic potential of HO-1 activity modulation, or CO/biliverdin/bilirubin administration, *in vivo*, in regard to atherosclerosis. However, no study has focussed on elucidating the role of BVR specifically

in atherosclerosis or other inflammatory conditions and, given the recent realisation of the pleiotropic functions of the reductase, this represents an evidence chasm.

Gilbert's Syndrome

Gilbert's syndrome patients are generally asymptomatic and have moderately elevated levels of bilirubin, and this confers protection against CVD (Schwertner *et al*, 1994). The syndrome was first clinically described over a century ago by the French gastroenterologist Gilbert and his co-worker Lereboullet in 1901. It is characterised by mild unconjugated hyperbilirubinemia, not overtly secondary to hemolysis and without hepatic disease (i.e. inflammation, fibrosis, etc). Diagnostic criteria for Gilbert's syndrome include a consistent mild elevation of serum bilirubin levels (i.e. 17-102µM or 1-6mg/dL). This elevation in bilirubin levels is attributable to an increase in unconjugated bilirubin levels only – conjugated bilirubin levels remain within normal limits (i.e. <20% of the total bilirubin). On this basis, 3-10% of the general population are thought to have Gilbert's syndrome with men more frequently affected than women (12.4% vs. 4.8% respectively). The mean bilirubin concentration is also significantly higher in males than in females (Olsson *et al*, 1988).

The pathogenesis of Gilbert's syndrome is explained by the approximately 70% reduced hepatic glucuronidating activity in such patients (Bosma *et al*, 1995). Hepatic bilirubin conjugation with a polar group – i.e. UDP-glucuronic acid – is essential for the biliary excretion of bilirubin because this renders bilirubin water-soluble, which allows it to form bile and exit into the duodenum. UDP-glucuronic acid is a ubiquitous intracellular molecule is derived from glucose metabolism. Bilirubin conjugation is mediated by the bilirubin

uridine diphosphoglucuronate-glucuronosyltransferase 1 (UGT1A1) which, in common with other glucuronosyltransferases, is a membrane-bound enzyme found mainly in the smooth endoplasmic reticulum. Bosma *et al* first discovered that the reduced expression of UGT1A1 in Gilbert's syndrome patients is accounted for by abnormalities in the promoter region of the corresponding gene whereas the coding region of the gene is normal (Figure 1.6). Gilbert's syndrome patients were found to be homozygous for two extra bases in the 5' promoter 'TATA' box – $[A(TA)_7TAA]$ in Gilbert's syndrome patients vs. $[A(TA)_6TAA]$ in normal subjects – and this abnormal allele had a frequency of 40% amongst normal subjects suggesting incomplete penetrance and other precipitating genetic/environmental factors (Bosma *et al*, 1995). The two extra bases substantially reduce the transcriptional activity of the promoter. The allele polymorphism with the extra 'TA' repeat is also referred to as UGT1A1*28.

This longer 'TATA' box – i.e. $[A(TA)_7TAA]$ – is almost exclusively associated with Gilbert's syndrome in Caucasians. Other variants – $[A(TA)_5TAA]$ and $[A(TA)_8TAA]$ – are found predominantly in the black population and are also associated with Gilbert's syndrome (Lolascon *et al*, 1999).

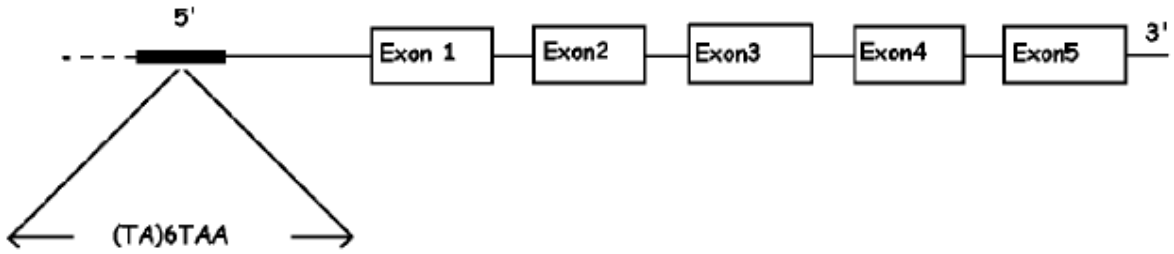

Figure 1.6 ***Organisation of the UGT1A1 gene***. The first exon is variable depending on the isoform of the enzyme whereas exons 2-5 remain the same. Solid lines between exons indicate introns. Indeed over 100 UGT1A1 variants have been detected (e.g. due to alternative splicing) thus leading to a range of serum bilirubin concentrations from low serum bilirubin to life-threatening jaundice. Adapted from Radu and Atsmon, 2001.

The inverse relationship between serum bilirubin levels and risk of coronary artery disease (CAD) was first suggested in 1994 (Schwertner *et al*, 1994), with the strength of correlation being similar to that of low HDL cholesterol levels or high systolic blood pressure. Several years later, a prospective study by Vitek *et al* found that Gilbert's syndrome patients had an approximately six-fold lower risk of developing ischemic heart disease (IHD) compared to the general population – prevalence of IHD was 2% in Gilbert's syndrome patients vs. 12.1% in the general population. This study incorporated a small number of females and also older (i.e. >40yrs) subjects (Vitek *et al*, 2002). Importantly, the total serum bilirubin levels were found to correlate with total serum antioxidant status, suggesting a likely mechanism of action of bilirubin.

More recently, a retrospective study by Lin *et al* examined the relationship between the UGT1A1*28 allele and three physician-verified cardiovascular endpoints, namely coronary heart disease (CHD) (i.e. angina pectoris or coronary insufficiency), CVD (i.e. CHD or death thereof, stroke, congestive heart failure, transient ischemic attack or intermittent claudication) or MI. Subjects homozygous for the UGT1A1*28 allele had only a 36% and 30% risk of CVD and CHD respectively relative to those heterozygous for the UGT1A1*28 allele, or to those subjects not in possession of this allele. However, the UGT1A1*28 allele was not found to be significantly associated with lower risk of MI. Furthermore, low serum bilirubin levels were significantly associated with higher risk of CHD, CVD and MI (Lin *et al*, 2006).

In summary, Gilbert's syndrome affects a large number of the global population (some 5%) and this confers protection against CVD. Gilbert's syndrome arises due to homozygous abnormalities in the promoter region of UGT1A1, the enzyme responsible for conjugation (and hence clearance) of bilirubin (Figure 1.7). Circulating unconjugated bilirubin levels

therefore rise and the protection against CVD may be conferred by increased serum antioxidant capacity (Vitek *et al*, 2002). Recent meta-analyses have confirmed this inverse relationship between serum bilirubin and CVD (Schwertner and Vitek, 2008).

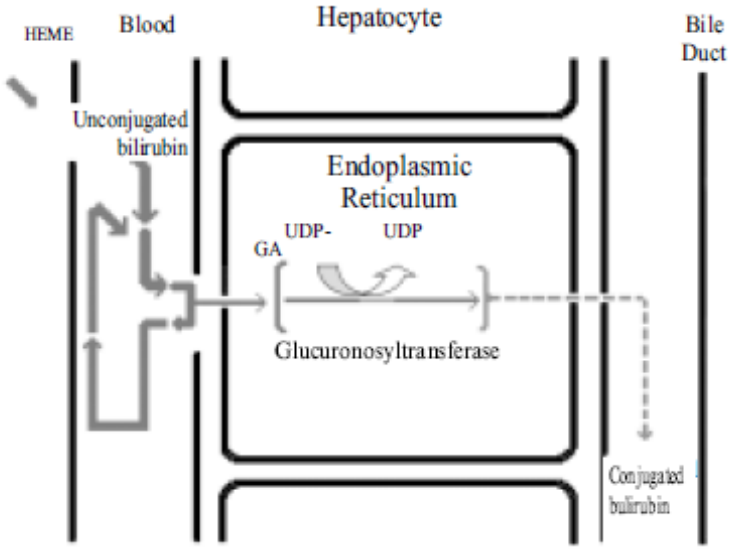

Figure 1.7 ***Bilirubin conjugation in a liver cell and excretion into the bile duct***. Adapted from Radu and Atsmon, 2001.

Bile Pigments

The bile pigments, biliverdin and bilirubin, are derived primarily from the degradation of heme via the heme-bilirubin catabolic pathway. Although both pigments share a common porphyrin structure, the pigments have markedly different three-dimensional structures (Figure 1.8).

Historically, both biliverdin and bilirubin were regarded as toxic metabolites with no biological function. Recently however, much attention has focussed on the role of these bile pigments, particularly bilirubin, in CVD. It has become clear that whilst heme is a pro-

oxidative and pro-atherosclerotic molecule, its degradation results in the production of biliverdin and bilirubin both of which have anti-atherosclerotic properties.

It has also been recently found that bile pigments confer regulation of numerous cell signalling systems resulting in antioxidant (Stocker *et al*, 1987), anti-inflammatory (Qin, 2002), anti-apoptotic (Dudnik *et al*, 2001), anti-complement (Nakagami *et al*, 1993), anti-mutagenic (Tang and Edenharder, 1997), anti-viral (Mori *et al*, 1991) and anti-proliferative (Tell and Gustincich, 2009) effects.

Both biliverdin and bilirubin possess anti-nitrosative characteristics and have antioxidant activity towards peroxynitrite (Kaur *et al*, 2003); an oxidant derived from the reaction between free radical superoxide and free radical nitric oxide.

Once bilirubin has been formed, it binds serum albumin in the systemic circulation and is then delivered to the liver where it is both actively and passively absorbed into hepatocytes across the sinusoidal membrane (after albumin has dissociated). Once inside the hepatocyte, bilirubin binds to ligandin and Z protein in the cytosol and is carried to the endoplasmic reticulum where it is conjugated by UGT1A1 (Kamisako *et al*, 2000). The catalytic site of UGT1A1 is on the lumen side of the endoplasmic reticulum and hence both UDP-glucuronic acid and bilirubin must be transported into the lumen. This is thought to occur via a carrier-mediated and protein-mediated mechanism respectively. Conjugation renders bilirubin hydrophilic and allows it to be transported across the canalicular membrane by multidrug resistance protein 2 (MRP2). The bile duct directs the bilirubin conjugates into the duodenum and as these enter the gastrointestinal tract, bacterial enzymes hydrolyse the bilirubin esters to form unconjugated pigment (Kamisako *et al*, 2000). Approximately 300mg of bile pigment is excreted from the human body everyday (Stocker, 2004).

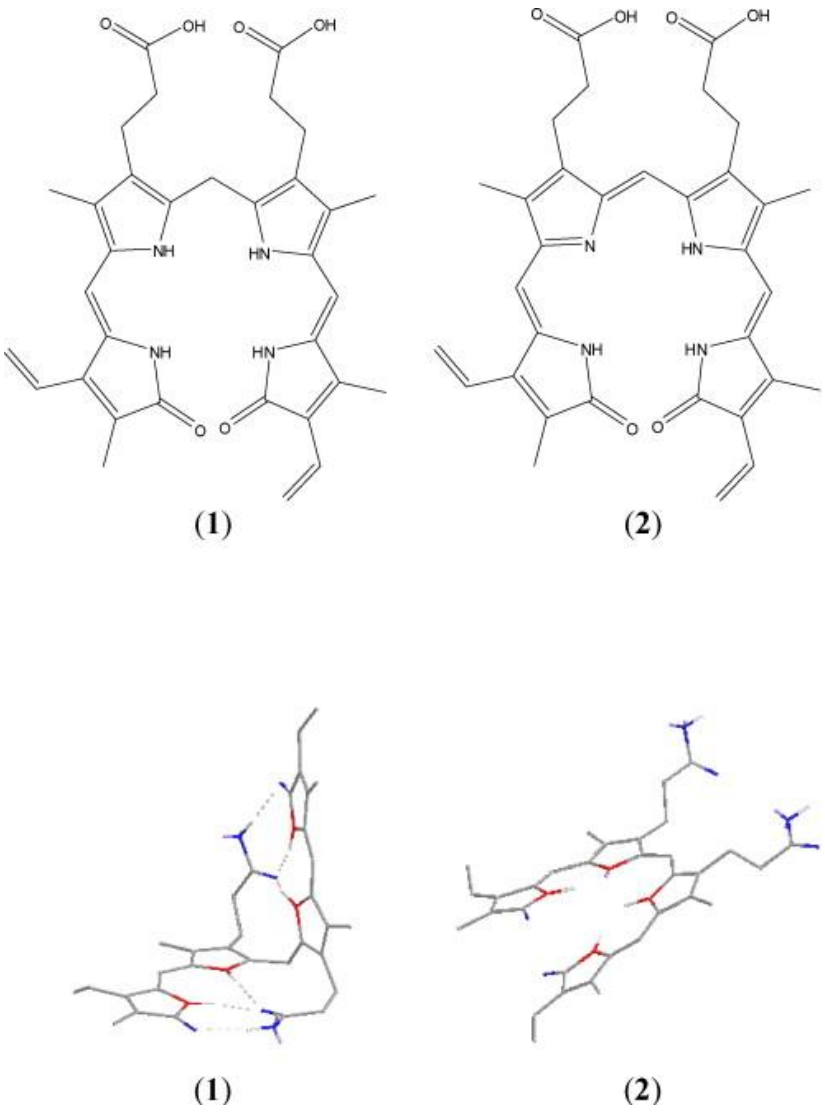

Figure 1.8 ***Two-dimensional (above) and three-dimensional (below) structures of biliverdin (2) and bilirubin (1)***. Nitrogen atoms are coloured blue whilst oxygen atoms are coloured red. Adapted from Bulmer *et al*, 2008.

Biliverdin in Inflammation

In recent years, both biliverdin and CO have been the focus of numerous studies seeking to elucidate the mechanism of the protective effects of HO-1 in various disease models. Several studies have also shown that biliverdin can in fact modulate various intracellular

signalling pathways. Investigators have also demonstrated the therapeutic benefit of biliverdin administration in animal models of inflammatory diseases.

Biliverdin has been shown to inhibit the following cell signalling molecules/pathways: (PKCs), NFκB, the JNK-SAPK-AP-1 signalling pathway, serum-induced smooth muscle cell proliferation via MAPK, and retinoblastoma (Kapitulnik and Maines, 2009). Inhibition of these pathways confers anti-inflammatory and anti-proliferative effects. Moreover, biliverdin is a feedback inhibitor of BVR (Kutty and Maines, 1981).

Plasma concentrations of biliverdin can reach as high as 40μM in patients with obstructive jaundice (Tickner and Gutteridge, 1978) however, during normal heme metabolism; biliverdin is present only in trace amounts. Biliverdin is rapidly reduced by BVR in most mammalian tissues and hence some of the effects of biliverdin administration arise due to increased bilirubin formation (Deguchi *et al*, 2008). This is an important consideration when interpreting studies in which biliverdin is administered to animal models, and some effect is observed over a given period of time. As serum biliverdin enters cells, it is rapidly converted to bilirubin by BVR and hence, some (if not all) of the effects of biliverdin administration are likely due to increased *intracellular* bilirubin, as opposed to elevated *serum* biliverdin or bilirubin (Figure 1.9).

Numerous studies have examined the therapeutic potential of biliverdin (or bilirubin) administration in animal models of transplantation. Biliverdin has been specifically demonstrated to increase function of liver (Fondevila *et al*, 2004), lung (Wang *et al*, 2010), intestinal (Nakao *et al*, 2004) and heart transplants (Yamashita *et al*, 2004) in animal models, via its anti-inflammatory and anti-oxidant capacities. In addition to transplantation however, biliverdin has been shown to have therapeutic potential in animal models of cerebral

infarction (Deguchi *et al*, 2008) and also acute lung injury (Nakao *et al*, 2005). A selection of such studies are briefly discussed and summarised below.

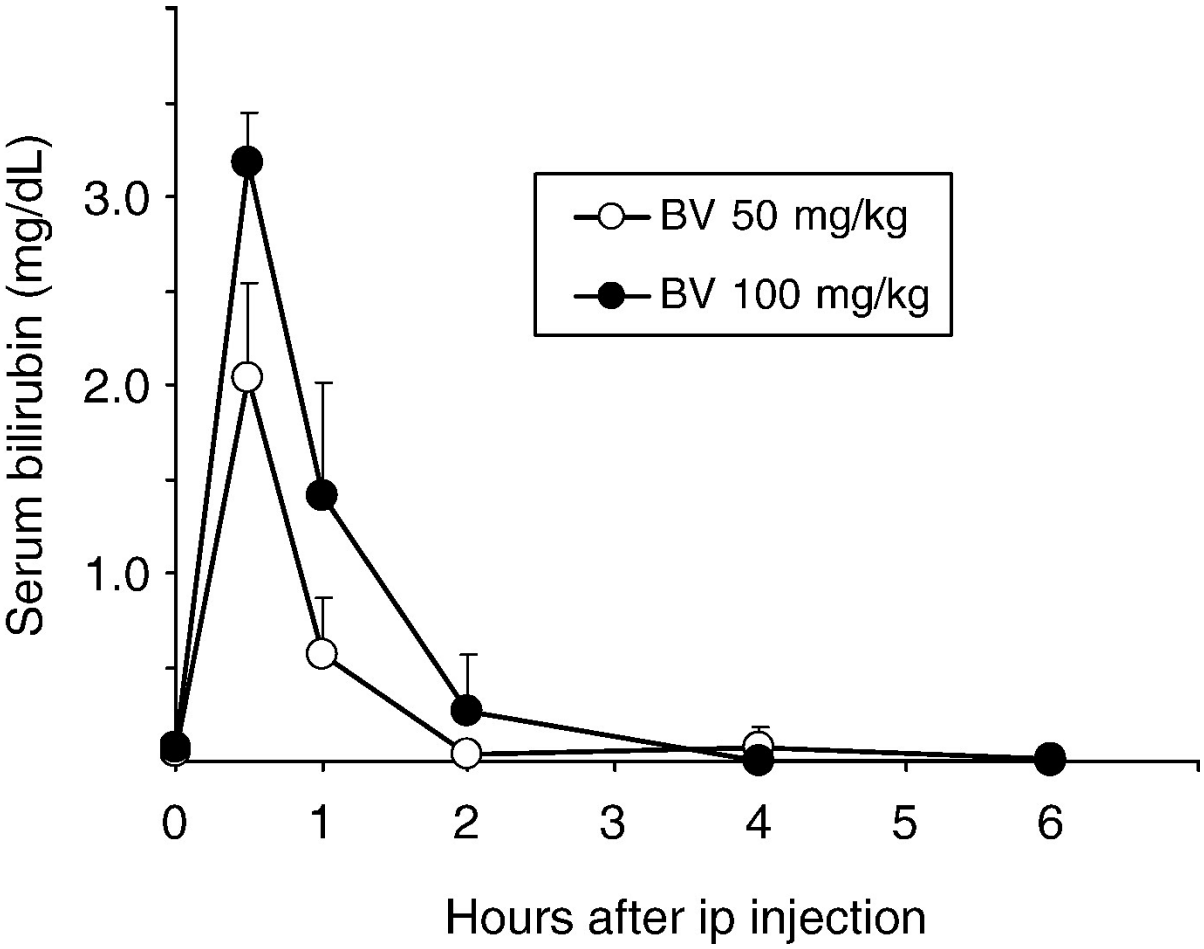

Figure 1.9 ***In vivo (rat) total serum bilirubin levels following intraperitoneal (IP) administration of biliverdin-IXα (BV)***. Serum bilirubin rises dose-dependently and peaks very quickly after approximately 30mins before returning to control levels after 3hrs. Taken from Deguchi *et al*, 2008.

The first study to examine the potential benefit of biliverdin administration in an inflammatory context examined the effect of the bile pigment in a hepatic ischemia/reperfusion injury (IRI) rat model (Fondevila *et al*, 2003). Rat livers reperfused with

biliverdin-containing perfusate showed significantly higher liver function, as assessed by liver enzyme release (i.e. glutamic-oxaloacetic transaminase and glutamic-pyruvic transaminase) and histological assessment. Biliverdin-perfused livers also showed greater portal vein blood flow and produced more bile.

Biliverdin administration was subsequently shown to prolong cardiac allograft survival in mice via attenuation of alloimmune responses (Yamashita *et al*, 2004). Biliverdin administration (50µmol/kg) almost doubled cardiac graft survival in a major histocompatability complex (MHC) class I and class II mismatched transplant model. Moreover, this tolerance was donor-specific such that mice accepted a second graft from the same donor strain but did not accept a second graft from a third-party donor (in the presence of biliverdin). Immunohistochemical analyses showed that biliverdin treatment reduced leukocyte infiltration and also inhibited T cell proliferation. Most importantly perhaps, this study suggested that at least some of the anti-inflammatory effects of biliverdin are related to its ability to inhibit the activation of specific transcription factors, namely NFAT and NFκB, as shown by the suppression of nuclear factor-DNA binding in an electrophoretic mobility shift assay.

Another study examined the therapeutic potential of biliverdin administration in *syngeneic* transplants (Nakao *et al*, 2004) in rats. Biliverdin was shown to increase recipient survival following transplant of syngeneic small intestine. Biliverdin treatment also increased expression of biliverdin reductase by a small degree in muscularis externa tissue in non-operated controls. Furthermore, biliverdin exerted its effects via its ant-inflammatory capacity – specifically via attenuation of expression of pro-inflammatory NFκB promoter-driven genes such as ICAM-1 and iNOS. Most importantly however, biliverdin treatment was

shown to *increase* NFκB DNA binding and, pharmacological inhibition of NFκB activity resulted in the loss of the ability of biliverdin treatment to prevent graft permeability after transplantation. This increased NFκB-DNA binding was shown to be present prior to transplantation.

A more recent study examined the effect of biliverdin treatment in lung graft transplants in rats (Wang *et al*, 2010). Biliverdin was administered intraperitoneally to both brain dead donors and recipients after confirmation of brain death and transplantation. Biliverdin treatment exerted a number of effects including reduction of the following pro-inflammatory parameters; wet/dry ratio of lung graft, myeloperoxidase (involved in oxidative stress) activity in lung graft and TNFα levels in serum. As one might expect, biliverdin also had an anti-oxidative effect – it reduced malanodialdehyde (a reactive species involved in oxidative stress) levels in lung graft and increased protein expression of superoxide dismutase (an antioxidant enzyme) in lung graft. Histologically, biliverdin treatment improved a variety of parameters in lung graft including, leukocyte infiltration. Brain death resulted in an increase in protein levels of HO-1, BVR and NFκB in lung graft. In the biliverdin treatment group, HO-1 and NFκB expression were reduced whilst BVR expression was increased.

A study examined the effect of biliverdin treatment on NFκB-DNA binding in HEK293 cells (Gibbs and Maines, 2007). Biliverdin was shown to suppress the transcriptional activity of the nuclear factor in a time- and concentration dependent manner in an electrophoretic mobility shift assay, in response to TNFα stimulation. The authors offer two possible explanations for this observation – that biliverdin interacts and therefore inhibits NFκB directly or, more likely, that biliverdin indirectly exerts an indirect inhibitory effect on NFκB.

The latter theory is supported by evidence that biliverdin alters activities of protein kinases – i.e. inhibits activity of PKCs (Maines, 2005) – and this may suppress intracellular signalling events associated with NFκB activation. Specifically, it has been suggested that biliverdin may cause IκB kinase (IKK) inhibition, thus resulting in the inhibition of IκBα degradation and sequestration of NFκB in the cytoplasm (Gibbs and Maines, 2007). There is a clear discrepancy between this study which reports a *decrease* in NFκB-DNA activity upon biliverdin treatment and the aforementioned studies (Nakao *et al*, 2004 and Yamashita *et al*, 2004) which showed an *increase* in NFκB-DNA binding. These discrepancies may be explained by the different time points, concentrations of biliverdin utilised, cell types, etc. The issue is further complicated by the 'Janus nature' of NFκB.

A recent seminal study demonstrated a novel mechanism in which BVR can in fact, at least in part, account for some of the anti-inflammatory effects of biliverdin (Wegiel *et al*, 2009). The authors show that functional (i.e. biliverdin-reducing) BVR is expressed on the cell-surface of RAW 264.7 cells (mouse macrophage cell line). Biliverdin binding to cell-surface BVR induces interaction of the BVR with the p85α regulatory subunit of PI3K, and BVR is itself phosphorylated on tyrosine residues. This results in downstream Akt phosphorylation and activation. The authors show that Akt activation is associated with expression of the anti-inflammatory interleukin-10 cytokine and that biliverdin treatment therefore leads to interleukin-10 production via the biliverdin-$BVR_{cell\text{-}surface}$-PI3K-Akt pathway in macrophages. This mechanism is shown to protect against LPS-induced liver injury (i.e. alanine aminotransferase release) *in vivo* in mice. Importantly, the protective action of biliverdin is lost when BVR is knocked down with Ad-siRNA.

Although the relationship between hyperbilirubinemia (i.e. due to Gilbert's syndrome) and CVD has now been well established, the potential benefit of hyperbilirubinemia in protection against various vascular complications (e.g. due to diabetes) requires further investigation. Indeed it has been shown that patients suffering from both diabetes and Gilbert's syndrome have reduced diabetic vascular complications compared to patients without hyperbilirubinemia (Inoguchi *et al*, 2007). Based on these findings, Fujii *et al* examined the effect of biliverdin administration on the severity of diabetic nephropathy in a rodent model of type II diabetes – i.e. diabetic *db/db* mice (Fujii *et al*, 2010). Uniquely, biliverdin was administered orally for a fortnight or more and did not give rise to substantively elevated serum bilirubin levels. Importantly, twelve weeks of biliverdin treatment reduced mRNA levels of NADPH oxidase 4 (NOX4) in both kidney and glomeruli tissue in *db/db* mice. Indeed, NOX4 is highly expressed in renal tissue and expression is elevated in the diabetic kidney (Gorin *et al*, 2005). NOX4 is a major source of superoxide in the kidney. Unsurprisingly therefore, superoxide generation is also reduced by biliverdin treatment in *db/db* mice. This study therefore shows that biliverdin has therapeutic potential in the treatment of diabetic nephropathy, partly due to its effects on the attenuation of oxidative stress generated via NOX4.

In summary, biliverdin posseses anti-oxidant, anti-inflammatory, anti-mutagenic, anti-proliferative and anti-apoptotic properties. Hence, biliverdin is now recognised as a potential therapeutic option for the treatment of numerous chronic inflammatory diseases, including atherosclerosis (Ollinger *et al*, 2007). Further animal studies are required however before biliverdin can be administered to humans. Biliverdin has also been shown to be able to modulate various cell signalling pathways – most relevantly, it can inhibit NFκB activation

and also inhibit PKCs. Indeed biliverdin is as effective as a commercially available peptide in inhibiting PKC isozymes (Maines, 2005). Whether biliverdin binds to and inhibits NFκB directly, or whether biliverdin exerts its inhibitory effect on NFκB by interfering with its transduction signals (e.g. via conventional PKC inhibition) is unclear (Gibbs and Maines, 2007). Biliverdin, in contrast to bilirubin, can also inhibit BVR promoter activity (Gibbs *et al*, 2010). Although biliverdin is often investigated in *in vivo* disease models, it must be remembered that its effects may in fact arise due to elevated intracellular bilirubin levels.

Bilirubin in Inflammation

In common with both the bile pigment from which it is formed and the enzyme which catalyses this reaction, bilirubin possesses recently discovered pleiotropic activities. In this regard, bilirubin can function in anti-oxidant, anti-inflammatory, anti-apoptotic and anti-mutagenic capacities, in addition to affecting cell signalling. Interestingly, bilirubin has widespread inhibitory effects on protein phosphorylation (Hansen *et al*, 1996) and this may, at least in part, explain some of the non-canonical activities of the pigment.

Bilirubin has been known to inhibit leukocyte adhesion and rolling to endothelium for over a decade. Indeed, an early study showed that bilirubin could inhibit monocyte transmigration through human aortic endothelium, in response to mildly oxidised LDL (Ishikawa *et al*, 1997). Prior to this discovery, studies had established that pharmacological HO-1 induction could suppress acute inflammation in a variety of systems, including for example LPS-induced endotoxemia in rats (Otterbein *et al*, 1997). This prompted Hayashi *et al* to elucidate the specific downstream mechanism by which HO-1 induction suppressed leukocyte adhesion (Hayashi *et al*, 1999). It was found that exogenously applied bilirubin could dose-

dependently inhibit both leukocyte rolling and adhesion, as elicited by H_2O_2 in mesenteric venules, in an *in vivo* intravital assay. Indeed, just 5µM of bilirubin was sufficient to attenuate the H_2O_2-induced adhesion.

Subsequent studies have found that bilirubin downregulates adhesion molecules. Kawamura *et al* found that bilirubin attenuates TNFα-induced VCAM-1 production in human aortic endothelial cells – as evidenced by an ELISA for the soluble VCAM-1 ectodomain released into the conditioned medium (Kawamura *et al*, 2005). Another study showed that bilirubin could suppress VCAM-1-associated ROS generation (Keshavan *et al*, 2005). Low-level ROS generation by NADPH oxidase is induced upon binding of $\alpha_4\beta_1$ integrin to endothelial VCAM-1, and this has the effect of increasing the activities of MMP-2 and -9. In turn, the MMPs degrade intercellular tight junctions and therefore facilitate leukocyte transmigration. In this regard, bilirubin was also shown to inhibit the activities of MMP-2 and MMP-9 in murine endothelial cells, downstream of VCAM-1 activation by an anti-VCAM-1 antibody (Keshavan *et al*, 2005).

A recent *in vivo* study also demonstrated that bilirubin can protect against LPS-induced lung injury in rats, at least in part via its ability to inhibit LPS-induced leukocyte-endothelium interactions (Kadl *et al*, 2007). Hence, histological analyses revealed that bilirubin treatment suppressed LPS-induced expression of endothelial ICAM-1 and VCAM-1. In addition to this, bilirubin treatment could suppress LPS-induced release of TNFα by various cell types, including endothelial cells and human PBMCs, in cell culture experiments.

The mechanism by which bilirubin exerts its anti-inflammatory effects was examined in two different studies by Mazzone *et al* (Mazzone *et al*, 2009 and Mazzone *et al*, 2009). The first study corroborated previous findings – that bilirubin could attenuate expression of cell-

surface adhesion molecules (i.e. ICAM-1, VCAM-1 and E-selectin) in response to inflammatory cytokines (i.e. TNFα) in endothelial cells. Moreover, this correlated with functional analyses showing that bilirubin could inhibit human polymorphonuclear leukocyte adherence to TNFα-activated HUVECs.

In their subsequent study, the authors showed that bilirubin exerted its effects on adhesion molecule expression via inhibition of the NFκB signalling pathway (Mazzone *et al*, 2009). The authors showed that bilirubin (30nM) attenuates nuclear translocation of the NFκB p65 subunit in H5V (murine endothelial) cells. Furthermore, application of an NFκB activation inhibitor – pyrridoline dithiocarbamate – additively inhibited the mRNA expression of E-selectin and VCAM-1 with bilirubin, in response to TNFα stimulation. However, this particular aspect of methodology could have been improved by measuring cell-surface protein expression of adhesion molecules, as opposed to mRNA levels.

Another study however, has shown that bilirubin can inhibit NFκB activation in $CD4^+$ T cells (Liu *et al*, 2008). Furthermore, bilirubin was shown to directly inhibit the binding of NFκB to DNA in an electrophoretic mobility shift assay (EMSA). Importantly, bilirubin suppressed IκB phosphorylation and this is a potential mechanism of inhibition of NFκB activation. Interestingly, BVR has completely the opposite effect on NFκB activation (Gibbs and Maines, 2007).

Bilirubin is also a potent inhibitor of PKCs (Sano *et al*, 1985). Importantly, PKCζ is absolutely necessary for TNFα-induced NFκB signalling in endothelial cells (Nigro *et al*, 2010). BVR on the other hand activates PKCζ, thus potentiating TNFα-induced NFκB signalling (Lerner-Marmarosh *et al*, 2007).

In summary, bilirubin has been shown to exert potent anti-inflammatory effects in various animal models. Mazzone *et al* have demonstrated that, in endothelial cells, bilirubin downregualtes TNFα-induced adhesion molecule expression via inhibition of NFκB activation (Mazzone *et al*, 2009). Bilirubin is also a potent inhibitor of PKCs (Sano *et al*, 1985)) and this may contribute to the pigment's anti-inflammatroy properties. BVR has the opposite effect on NFκB and PKCs as compared to bilirubin – it activates NFκB (Gibbs and Maines, 2007) and PKCζ (Lerner-Marmarosh *et al*, 2007).

Bilirubin as an Antioxidant

Reactive oxygen species (ROS) have a key role in the process of atherosclerosis and for example, induce macrophage infiltration and inactivate nitric oxide. Bilirubin also has indirect antioxidant abilities – i.e. independent of its scavenging activity against reactive oxygen and nitrogen species. Of the enzymatic pathways responsible for generating ROS, NADPH oxidase, which produces superoxide, is the most important in the vasculature. Bilirubin can downregulate NADPH oxidase (Kwak *et al*, 1991), and in addition to this can also inhibit iNOS expression (Lanone *et al*, 2005). iNOS is associated with several inflammatory diseases including atherosclerosis (Kroncke *et al*, 1998).

A seminal study by Baranano *et al* showed that 10nM of bilirubin could protect HeLa cells against 10,000-fold molar excesses of H_2O_2 (Baranano *et al*, 2002). Novelly, knockdown of BVR with siRNA in HeLa cells increased ROS levels and also increased sensitivity to oxidative stress. This led the authors to propose a biliverdin-bilirubin antioxidant redox cycle in which the linear terapyrrole bile pigment is kept in its reduced (bilirubin) form by BVR. In the

putative cycle, bilirubin reduces ROS, itself being specifically oxidised back to biliverdin, which is then subsequently reduced back to bilirubin by BVR (Figure 1.10). This model, in which bilirubin is recycled in an NADPH-dependent manner, was suggested to explain the discrepancy between the antioxidant capacity, and the relatively scarce intracellular concentrations of, bilirubin as compared to other established antioxidants. Indeed in comparison to glutathione, bilirubin has an intracellular concentration of <0.1% (Baranano *et al*, 2002).

Sedlak *et al* have demonstrated that bilirubin is primarily involved in cytoprotection against lipid peroxidation (Sedlak *et al*, 2009). The authors show that knockdown of BVR with siRNA in HEK293 cells preferentially increases H_2O_2-mediated lipid oxidation, as opposed to protein oxidation. However, it is suggested that bilirubin may protect against protein oxidation in hydrophobic environments (i.e. membrane proteins).

Although it is well accepted that both biliverdin and CO can function protectively downstream of HO, by for example acting as anti-inflammatory compounds, few studies have examined to what extent, if any, BVR is required for cellular protection following HO-1 induction. A recent study examined whether conversion of biliverdin to bilirubin was necessary to elicit the protective effects of HO-1 induction (Jansen *et al*, 2010). It was shown that bilirubin is a more potent anti-oxidant than biliverdin, in terms of superoxide scavenging ability and also protection against peroxynitrite-mediated protein tyrosine nitration, in an *in vitro* system. BVR knockdown in HUVECs with siRNA resulted in an increase in intracellular oxidative stress under basal conditions (as evidenced by dihydroethidium staining which specifically detects superoxide). Furthermore, HO-1 and BVR knockdown increased protein tyrosine nitration (an indicator of intracellular oxidative

stress) by the same amount. The protective effect of hemin on protein tyrosine nitration was lost in both HO-1 and BVR silenced cells whereas the protective effect of biliverdin was lost only in BVR silenced cells. Bilirubin was also shown to increase the expression of GTP-cyclohyrolase-1 (GCH-1) in EA.hy 926 (human endothelial) cells. GCH-1 is the rate-limiting enzyme in tetrahydrobiopterin (BH_4) synthesis, and BH4 prevents eNOS uncoupling and subsequent ROS generation (Jansen *et al*, 2010). These findings indicate an important role for BVR in conferring the antioxidant activities of HO-1.

The existence of any physiologically meaningful biliverdin-bilirubin redox amplification cycle is however an ongoing issue of contention (Sedlak and Snyder, 2009). Maghzal *et al* conducted a recent study, the results of which contradict the existence of a biliverdin-bilirubin redox antioxidant cycle (Maghzal *et al*, 2009). In contrast to previous studies, the authors showed that BVR overexpression in HeLa cells does not affect cell viability in the presence of H_2O_2. In mutant yeast cells which are completely deficient of endogenous heme oxygenase and BVR activity, BVR overexpression fails to protect against H_2O_2-induced cell death. Moreover, overexpression of the reductase in HeLa cells does not decrease H_2O_2-induced ROS and also, H_2O_2-mediated bilirubin oxidation yields relatively small amounts of biliverdin. However, the central premise of the biliverdin-bilirubin redox cycle is that bilirubin oxidation specifically results in the formation of biliverdin. Indeed, Maghzal *et al* argue that biliverdin formation (following oxidant-mediated bilirubin oxidation) is the limiting factor in the proposed scheme, preventing the redox cycle from regenerating meaningful concentrations of bilirubin.

Recent *in vitro* experiments also argue against the putative biliverdin-bilirubin redox amplification cycle (Jansen *et al*, 2010). In this study, HPLC analyses detected no significant

conversion of bilirubin to biliverdin by a variety of oxidants, including H_2O_2. This is in agreement with the notion that biliverdin formation is in fact the limiting factor in the putative cycle.

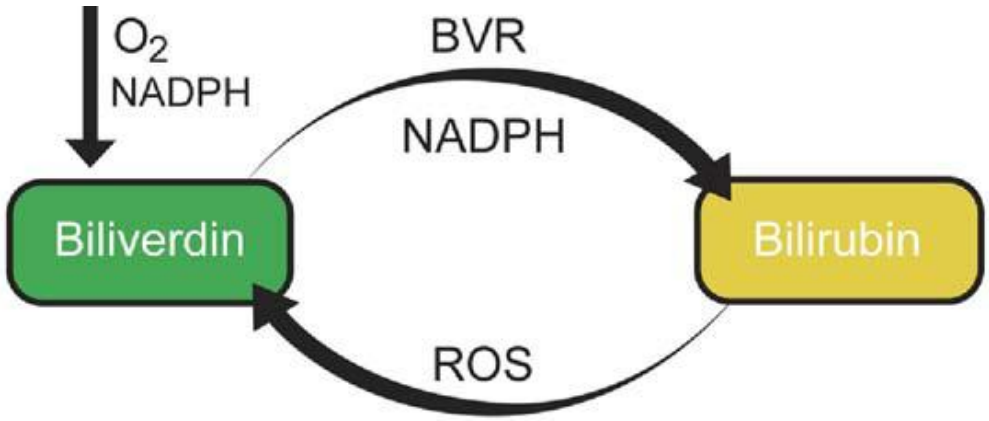

Figure 1.10 ***Bilirubin's antioxidant capacity may be part of a biliverdin-bilirubin redox cycle***. In this regard, bilirubin is not acting as a solely stoichiometric antioxidant but instead functions in a catalytic manner – ROS oxidise bilirubin to biliverdin, after which BVR reduces the newly-formed biliverdin back to bilirubin. A cycle of this sort confers amplification such that nanomolar concentrations of bilirubin can protect against 10,000-fold greater concentrations of oxidants. Adapted from Huffman *et al*, 2009.

Although further elucidation is required as to the (patho-)physiological relevance of any biliverdin-bilirubin cycle, it may be the case that oxidation of *intracellular* bilirubin does not specifically result in biliverdin formation. However, the notion that bilirubin is a pathophysiologically important *extracellular* antioxidant, responsible for the inverse correlation between serum bilirubin levels and risk of cardiovascular disease, is well accepted. In interpreting studies which aim to raise intracellular bilirubin concentratuions via BVR-overexpressing cell culture systems, there are two very important considerations; firstly, that HO is rate-limiting for bilirubin formation and secondly, that biliverdin (or heme)

substrate may need to be incorporated to generate meaningful levels of bilirubin (Sedlak and Snyder, 2009). This may, in part, explain some of the discrepancies between the recent findings of Maghzal *et al* and Jansen *et al*, which argue against the putative biliverdin-bilirubin redox cycle, and previous studies.

Bilirubin Inhibits LDL Oxidation

LDL is highly susceptible to oxidation and the ability of bilirubin to prevent oxidative modification of LDL was first demonstrated *in vitro* by Wu *et al* (Wu *et al*, 1994). The authors showed that physiological (i.e. <20μM) concentrations of bilirubin could inhibit Cu^{2+}-mediated LDL oxidation, as evidenced by TBARs assay and agarose gel electrophoresis.

These findings were corroborated in a study which showed that exogenous bilirubin supplementation can suppress oxidation of human blood plasma and also isolated LDL, following exposure to a pro-oxidant (Neuzil and Stocker, 1994). This established the potential role of bilirubin as an important antioxidant involved in the prevention of LDL oxidation during atherogenesis, and therefore provided the basis for investigations seeking to establish a relationship between serum bilirubin levels and cardiovascular risk.

That bilirubin generation is an important anti-atherogenic defence mechanism, involved in suppression of LDL oxidation, is demonstrated by the ability of ox-LDL to induce HO-1 (Siow *et al*, 1995; Siow *et al*, 1999 and Ishikawa *et al*, 1997). As HO-1 is the rate-limiting enzyme for the formation of bilirubin, its upregualtion is correlated with increased bilirubin production. There therefore exists a feedback loop in which elevated ox-LDL levels bring

about increases in bilirubin generation, in addition to another important anti-inflammatory mediator – CO.

As previously discussed, bilirubin provides protection against atherosclerosis, coronary artery disease and inflammation, at least in part via its potent antioxidant capacity (Gullu *et al*, 2005). However, given the pleiotropic nature of bilirubin, studies have sought to ask what contribution, if any, bilirubin's capacity to specifically inhibit LDL oxidation makes to its ability to inhibit atherogenesis. Indeed a recent study found that plasma LDL from Gilbert's syndrome patients is less susceptible to oxidation and that, in these LDL oxidation susceptibility experiments, the lag phase was prolonged in Gilbert's syndrome patients. (Yesilova *et al*, 2008). Interestingly, there was no statistically significant difference between TBARS levels in Gilbert's syndrome patients and healthy controls. This indicates protective activities of bilirubin, other than its ability to inhibit LDL oxidation.

In another study, the antioxidant capacity of Gilbert's syndrome patients was also not significantly different to normal controls (Bulmer *et al*, 2008). However, a trolox-equivalent antioxidant capacity (TEAC) assay did reveal a statistically significant difference between Gilbert's syndrome patients and normal controls, as did a ferric reducing ability of plasma (FRAP) assay. As discovered previously by Yesilova *et al*, the lag phase of serum oxidation was demonstrated to be significantly higher in the Gilbert's syndrome patients.

In summary, numerous studies have shown the potent anti-inflmmatory and antioxidant effects of bilirubin in *in vivo* models of inflammatory disease. That bilirubin has therapeutic potential in the treatment of atherosclerosis is perhaps best demonstrated by Gilbert's syndrome patients, who are protected against CVD. Bilirubin exerts these effects via its well-

established antioxidant capacity (which may or may not be part of a biliverdin-bilirubin redox cycle) and importantly, by also affecting cell signalling (Figure 1.11).

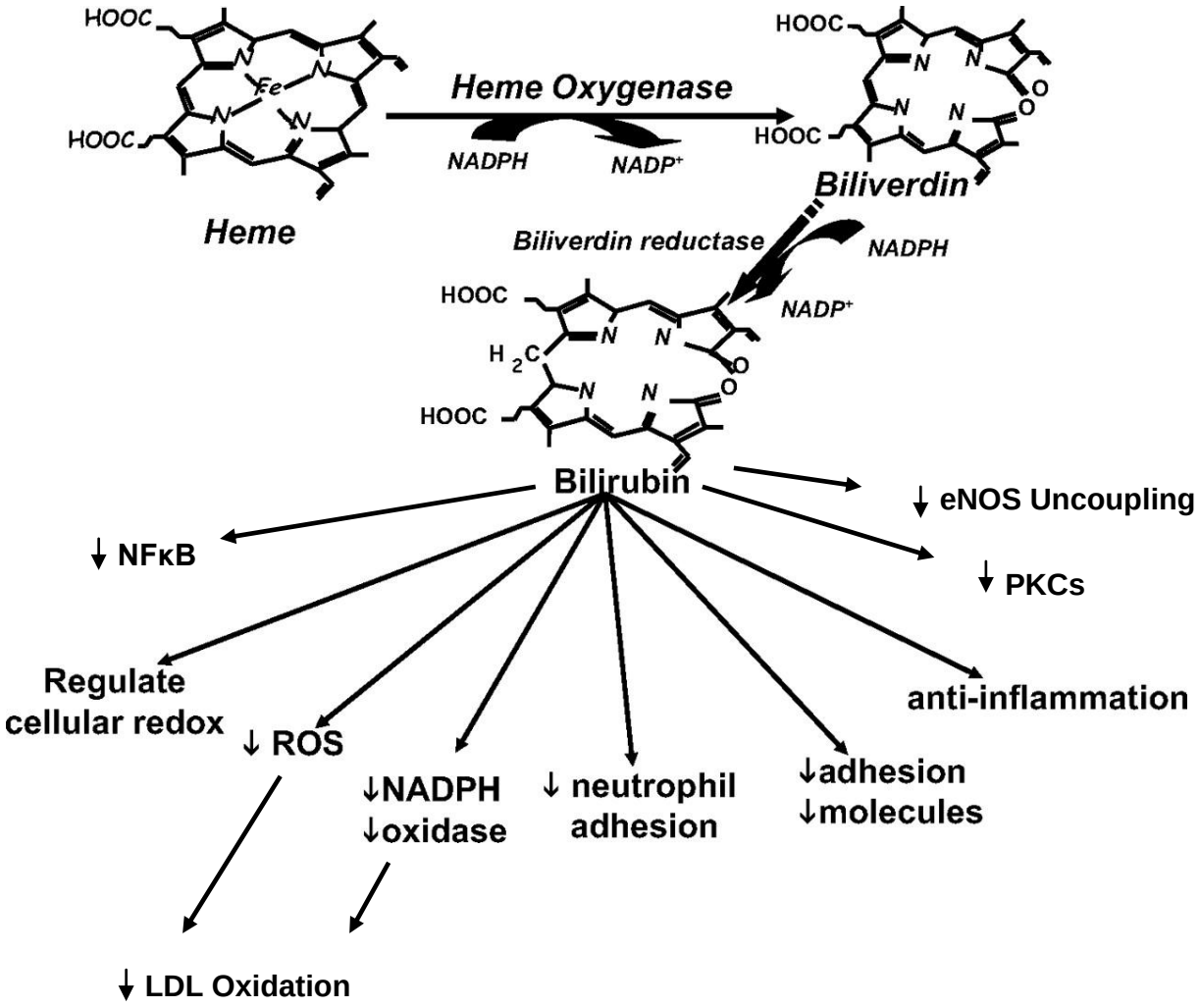

Figure 1.11 ***Bilirubin exerts its antioxidant and anti-inflammatory effects in a pleiotropic manner***. The pigment inhibits NADPH oxidase, a major source of superoxide in the endothelium (Kwak *et al* 1991). Bilirubin also downregulates TNFα-induced adhesion molecule expression in endothelial cells (Mazzone *et al*, 2009), and this reduces leukocyte adhesion. This is thought to occur, at least in part, via bilirubin-mediated inhibition of NFκB (Mazzone *et al*, 2009). A controversial BVR-mediated biliverdin-bilirubin redox cycle has been proposed to explain the observation that very low intracellular bilirubin concentrations can have potent antioxidant effects (Baranano *et al*, 2002). Furthermore, bilirubin can directly protect against serum LDL oxidation (Yesilova *et al*, 2008). Bilirubin is a potent inhibitor of PKCs (Sano *et al*, 1985). Bilirubin also protects against eNOS uncoupling (Jansen *et al*, 2010). Adapted from Abraham and Kappas, 2008.

NO in Atherosclerosis

Nitric Oxide (NO), along with CO and hydrogen sulfide (H_2S), is one of three endogenously generated gaseous signalling molecules implicated in cardiovascular homeostasis. NO is produced by three different nitric oxide synthase (NOS) isoforms – neuronal NOS (nNOS), inducible NOS (iNOS) and endothelial NOS (eNOS). NO output levels from each of the isoforms differ vastly such that iNOS>>nNOS>eNOS (Fleming, 2010).

Historically, NO was identified as the endothelium-derived relaxing factor (EDRF) due to its vasodilatory effects, although it is now known that NO, derived from eNOS, has other anti-atherosclerotic activities (Chowdhary and Townend, 2001). Amongst these other functions, NO is known to mitigate oxidative stress, act as an anti-coagulant, and to inhibit leukocyte-endothelial adhesion, VSMC proliferation in atherosclerosis and LDL oxidation (Napoli *et al*, 2006). Indeed, NO concentrates in the hydrophobic core of LDL where it acts as an antioxidant (Denicola *et al*, 2002).

Importantly, recent studies from our lab have demonstrated that induction of NO production, via eNOS S1177 phosphorylation, attenuates LDL oxidation in both HUVEC-culture experiments and *in vivo*, in apoE$^{-/-}$ mice (Ahmed *et al*, 2009). BVR is not known to affect NO generation via eNOS in any cell type.

NO has a variety of anti-inflammatory effects (Figure 1.12). Indeed, a recently developed anti-atherosclerotic drug, chunghyuldan, was shown to exert its effects in VCAM-1 expression via upregulation of eNOS expression (Park *et al*, 2005). Chunghyuldan was demonstrated to increase mRNA levels NOS, whilst decreasing cell-surface expression of VCAM-1 in HUVECs under basal conditions. This was associated with dose-dependent

increases in NO production. The compound also inhibited TNFα-induced VCAM-1 mRNA levels. Importantly, the effect of chunghyuldan on VCAM-1 expression is lost in the presence of an NOS inhibitor, L-NMMA. This demonstrates that the drug exerts its effects on VCAM-1 expression via NO. Furthermore, inhibition of basal NO generation is associated with increased MCP-1 expression in HUVECs (Zeiher *et al*, 1995). This study also showed that inhibition of basal NO production promotes NFκB translocation to the nucleus in HUVECs, in a gel mobility shift assay. Moreover, TNFα-induced increases in NFκB activation were suppressed by an NO donor.

A more recent study corroborated these findings and, in addition, showed that NOS inhibition increased Ca^{2+} influx and tissue factor expression in human coronary arterial endothelial cells, in the presence of monocyte binding (Sakamoto *et al*, 2005). Tissue factor is involved in coagulation and is therefore pro-thrombogenic. TNFα does not increase NO generation when applied to isolated rat hearts (Paz *et al*, 2003). However, the cytokine does downregulate eNOS mRNA.

NO bioavailability is decreased in atherosclerosis for two reasons – NO inactivation by ROS and reduced NO synthesis, due to changes in eNOS activity (Li and Forstermann, 2009). Under normal physiological conditions, NO concentrations are in the nM-to-pM range (Ignarro *et al*, 1999). ROS can be generated from a variety of sources however, of the enzymatic pathways; specific NAD(P)H oxidase (NOX) isoforms are the most important in the vessel wall (Violi *et al*, 2009). NOXs generate superoxide, which has a short half-life and which can readily dismutate to hydrogen peroxide, a species which also contributes to the oxidative milieu. In turn, this can lead to eNOS uncoupling thus exacerbating the NO/superoxide imbalance (Muller and Morawietz, 2009). NOX activity can be regulated by

cytokines (e.g. TNFα), growth factors, and shear stress (Frey *et al*, 2009). Indeed, TNFα-induced ROS generation via NOX requires PKCζ activation, an atypical PKC isoform that is highly expressed in endothelial cells (Rahman *et al*, 2000). Furthermore, increased NOX activity by angiotensin II occurs via the ERK1/2 MAPK pathway (Xie *et al*, 2001). NO has a crucial role in the deactivation of ROS, and this contributes to both the antioxidant and anti-inflammatory effects of NO. Indeed, ROS activate NFκB such that catalase overexpression inhibits TNFα-induced NFκB activation in endothelial cells (Schreck *et al*, 1991).

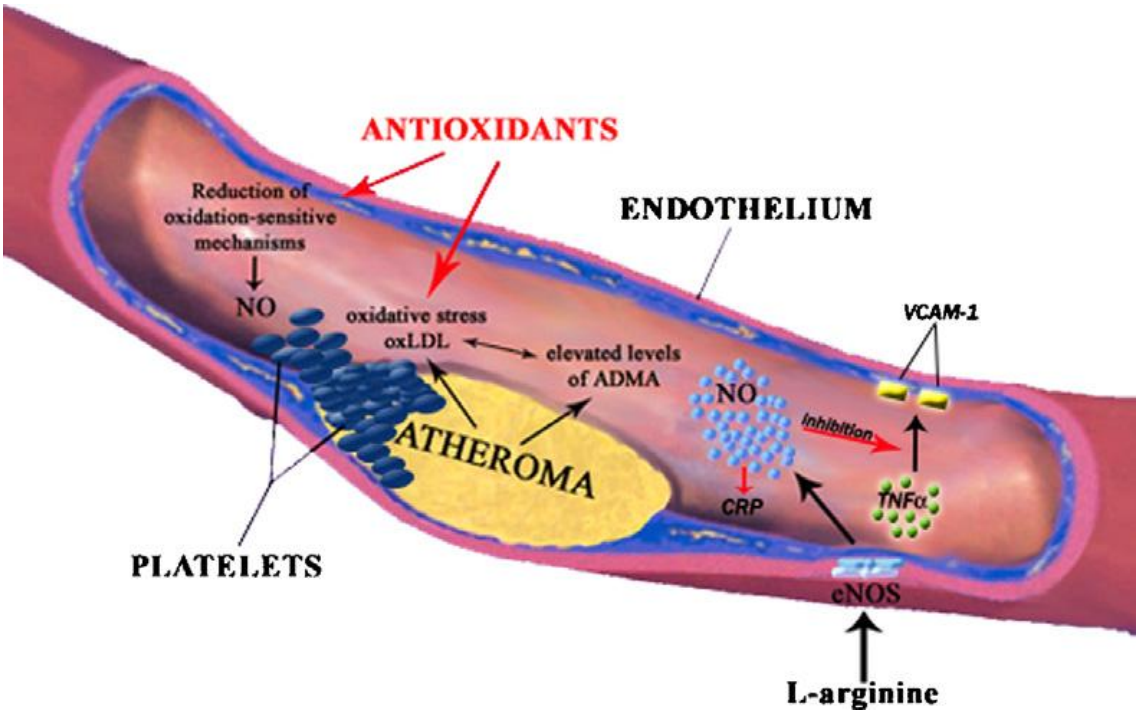

Figure 1.12 ***The anti-inflammatory role of NO in atherosclerosis***. On the right, eNOS generates NO. This reaction involves the oxidation of L-arginine to L-citrulline and 2mol of O_2 and 1.5mol of NADPH are required to produce 1mol of NO. NO is known to inhibit VCAM-1 expression. Loss of NO increases TNFα-induced VCAM-1 expression, possibly via a mechanism involving NFκB activation (Lazzerini *et al*, 2009). Loss of NO also leads to an increase in the circulating inflammatory marker, C-reactive protein (CRP). On the left, loss of NO increases oxidative stress and platelet aggregation. Antioxidants can alleviate oxidative stress. In the centre, asymmetric dimethylarginine (ADMA) levels are depicted to have increased. Indeed, ADMA is an endogenous competitive inhibitor of nitric oxide synthases, and hence decreases NO generation. Plasma ADMA levels are increased in atherosclerosis patients (Cooke, 2004). This perpetuates the oxidative milieu, causing LDL oxidation. Taken from Napoli *et al*, 2006.

In summary, NO is critical for endothelial homeostasis and its reduced bioavailability is a substantial contributor to the pathophysiology of atherosclerosis. NO is a vasodilator, an important antioxidant (preventing for example LDL oxidation) and an inhibitor of TNFα-induced NFκB activation, and downstream pro-inflammatory signalling. Strategies to increase its bioavailability are therefore likely to be beneficial in the treatment of atherosclerosis.

Akt in Atherosclerosis

Akt, a serine/threonine kinase, is activated by phosphatidylinositol 3, 4, 5-trisphosphate (PIP_3) and also by phosphatidylinositol-dependent protein kinases. PI3K/Akt-dependent pathways are critical in endothelial homeostasis and angiogenesis – Akt promotes cell survival, improves endothelial function via eNOS activation and NO release, regulates cell migration and is involved in neovascularisation in ischemic tissues (Shiojima and Walsh, 2002). Endothelial cell migration is critical for angiogenesis (Carmeliet, 2000), following myocardial infarction for example, and the PI3K/Akt pathway confers the pro-angiogenic properties of VEGF in these cells (Morales-Ruiz *et al*, 2000). Indeed, some of the pleiotropism of statins, for example their pro-angiogenic effects, is attributable to activation of the PI3K/Akt pathway (Kureishi *et al*, 2000). In addition, Akt has been demonstrated to protect endothelial cells against ox-LDL-induced cytotoxicity (Ou *et al*, 2010). Other pharmacological strategies have also demonstrated that Akt activation is a viable strategy to limit atherosclerosis, via improved endothelial function and angiogenesis (Lovren *et al*, 2009).

On the other hand, there is evidence to suggest that Akt can *activate* NFκB in endothelial cells, via IKK activation (Meng *et al*, 2002 and Liu *et al*, 2010). This would lead to the transcription of pro-inflammatory genes involved in the initiation and progression of atherosclerosis. There is also evidence demonstrating that Akt is activated downstream of NFκB activation, suggesting a positive feedback loop (Meng *et al*, 2002).

A recent study by Pachori *et al* suggested that BVR activates Akt in H9c2 cells (cardiomyocytes). Co-immunoprecipitation experiments revealed that BVR associates with the p85 regulatory subunit of PI3K (Pachori *et al*, 2007). That BVR activates the PI3K/Akt pathway was alluded to in the analyses of the structure of BVR which revealed that the reductase has two potential SH2 docking sites, which could interact with the SH2 domains in PI3K (Maines, 2005). Zeng *et al* corroborated these findings in their study which showed that BVR-transfected HK-2 (kidney) cells have substantially increased Akt activation, which could be reduced with PI3K inhibitors (Zeng *et al*, 2008). However, studies to date have not sought to demonstrate the BVR/PI3K/Akt pathway in endothelial cells.

Regulation of eNOS

The NO output from eNOS can be regulated via a number of different mechanisms including shear stress, phosphorylation, ROS and transcriptional control. Although eNOS was historically known as a Ca^{2+}/Calmodulin-dependent enzyme, it is now known that eNOS can be activated independent of sustained increases in intracellular calcium levels (Fleming, 2010). Precise, temporal regulation of eNOS activity is achieved via multi-site phosphorylation at specific serine, threonine and tyrosine residues and, various kinases and

phosphatases are therefore important in eNOS regulation. eNOS exists as a homodimer that is found localised in the plasma membrane caveolae and Golgi apparatus.

Under basal conditions, eNOS is constitutively phosphorylated on Thr495 by PKC. This prevents association with calmodulin. Under conditions of oxidative stress, eNOS phosphorylation on Tyr657 by Proline-rich tyrosine Kinase (PYK2) inhibits NO production.

Upon stimulation, the eNOS signalling complex undergoes structural changes, including the dissociation of caveolin-1. Thr495 is dephosphorylated which consequently allows calmodulin to bind to and activate the enzyme. Serine residues associated with activation (i.e. including Ser1177) are now phosphorylated. Indeed, phosphorylation of Ser1177 (located at the carboxyl-terminal end of the protein) is absolutely required for eNOS activation.

The phosphorylation of eNOS-Ser1177 involves at least four kinases – Akt, PKA, PKG and AMPK and is calcium-independent (Boo and Jo, 2003). Historically, the most salient of these was Akt. This was originally demonstrated in a seminal study by Dimmeler *et al* in which the PI3K/Akt pathway was shown to mediate the activation of eNOS (i.e. Ser1177 phosphorylation) in response to shear stress in HUVECs (Dimmeler *et al*, 1999). This was associated with increased NO generation and inhibition of the PI3K/Akt pathway with wortmannin (a PI3K inhibitor) attenuated the shear stress-induced eNOS Ser1177 phosphorylation.

Since then, inhibition of the PI3K/Akt pathway has been shown to inhibit eNOS Ser1177 phosphorylation in response to various other stimuli including VEGF agonist and insulin-like growth factor (Boo and Jo, 2003). Moreover a mutant form of eNOS, eNOS S1177D, is

utilised experimentally as a constitutively active version of eNOS, which generates substantial NO under basal conditions. This mutant is effective because the aspartic acid residue serves as a phosphomimetic.

A recent study examined the mechanism of action of kallistatin in the prevention of TNFα-induced endothelial cell apoptosis and oxidative stress (Shen *et al*, 2010). Kallistatin was shown to inhibit TNFα-induced endothelial cell apoptosis via the PI3K/Akt/eNOS^{Ser1177} pathway. This protective effect was lost with L-NAME (a NOS inhibitor) and eNOS knockdown (with siRNA) also attenuated kallistatin's inhibition of TNFα-induced apoptosis. Furthermore, TNFα treatment increased NOX activity and intracellular ROS generation – kallistatin inhibited this oxidative stress via NO generation, via the PI3K/Akt/eNOS pathway. Together, these findings suggest that strategies which aim to increase endothelial intracellular NO generation, via upregulation of eNOS Ser1177 phosphorylation, are likely to be beneficial in atherosclerosis and CVD.

Attenuated eNOS activity and consequently, reduced NO bioavailability, is a central feature of the pathophysiology of atherosclerosis. In this regard, various therapeutic strategies for atherosclerosis, either in use or in development, centre on increasing the bioavailability of NO (Li and Forstermann, 2009).

BVR & NO

At the time of writing, there is no published evidence to suggest that BVR directly influences NO release via eNOS. However, because BVR is involved in cell signalling (e.g. via its capacity as a dual-specificity kinase) it is possible that it is involved in eNOS regulation in

physiological and/or pathophysiological settings. Given the numerous signalling pathways that BVR affects – via its dual-specificity kinase activity, its role as a transcription factor, its role as an anchor protein or the bilirubin it produces – it is likely that the enzyme has multilateral influence on NO generation via eNOS.

Previous studies have shown that BVR activates the PI3K/Akt pathway in HEK293, HK-2 and H9c2 cells (Zeng *et al*, 2008 and Pachori *et al*, 2007). It is therefore possible that BVR induces NO release via a PI3K/Akt/eNOS pathway in endothelial cells.

Confounding the situation however, BVR is known to *activate* both PKCζ and ERK1/2 (Maines, 2007 and Lerner-Marmarosh *et al*, 2008). PKCζ is involved in TNFα-induced ROS generation via NOX in endothelial cells (Rahman *et al*, 2000), and also NFκB activation. The ERK1/2 pathway is also associated with increased NOX activity (Xie *et al*, 2001). Hence, one might expect that BVR acts to decrease the bioavailability of NO via the increased ROS production from NOX. On the other hand, ERK1/2 activation increases NO release via the ERK1/2/eNOS/NO pathway in HUVECs (Urano *et al*, 2008). Moreover, BVR overexpression in HEK293A cells increased both basal and TNFα-induced (NFκB-mediated) iNOS expression (Gibbs and Maines, 2007).

PKCζ is activated by BVR and is an important mediator of endothelial dysfunction due to its critical role in TNFα-induced inflammation (Nigro *et al*, 2010). Moreover, PKCζ decreases eNOS protein stability in response to TNFα stimulation, via a mechanism involving ERK5 (Nigro *et al*, 2010). On the other hand, the bilirubin produced by BVR has potent antioxidant and anti-inflammatory effects.

In summary, published findings have not yet established a BVR/PI3K/Akt/eNOS/NO pathway although one could hypothesise its existence on the established dogma that BVR strongly activates Akt. However, BVR also has several other (putative) positive/negative effects on NO production, confounding the situation. For this reason it is necessary for investigators to establish the dominant effect on NO production, and mechanisms thereof, in specific cell types.

Leukocyte-Endothelium Interaction in Atherosclerosis

During the early phase of atherosclerosis, leukocytes must be recruited from the circulation to the vascular endothelium where diapedesis subsequently occurs. Vascular adhesion molecules are expressed on both the vascular endothelium and circulating leukocytes in response to inflammatory stimuli, and are important in this process. Several different classes of adhesion molecule exist including the, integrins, ICAM-1 and VCAM-1, selectins and the junctional adhesion molecules (JAMs). The different adhesion molecules serve different functions during the process of leukocyte recruitment and transendothelial migration. Their importance in atherosclerosis has been demonstrated in numerous *in vivo* functional inactivation studies. For example, atherosclerotic fatty streaks in mice on a high-fight diet with homozygous mutations in ICAM-1 were substantially reduced compared to controls (Nageh *et al*, 1997). In cell culture experiments, the different adhesion molecules have different temporal expression profiles. With the exception of integrins, most of the vascular adhesion molecules have soluble forms which can be found in the circulation (Blankenberg *et al*, 2003).

The selectins (L-, P- and E-selectin) are C-type lectins that are involved in the initial capture, tethering and rolling of leukocytes along the endothelium (McEver, 2002). E-selectin is not constitutively expressed rather, only synthesised under inflammatory conditions. VCAM-1 is required for the slow rolling of monocytes whereas ICAM-1 is also involved in adhesion strengthening (Mestas and Ley, 2008). Augmented expression of these adhesion molecules has been observed in atherosclerotic plaques, in numerous *in vivo* models (Mestas and Ley, 2008).

Transcriptional control of the adhesion molecules, ICAM-1, VCAM-1 and E-selectin is largely via the NFκB transcription factor in endothelial cells. A study by Chen *et al* showed that inhibitors of IκBα phosphorylation block adhesion molecule expression in HUVECs, in response to TNFα (Chen *et al*, 1995). The authors show that IκBα is almost completely degraded after 30mins and that this correlates with NFκB DNA-binding activity, in HUVECs. Furthermore, inhibitors of serine proteases attenuated TNFα-induced IκBα degradation and consequently, NFκB activation. These inhibitors also blocked the transcription of the adhesion molecules.

A recent study by Zhou *et al* revealed that TNFα-induced adhesion molecule expression in HUVECs was mediated via TNF receptor-1 (TNFR-1) and importantly, they demonstrated that this process was completely dependent on NFκB activation (Zhou *et al*, 2007). Indeed, HUVECs express both TNFR-1 and TNFR-2 (at low levels) however the authors demonstrate that TNFR-1 is solely responsible for NFκB activation and consequently, downstream mRNA and protein expression of ICAM-1 and VCAM-1 (Figure 1.13). In this regard, the ERK1/2, p38 MAPK and JNK kinase pathways are shown to not contribute to TNFα-induced adhesion molecule expression in HUVECs, at the specific time-point studied. Consistent with these

findings, Rajan *et al* utilised a pharmacological inhibitor strategy to show that the p38 pathway does not contribute to TNFα-induced adhesion molecule expression in endothelial cells (Rajan *et al*, 2008). On the other hand, an earlier study by Read *et al* showed that maximal E-selectin expression in HUVECs depended on both NFκB activation and JNK/p38 activation (Read *et al*, 1997).

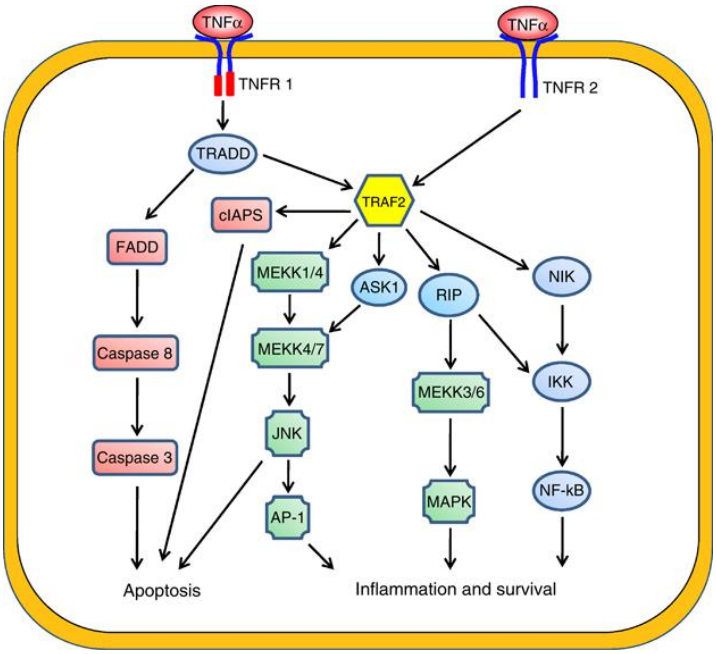

Figure 1.13 ***Intracellular signalling pathways activated by TNFα***. Zhou *et al* recently showed that TNFR-1 was solely associated with NFκB activation in HUVECs. TNFα binding induces receptor trimerisation and the recruitment of the TNFR-1-associated death domain (TRADD) adaptor protein and in turn, this recruits TNFα Receptor-Associated Factor-2 (TRAF-2). TRAF-2 activates IκB kinase (IKK) via receptor-interacting protein (RIP). IKK phosphorylates IκBα, resulting in IκBα ubiquitination and degradation. This releases NFκB. RIP is essential for TNFα-induced NFκB activation. Importantly, PKCζ is absolutely necessary for NFκB activation and is implicated both upstream and downstream of the IKK complex (Moscat *et al*, 2006). TRAF-2 also activates the ERK1/2, p38 MAPK and JNK kinase pathways. TNFα can also bring about apoptosis via degradation of inhibitor of apoptosis proteins (IAPs) and caspase activation via Fas-associated protein with death domain (FADD). Taken from Wu and Zhou, 2010.

In summary, adhesion molecules are critical in mediating the leukocyte-endothelial interactions required in atherosclerotic inflammation. Importantly, studies have shown that adhesion molecule expression in response to TNFα is largely via NFκB activation. However, the promoter regions of the adhesion molecules (and chemokines such as MCP-1) contain other transcription factor binding sites (e.g. AP-1). Hence these other pathways – i.e. ERK1/2, p38 MAPK and JNK kinase pathways – may contribute to some extent, depending on the system under study.

BVR & Adhesion Molecules

In short, the cell signalling pathways *activated* by BVR predominantly terminate on pro-inflammatory transcription factors, resulting in for example, adhesion molecule expression (Figure 1.14). This includes the NFκB, JNK, p38 and and AP-1 pathways (Kapitulnik and Maines, 2009). The protective effect of bilirubin, the product of BVR, in downregulating adhesion molecule expression, was recently demonstrated (Mazzone *et al*, 2009). However, the dual-specificity kinase activity and phosphorylation targets of BVR are consistent with a pro-inflammatory effect.

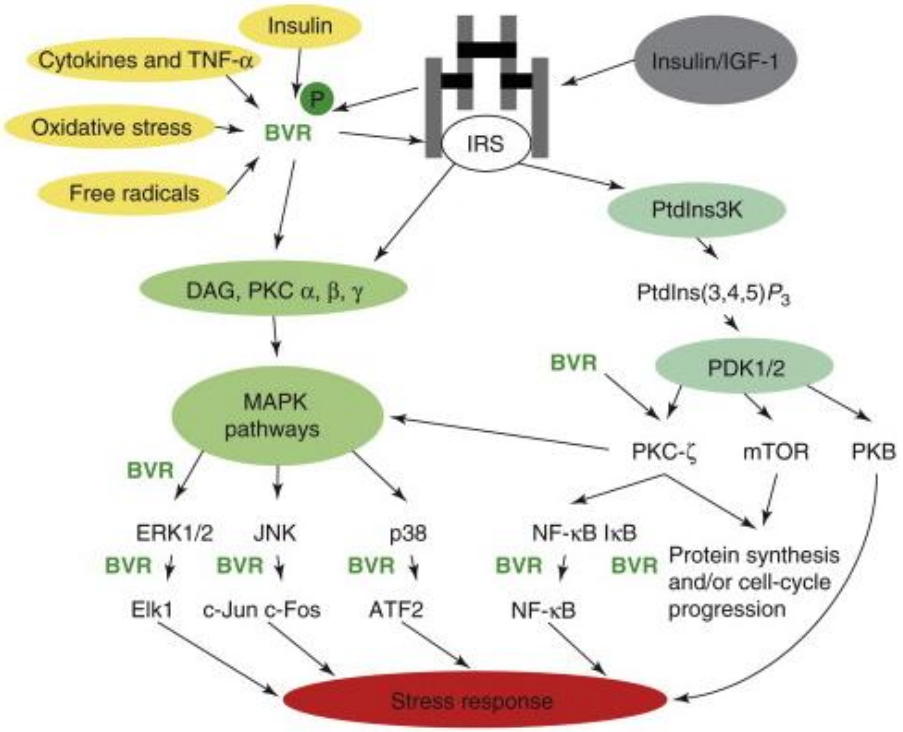

Figure 1.14 ***BVR promotes pro-inflammatory gene transcription***. Insulin, cytokines and oxidative stress all increase the kinase and reductase activities of BVR. BVR augments the activities of PKCs and PI3K, the later via IRS-1. Indeed, BVR competes to be phosphorylated by IRS-1 and in return BVR phosphorylates IRS-1. This leads to activation of the PI3K/Akt pathway. BVR also activates the ERK1/2, JNK and p38 pathways. Taken from Kapitulnik and Maines, 2009.

A study by Lerner-Marmarosh *et al* demonstrated that BVR may function as an essential part of the TNFα/PKCζ/NFκB pathway in HEK293A cells (Lerner-Marmarosh *et al*, 2007). BVR achieves this, in part, by reducing biliverdin – a potent inhibitor of PKCs (and PKAs) – to bilirubin, therefore increasing PKCζ activity. Also, the authors show that BVR increases PKCζ autophosphorylation, therefore increasing PKCζ activity. PKCζ phosphorylates BVR, thus increasing its activity. BVR was shown to co-immunoprecipitate with PKCζ, following stimulation of HEK293A cells with TNFα. This was not observed under basal conditions. Furthermore, TNFα stimulation increased PKCζ activity and BVR overexpression increased this effect. Most importantly, TNFα-induced NFκB activation was shown to be mediated by

PKCζ – and crucially, BVR overexpression enhanced this TNFα-induced NFκB activation (Figure 1.15). Indeed, BVR overexpression alomost doubled TNFα-induced promoter activity from an NFκB promoter-luciferase reporter construct. Interestingly, TNFα stimulation increased the reductase (as well as the kinase) activity of BVR such that BVR activity (i.e. rate of bilirubin production) doubled 30mins after TNFα was applied. This effect was transient and began to decline after 30mins. Moreover, TNFα stimulation altered the cellular distribution of BVR from a predominantly cytoplasmic localisation under basal conditions to a more nuclear, cell-membrane-associated distribution with TNFα. PKCζ also associates with the cell membrane following TNFα stimulation (Lerner-Marmarosh *et al*, 2007).

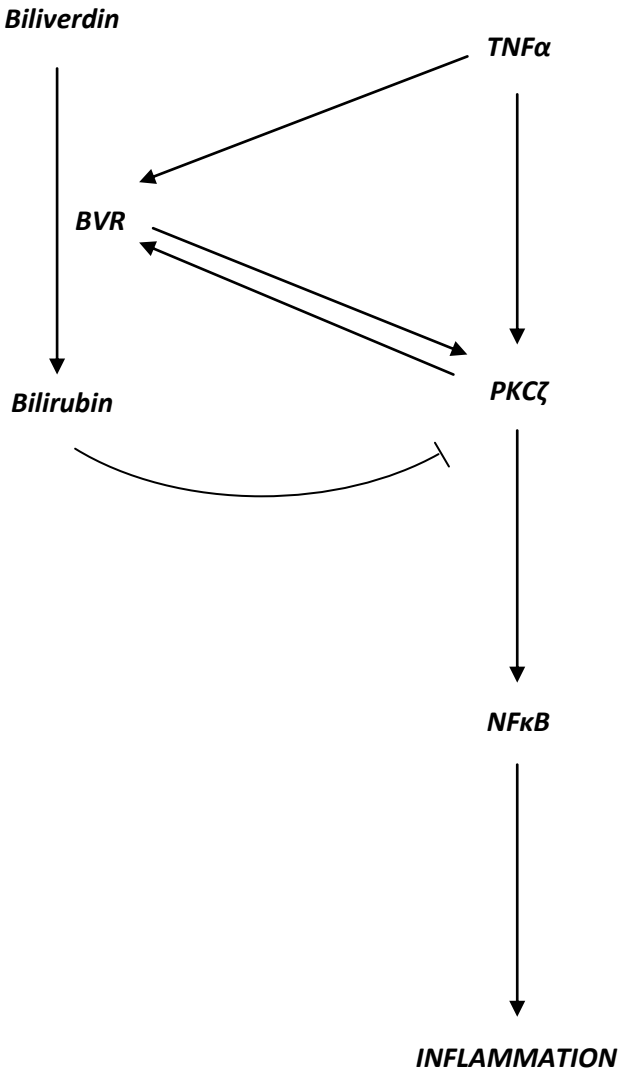

Figure 1.15 ***The TNFα/BVR/PKCζ/NFκB axis in TNFα-induced inflammation***. TNFα increases the kinase activity of BVR and induces BVR-PKCζ interaction. In turn BVR increases PKCζ activity and, PKCζ increases BVR activity (Lerner-Marmarosh *et al*, 2007). PKCζ is absolutely necessary in TNFα-induced NFκB activation (Nigro *et al*, 2010). On the other hand, bilirubin, produced by BVR, is a potent inhibitor of PKCs.

In summary, these findings suggest a critical augmenting role for BVR in TNFα-induced inflammation. TNFα signalling is implicated in transducing cardiovascular risk factors into endothelial dysfunction (Figure 1.16). BVR affects TNFα-induced inflammation by increasing PKCζ activity and consequently, increasing downstream NFκB signalling (Figure 1.15).

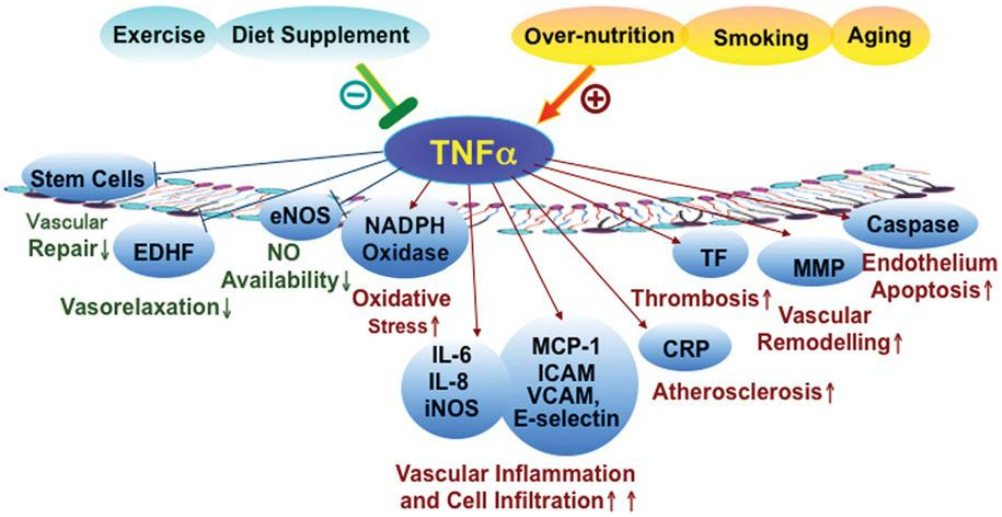

Figure 1.16 ***TNFα has a critical role in mediating cardiovascular inflammation***. Lifestyle factors determine endothelial dysfunction and the cytokine is crucial in initiating these changes. Importantly, TNFα-induced NFκB activation is *enhanced* by BVR and PKCζ is critical in this process (Lerner-Marmarosh *et al*, 2007). Taken from Zhang *et al*, 2009.

AIMS

Aims

It is clear that bilirubin, produced by BVR, functions in an anti-inflammatory and antioxidant capacity. However, the dual specificity kinase activity of BVR confers pro-inflammatory activities to the HO-1/BVR axis. For example, TNFα increases BVR activity and BVR in turn increases PKCζ activity, therefore contributing to NFκB activation. Published studies have not yet utilised BVR overexpression strategies in endothelial cells, the site of the initiation of atherosclerosis. Whilst BVR-mediated Akt activation has been demonstrated in HK-2 and HEK293 cells, endothelial cells have not yet been examined. We aim to demonstrate the existence of a BVR/PI3K/Akt/eNOS/NO pathway in HUVECs. A recent study by our group (and numerous others) showed that NO release by eNOS can protect against LDL oxidation in a cell culture system (Ahmed *et al*, 2009). We therefore aim to examine whether BVR overexpression in HUVECs is associated with reduced LDL oxidation. We also aim to investigate the role of BVR in leukocyte-endothelium adherence (i.e. adhesion molecule expression and monocyte adherence). This is partly due to a recent study by Mazzone *et al* which showed that bilirubin could attenuate TNFα-induced adhesion molecule expression (Mazzone *et al*, 2009).

MATERIALS & METHODS

Materials

Human umbilical vascular endothelial cells (HUVECs) were obtained from umbilical cords, from complication-free full-term deliveries. This was courtesy of ethical permission from Birmingham Women's Hospital NHS Trust. The ethical approval reference number for the present study was: 09/H1211/83. Umbilical cords remained connected to the placenta and were immediately refrigerated at +4°C post-partum in plastic bags, following standard clamping and cutting procedures.

Methods

All tissue culture work, and other work requiring aseptic conditions, was carried out in a class II microbiological safety cabinet. Tissue culture media, plastics (e.g. cell culture flasks), and supplements were purchased as sterile. Any solutions that were required to be made to be sterile (e.g. BSA-PBS solutions) were passed through a syringe-driven sterilizing filter (0.22µm pore). Glassware was washed and autoclaved prior to use. Cell culture media was stored in accordance with manufacturer guidelines (i.e. at 4°C) and used before the expiry date.

Tissue Culture

Cell cultures were maintained in a humidified incubator at 37°C in an atmosphere of 95% air and 5% CO_2. Cells were seeded onto T75 flasks which had been pre-incubated with 0.2%

gelatin for 5-10mins for adherent cells. Cell monolayer confluence was assessed daily for all cell types using a light microscope. Unless stated otherwise, cell culture medium was replaced every other day – this involved aspiration of the current medium, two washes with PBS and finally the addition of fresh medium. For adherent cells, approximately 11mL of cell culture medium was introduced into each T75 flask. Cells were generally passaged once 85-95% confluence was achieved, using trypsin-EDTA solution.

Isolation of HUVECs

HUVECs were isolated, characterised and cultured as previously described (Bussolati *et al*, 2001). Approximately 15mins prior to requirement, 20mL vials of 0.1% collagenase solution (i.e. one vial for each cord) were transferred from the -20°C freezer to the 37°C water bath.

Excessively hematic cords were discarded due to the inherent difficulties of manipulating such tissues. Crucially, each cord was examined for trauma arising from clamping – this would indicate possible damage of the endothelial basement membrane and may therefore lead to contamination of the isolation with non-endothelial cells (i.e. fibroblasts and VSMCs). Following selection of suitable sections of cords, each cord was cut cleanly at either end with a scalpel. Cannulae were then introduced at either extremity of the umbilical vein and held securely in place with nylon straps. The cannulated umbilical vein was then washed with PBS using a 50mL syringe until the effluence was clear and free of hematic contamination. Next, 20mL of the 0.1% collagenase solution (per 30-40cm section of cord) was injected into the washed umbilical vein with a 20mL syringe and either extremity was

then promptly clamped. The cord was then wrapped in clean aluminium foil and placed into the 37°C incubator for 20mins.

After 20mins, the cord was unwrapped in the hood and gently massaged for 1-2mins to encourage HUVEC detachment. Detached cells were collected into a 50mL tube by flushing the umbilical vein with M199 medium. The cell suspension was then centrifuged at 100g for 5mins before the supernatant was removed. The cell pellet was resuspended in an appropriate volume of complete M199 medium and then seeded into T75 flasks pre-coated with 0.2% gelatin before being placed in a 37°C incubator overnight. The following day, non-adherent cells (e.g. erythrocytes) were removed by washing each flask twice with PBS and then adding fresh complete M199. Confluence was generally achieved 4-6 days after isolation. Generally, HUVECs arising from three different sections of cord (i.e. from three different donors) were pooled and grown to confluence in two T75 flasks. Other lab members ensured adequate purity of isolations (at regular intervals) using this method by staining for the von Willebrand Factor (vWF), an endothelial cell marker. Experiments were performed on second or third passage HUVECs unless stated otherwise.

Cell Cryopreservation

Reserve stocks of each cell line and HUVECs were stored at -80°C and maintained via cryopreservation. The controlled-rate freezing method was used to freeze the cells at a rate of approximately -1°C/min, using the NALGENE 'Mr Frosty' freezing container. This protocol (see manufacturer instructions) minimises cell damage due to ice crystal formation and osmotic imbalance.

Reconstitution of the cryopreserved cells was performed by rapidly warming the cryovials at 37°C in a water bath. For non-adherent cells (i.e. THP-1 cells), residual DMSO was removed prior to seeding by pelleting the cells (via centrifugation at 100g for 5mins), removing the supernatant and then adding fresh culture medium. For adherent cells, 12-16hrs was allowed for cell attachment before two washes with PBS to remove residual DMSO.

Adenoviral-mediated Infection

A number of adenoviruses were utilised during the studies (Table 2.1) and the infection protocol used was the same for each of the different cell types that were infected. Adenoviruses were propagated in HEK-293 cells, purified in house via a double caesium chloride (CsCl) gradient, titred and then stored at -80°C in viral storage buffer as described previously (Channon *et al*, 1996). Unless stated otherwise, viruses were administered to cells at a concentration of 50 plaque-forming units (PFU) per cell. The transduction was carried out in the same culture medium that was used to grow the cells (e.g. complete M199 for HUVECs) and the cells were incubated with the virus for at least 20hrs before the experiment commenced.

Virus	***Titre (PFU/mL)***
CMV	1.23×10^{10} / 1.73×10^{10}
Adβ-Gal	1.38×10^{11}
AdBVR	5.25×10^{9} / 6.14×10^{9} / 1.67×10^{11}
AdHO-1	4.32×10^{11}
AdeNOS-WT	7.25×10^{9}
AdeNOS-S1177D	7.13×10^{9}

Table 2.1 ***Viruses utilised during the study and corresponding titres***.

Western Blotting

All cell lysates for Western blotting were harvested from 80-100% confluent cell monolayers growing in tissue culture plates. One hour prior to requirement RIPA lysis buffer was prepared on ice from a 10x RIPA lysis buffer stock, using d.H_2O as a diluent. The solution was then supplemented with an 'inhibitor cocktail' of protease and phosphatase inhibitors at 1% (v/v) each, to prevent degradation and dephosphorylation of proteins respectively. This solution was left on ice for at least 30mins prior to use and was stored (after wrapping in foil to protect from light) for up to one week. For each well of a 6 well plate, approximately 90µL of the RIPA solution was added.

To harvest the cell-lysate, culture medium was aspirated from each well before ice cold PBS was added to each well. The plate was then left on ice for 2-3mins before this was repeated. The ice cold PBS was then aspirated and the RIPA solution was added to the centre of each well, before the plate was agitated to ensure complete coverage. The plate was then left on ice for at least 20mins before a cell scraper was used to harvest the lysates. The lysates were collected into tubes which were subsequently centrifuged at 5000rpm for 5mins to remove insoluble cell debris. The supernatant was transferred to fresh tubes and frozen at -20°C until required.

Protein assays were carried out to estimate the total amount of protein present in cell lysates (for subsequent SDS-PAGE analysis) and to also estimate the total amount of LDL present in solution for our LDL oxidation experiments. The Bio-Rad *DC* protein assay was used for this purpose. The assay is a modification of the Lowry assay and employs colorimetric detection. A series of protein standards were prepared from a stock solution of 20mg/mL of BSA to give a range of concentrations from 0.2-1.4mg/mL. The BSA standards

were prepared in duplicate – one set of standards were diluted in PBS (for protein estimation of LDL concentration) whilst the other set were diluted in RIPA buffer (for protein estimation of cell lysate concentration). The standards were then assayed in triplicate (as described below for samples) to generate a standard line graph (BSA standard concentration vs. optical density) from which protein concentration of samples were calculated.

The protein assay was performed in near exact concordance with the manufacturer guidelines (the Bio-Rad 'DC Protein Assay Instruction Manual' – section 5.2 in this case). The plate was read within 1hr using a Multiskan Ascent 96 well plate reader at 690nm as per the instruction manual.

Once the resolving gel had been carefully poured into the plate assembly, avoiding the formation of air bubbles, it was immediately overlaid with several millilitres of 50% methanol. This prevents gel shrinkage and the formation of a meniscus. The gel was then allowed to polymerise for at least 30mins after which the 50% methanol was poured off. TEMED was then added to the stacking gel solution and following swift repulsing with a pipette, the gel was carefully poured on top of the resolving gel. An appropriate pre-cleaned sample loading comb was then inserted into the stacking gel and the gel was allowed to polymerise for at least 30mins.

SDS-PAGE: Loading & Running

Unless stated otherwise, 25µg of protein was loaded per well, in reducing buffer. The samples were placed on a heat block for 10mins at approximately 100°C to facilitate the reduction of disulfide bonds. Gels were initially electrophoresed at 80V. Once the

bromophenol blue dye had completely passed through the stacking gel, the voltage was increased to 140V.

SDS-PAGE: Semi-Dry Transfer

Following complete electrophoresis, the resolving SDS-PAG was separated from the glass plates. The gel was measured and then equilibrated in transfer buffer to remove buffer salts and detergents. Extra thick filter paper and nitrocellulose/PVDF was cut to the required dimensions. Generally, nitrocellulose membrane was used for transfer and the membrane was soaked in transfer buffer for 5mins before use. However on a few occasions PVDF was used. Unlike nitrocellulose, the PVDF membrane is hydrophobic and must be initially activated by incubating in 100% methanol for 5mins before being washed in transfer buffer. The extra thick filter paper was also soaked in transfer buffer for 5mins before being massaged to ensure complete saturation. The gel was then assembled in the Trans-Blot semi-dry electrophoretic transfer cell (Figure 2.1).

The required current was determined using the following equation: 0.8 x area of the gel (in cm^2) = required current (mA). All gels were allowed to transfer for 2hrs 30mins.

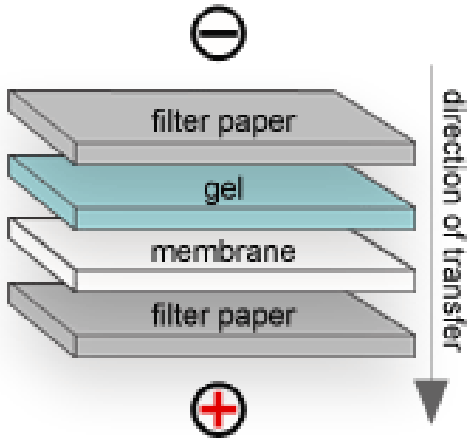

Figure 2.1 ***Assembly of the Trans-Blot semi-dry electrophoretic transfer cell***. Firstly, pre-soaked extra thick filter paper is placed on the platinum anode. A pipette tip is then gently rolled along the filter paper to remove air bubbles. The membrane is overlaid and rolled to remove air bubbles. The equilibrated gel is placed on top and air bubbles are rolled out before the other piece of filter paper is placed on top. Again, air bubbles must be rolled out and then any excess transfer buffer surrounding the 'stack' is soaked up with paper towels, to prevent short-circuiting. The cathode is then placed on top, being careful to avoid lateral movement which would disturb the stack, before being covered with the safety cover.

Membrane blocking & 1° Ab. Incubation

Once transfer was complete, the 'stack' was disassembled and the membrane was very briefly equilibrated in TBST on a platform rocker. Membranes were blocked for either 1hr at room temperature or overnight at +4°C with 5% dried skimmed milk (w/v) in TBST on a platform rocker. The membrane was then quickly washed twice with TBST to remove residual visible milk before being washed for a further 45mins on the rocker platform. The TBST was changed every 15mins.

After washing the membrane, the primary antibody solution was added (Table 2.2). Manufacturer time and temperature incubation guidelines for each antibody were adhered to. Each antibody was diluted in a 1% BSA-TBST (w/v) solution. To allow reuse of stored antibody dilutions, sodium azide (NaN_3) was added at 0.02% (w/v) to prevent microbial contamination.

Antibody	*Manufacturer*	*Description*	*Recognition*	*Optimal Dilution*
BVR	Abcam	Rabbit polyclonal	Human	1/5000
HO-1	Abcam	Rabbit polyclonal	Human	1/5000
Akt	Cell Signaling	Rabbit polyclonal	Human	1/1000
p-Akt (S473)	Cell Signaling	Rabbit polyclonal	Human	1/1000
eNOS	Cell Signaling	Rabbit polyclonal	Human	1/1000
p-eNOS (S1177)	Cell Signaling	Rabbit polyclonal	Human	1/1000
IκBα	BD Transduction Labs	Mouse monoclonal	Human	1/500
β-actin	Sigma	Mouse monoclonal	Human	1/15000

Table 2.2 ***Optimal dilutions of primary (1°) antibodies utilised during Western blotting***.

2° Ab. Incubation & ECL Detection

After primary antibody incubation, the membrane was thoroughly washed as previously described. The secondary antibodies (Table 2.3) were diluted in 5% skimmed milk-TBST (w/v) solution *pro re nata* and were disposed of after usage. As an exception, when detecting β-actin a secondary antibody concentration of 1/20000 was always used due to the high abundance of this protein in cell lysates.

Antibody	*Manufacturer*	*Description*	*Recognition*	*Optimal Dilution*
Peroxidase Anti-Rabbit IgG (H+L)	Vector Labs	Goat polyclonal	Rabbit	1/10000
Peroxidase Anti-Mouse IgG (H+L)	Vector Labs	Horse polyclonal	Mouse	1/10000
Peroxidase Anti-Biotin	Vector Labs	Goat polyclonal	(Biotin)	1/5000

Table 2.3 ***Secondary (2°) antibodies and relevant optimal dilutions utilised during Western blotting***.

Following 1hr incubation with the secondary antibody (or 30mins when detecting β-actin) on a platform rocker, the membrane was washed as previously described. The TBST was then drained from the membrane and ECL detection fluid was added. We utilised the EZ-ECL (Biological Industries) detection system in accordance with manufacturer instructions.

Quantitative NO Analysis

The Sievers nitric oxide analyzer (NOA) was used to indirectly measure the NO content of cell culture conditioned medium. The method is suitable for measuring low nanomolar to millimolar levels of NO in liquid samples. The underlying principle of the method is that the vast majority of NO in the liquid sample is oxidized to nitrite (NO_2^-) by dissolved oxygen, in the absence of oxyhemoglobin or superoxide. The NOA was therefore setup to measure nitrite via its reduction to NO by iodide. This reaction occurs in the purge vessel of the machine which contains the reducing agent, 1% sodium iodide (w/v) in glacial acetic acid:

$$I^- + NO_2^- + 2H^+ \longrightarrow NO + 0.5I_2 + H_2O$$

The amount of NO formed by this reaction is therefore directly proportional to the amount of nitrite in the sample which is in turn dependent on the amount of NO originally present. The NO enters the NOA (Figure 2.2) where it is detected by chemiluminescence. The detector relies on the reaction between NO and ozone (generated from an oxygen supply):

$$NO + O_3 \longrightarrow NO_2^* + O_2$$

$$NO_2^* \longrightarrow NO_2 + hf$$

The nitrogen dioxide produced in this reaction is in an excited state and decay of this species results in infrared photon emission (>600nm) in accordance with $E = hf$. Photon emission is therefore proportional to the NO content of the sample. Photon emission from this reaction is measured with a red-sensitive photomultiplier tube (PMT). To increase sensitivity, the PMT is cooled to <-12°C. The PMT amplifier processes the signal from the PMT and this was used in high gain mode (linear response up to approximately 400pmol nitrite). The PMT signal is represented in mV and changes in the PMT signal with time can be seen in real-time onscreen. Software was used to calculate the NO concentration in each sample by firstly finding the area under each sample peak. The NO concentration was then calculated by comparison with a standard graph, which was generated from the analysis of a set of serial dilutions of sodium nitrite. 100µL of each sample was injected into the centre of the purge vessel through the septum in the injection port with a syringe (Figure 2.2). The iodide reducing agent becomes more yellow as the reagent is depleted due to I_3^- formation and this can be used as an indication of when to change the solution.

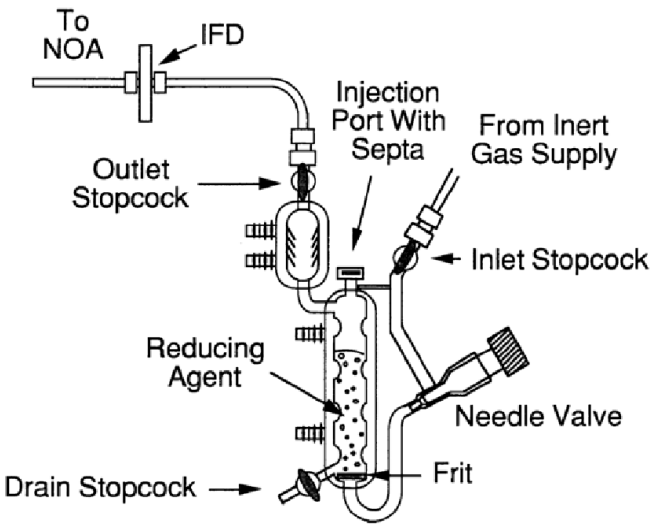

Figure 2.2 ***Purge vessel apparatus used for nitrite reduction***. Generally, about 5mL of the reducing agent was added to the purge vessel. The solution is simply discarded via the drain stopcock and replenished via the injection port. The inert gas that was used was nitrogen and this functions to purge the NO generated by the reduction reaction from the liquid phase. The NO is then drawn under vacuum to the NOA unit. The needle valve is used to adjust the flow of nitrogen such that the cell pressure is within a reasonable range. The polypropylene filter (IFD) protects the chemiluminescence reaction cell from liquid damage. Adapted from www.geinstruments.com.

Conditioned medium samples (0.5mL/well) for NO analysis were collected from confluent quiescent cells growing in 24 well plates. NO release was measured over the indicated times and 'stimulation' was therefore initiated by adding fresh culture medium. Fluid shear stress can activate eNOS and hence care was taken to prevent unnecessary movements. RPMI 1640 supplemented with 0.2% BSA was used for stimulation unless indicated otherwise. To control for background nitrite/NO inherently present in the culture medium, medium-only (cell-free) controls were incubated under the same experimental conditions. NO levels from these medium-only controls were subtracted from samples. All samples were collected into tubes and then stored at -80°C until analysis. Samples were analysed in triplicate.

Flow Cytometric Analyses

Flow cytometry was used to assess HUVEC-*surface* expression of adhesion molecules, specifically ICAM-1, VCAM-1 and E-selectin. The following antibodies were utilised:

Antibody	***Manufacturer***	***Description***	***Recognition***	***Optimal Dilution***
ICAM-1	Dako	Mouse monoclonal	Human	1/100
VCAM-1	Dako	Mouse monoclonal	Human	1/100
E-Selectin-Fluorescein	R & D Systems	Fluorescein-conjugated Mouse monoclonal	Human	1/25
IgG_1	Dako	Mouse monoclonal (negative control Antibody)	-	1/100
Anti-mouse IgG-FITC	Sigma	FITC-conjugated Goat polyclonal (2° Antibody)	Mouse	1/100

Table 2.4 ***Primary antibodies and relevant optimal dilutions utilised during flow cytometric analyses***.

Human recombinant TNFα cytokine composed of 157 amino acids, corresponding to the C-terminal extracellular domain of the full length transmembrane protein, was utilised at a working concentration of 10ng/mL, in order to induce cell-surface expression of the aforementioned adhesion molecules. Unless stated otherwise, stimulation with this cytokine was carried out for 6hrs (excluding any pre-incubation times with inhibitors) in 12 well plates (0.5mL/well). HUVECs were used in all experiments and were not pre-starved to quiescence. All stimulations were carried out in 'HUVEC starvation medium' (containing 5% FCS and no supplemental growth factors). If inhibitors were used in the experiment, cells were pre-incubated for one hour in the starvation medium with the inhibitors. The medium was then changed and fresh medium containing inhibitor and/or cytokine was added and incubated for 6hrs.

Antibodies were prepared at the indicated concentrations in 1% BSA (w/v) PBS solution. The cell culture plates were removed from the incubator and checked under the microscope for cytotoxicity. Each well was then washed twice with warm (i.e. 37°C) PBS before 60µL of trypsin-EDTA solution was added to each well. The plate was then jolted from side-to-side to ensure complete coverage before being placed in the incubator for 2-3mins. Cell detachment was then confirmed under the microscope before approximately 0.5mL of fresh starvation medium (at room temperature) was promptly added to each well. The contents of each well were transferred into a FACS tube on ice before approximately 2mL of ice cold PBS was added to each tube to remove medium/trypsin solution. The tubes were spun at 1200rpm for 6mins at +4°C before supernatant was discarded.

Primary antibodies were then added to the cell pellets. The Dako antibodies were added in a volume of 100µL/tube whereas the E-selectin antibody was added in a volume of 15µL/tube

in accordance with manufacturer guidelines in either case. Gentle vortexing and tapping of the tubes ensured thorough mixing and the tubes were left on ice for 30-45mins. Ice cold PBS was then added to each tube to wash off unbound antibody and the tubes were spun as previously described. Supernatant was discarded and 100µL/tube of secondary antibody was added and mixed, and left on ice for approximately 30mins. Tubes containing E-selectin antibody were omitted and left on ice because this antibody is already conjugated and so does not require the secondary antibody step. All tubes were then washed with ice cold PBS to remove unbound antibody, spun down and supernatant was discarded as previously described. The cell-antibody complexes were then fixed by the addition of 0.4mL of 2% paraformaldehyde (w/v) in PBS to each tube. Crucially, each tube was vortexed immediately after adding the fixative to prevent cell clumps being fixed. The tubes were sealed and stored at +4°C for up to three days before analysis. Prior to analysis, cells were pelleted and supernatant discarded as described previously and 0.3mL 1% BSA (w/v) PBS solution was added to each tube. This is to prevent the fixative from damaging the flow cytometer.

A 'BD FACSCalibur' flow cytometer was used to analyse the samples whilst a 'Summit' software package was used to view the results. Ten thousand events per tube were measured and median fluorescence was graphed.

Isolation of PBMs

Peripheral blood monocytes (PBMs) were isolated from whole human blood for the monocyte adhesion assays, using Ficoll and Percoll gradients. Healthy donors were asked to sign a consent form and were notified of how much blood was to be taken. Venipuncture

was performed (courtesy of Dr Kequing Wang) and blood was taken from the median cubital vein of the anterior forearm. The blood was then gently injected into a 50mL tube containing 100µL of 0.5M EDTA/50mL blood. The tube was inverted several times and either left at +4°C for no longer than 2hrs or processed immediately.

Peripheral blood mononuclear cells (PBMCs) must first be isolated, from which monocytes can be subsequently isolated. For every 50mL of whole blood, three 20mL tubes were prepared, each containing 8mL of the sterile density medium 'Ficoll-Paque PLUS'. Equal volumes of whole blood were carefully overlaid onto the gradients in each tube and spun at 400g for 30mins at room temperature. Crucially, the break setting was adjusted to zero to prevent disruption of the separation when the centrifuge is decelerating. The PBMCs present themselves as a 'buffy coat' – a white interphase ring. A Pasteur pipette was used to remove the PBMCs to a fresh 50mL tube, and care was taken to not disturb the layer of erythrocytes beneath. The PBMCs were then washed with PBS-citrate solution three times, with centrifugation at 150g for 8mins. The citrate in the solution prevents platelet contamination. If PBMCs were required for the experiment they were utilised at this stage.

If monocytes were required, the PBMCs were suspended in HUVEC starvation medium (15mL/50mL blood). Percoll gradients were prepared from a solution of isotonic Percoll. The isotonic Percoll is a solution of 90% Percoll (d = 1.130 g/mL) and 10% (v/v) 1.5M NaCl. From this isotonic Percoll solution, two solutions were prepared: a 1:1 solution (v/v) of isotonic Percoll and PBS-citrate and, an 11:9 solution (v/v) of isotonic Percoll and PBS-citrate respectively. Percoll gradients were made by carefully overlaying 4mL of the 11:9 Percoll solution with 4mL of the 1:1 Percoll solution. This was prepared three times in three different tubes and then 5mL of the PBMC suspension was carefully overlaid onto each

gradient. The tubes were then centrifuged at 400g for 30mins, with the break setting at zero. The lymphocytes are pelleted at the bottom of the tube whilst the monocytes are found dispersed in the upper two thirds of the gradient. The whole of the upper two thirds of the gradient was therefore transferred to a fresh 50mL tube before washing with PBS-citrate solution as previously described. The monocytes were then diluted in HUVEC starvation medium to the required concentration, after counting with a hemocytometer. Care was taken to avoid fluid shear stress during all steps because this can affect monocyte adhesion. The purity of monocyte isolation using this method was checked at regular intervals by other lab members, by staining for the monocyte-specific membrane marker CD14, which was typically 80-90%.

Static Monocyte Adhesion Assay

All monocyte adhesion assays were conducted on confluent HUVEC monolayers in 24 well plates under static conditions, with TNFα cytokine used to induce adhesion molecule expression. HUVECs were pre-incubated with inhibitors for one hour in HUVEC starvation medium in a volume of 250µL/well. After one hour the culture medium was aspirated from the wells and fresh starvation medium containing the inhibitor and/or TNFα at 10ng/mL was added. The stimulation was carried out for six hours, during which time monocytes were isolated from whole blood. 2 X 10^5 monocytes/well were then added in a volume of 400µL of HUVEC starvation medium – the culture medium already present (containing TNFα and/or inhibitor) was not aspirated. The monocytes were then allowed to adhere to the monolayer for one hour before non-adherent monocytes were washed off by washing the HUVEC monolayers once with PBS. Crucially, the culture medium was aspirated very gently

at this stage and the PBS was added with a Gilson pipette to avoid shearing off of bound monocytes. The PBS was then gently aspirated and 0.4mL/well of 1% glutaraldehyde (v/v) in PBS was added for fixation. The culture plate was then left at room temperature for 5mins before being stored at +4°C for up to one week for subsequent analysis.

The glutaraldehyde solution was aspirated and wells were washed twice with $d.H_20$. 0.4mL of Mayer's hematoxylin solution was then added to each well at a concentration of 4% (v/v), diluted in $d.H_20$. The plate was left at room temperature for 10-15mins before the hematoxylin solution was aspirated. Wells were then washed twice with 0.5mL of tap water. A further 0.5mL of tap water was subsequently added to prevent desiccation.

Images of adherent cells were captured using a confocal microscope. No fewer than five fields of view were imaged per well using a 10x lens. Fields of view were randomly selected from different quadrants of the well. 'Image-Pro Plus' software (Media Cybernetics) was used to count stained cells (i.e. adherent monocytes). The software can be programmed to count objects that have a relatively high optical density and can also discriminate on the basis of size (i.e. objects too large to be monocytes such as HUVEC nuclei can be excluded). This method proved to be highly accurate, as evidenced by concordance with results from human-counted images, and also very time-efficient.

ELISA for Human MCP-1

HUVECs were grown in 24 well plates. Cells were pre-incubated for one hour with inhibitors in HUVEC complete medium. The wells were then aspirated and fresh medium containing inhibitor and/or 10ng/mL of TNFα was added in HUVEC complete medium. The stimulation

was carried out in 0.5mL of the medium/well for 24hrs. The conditioned medium was then collected into tubes and centrifuged at 5000rpm for 5mins to remove detached cells. The supernatant was then transferred to fresh tubes and stored at -80°C for up to one month before analysis.

The 'Human CCL2/MCP-1 DuoSet' sandwich ELISA kit (R & D Systems) was used to measure the concentration of MCP-1 in the conditioned media, in complete accordance with the manufacturer instructions. Optical density was measured with a microplate reader at 450nm, with correction at 540nm. A standard curve was created from the optical densities of the recombinant MCP-1 standards and this was used to calculate MCP-1 concentration in the samples. Medium-only blanks were incorporated in the experiments and results were subtracted from the samples.

LDL Oxidation & TBARs Assay

The effect of BVR on lipid peroxidation was assessed via the thiobarbituric acid reactive substances (TBARs) assay. Native LDL isolated from human plasma was purchased from 'Sigma' and 'Sunnylab'. This native LDL solution contains EDTA and other small molecular weight contaminants which must be removed prior to the experiment by passing an appropriate volume of the native LDL solution through a Sephadex G25-M PD-10 size-exclusion column (Amersham Biosciences). The column was equilibrated with 50mL of sterile PBS (pre-filtered to 0.22µm) before the native LDL was applied to the column. Sterile PBS was also used for elution and approximately twelve 0.5mL fractions were collected into sterile tubes. The LDL fractions were then assayed for protein content as described

previously before fractions containing the highest concentrations of LDL (generally fractions 5-8) were pooled in serum-free Ham's F-10 medium containing 0.2% BSA to give a final LDL concentration of 100µg/mL (unless stated otherwise). Care was taken when handling the LDL solutions because fluid shear stress can cause LDL denaturation.

LDL oxidation experiments were conducted on confluent cell monolayers (not pre-starved to quiescence) in 12 well plates. 0.5mL of Ham's F-10 LDL solution was applied to each well, after washing each well with (LDL-free) Ham's F-10 to remove growth factors. The stimulation was conducted for 18hrs and cells were viewed under a light microscope at the end of the stimulation to check for cytotoxicity. Conditioned media were collected and centrifuged at 2200rpm for 10mins at +4°C to pellet detached cells. Supernatants were transferred to fresh tubes and EDTA and butylated hydroxytoluene (BHT) were added to give final concentrations of 2mM and 20µM respectively. EDTA and BHT prevent further LDL oxidation. Samples were frozen at -80°C for up to 2 weeks before analysis.

LDL oxidation was determined by measuring TBARs in the samples. Malondialdehyde (MDA) standards were prepared from an MDA stock of 500µM. The MDA stock was prepared by adding 4.17µL of MDA to 1mL of ethanol, before this solution was added to 49mL of d.H_20. A serial dilution was then performed to give a range of MDA concentrations from 0-100µM. These dilutions were prepared in the stimulating medium (i.e. Ham's F-10) for comparability. Essentially, this assay expresses TBARs in terms of MDA equivalents.

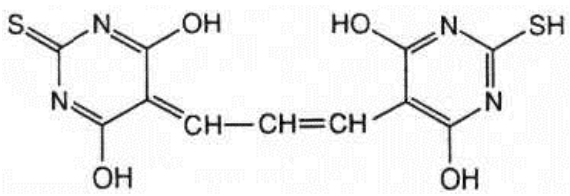

Figure 2.3 ***MDA***. MDA is the central three-carbon molecule and this is shown to have formed a 1:2 adduct with thiobarbituric acid in this diagram. This molecule can then be quantified using spectrophotometry.

200µL of TBARS reagent was added to 200µL of samples or MDA standards. The tubes were then heated at 100°C for 5mins prior to being centrifuged at 13000rpm for 6mins. Crucially, tubes were pierced approximately four times to prevent pressure build up and consequent sample loss. 150µL of sample/standard supernatant was then added in duplicate to a 96 well microplate. Absorbance was read immediately at 540nm in a microplate reader. Results were calculated by subtracting a blank (i.e. 0µM MDA) from readings before a standard curve was plotted ([MDA] vs. optical density). Mean MDA-equivalents in the samples were then calculated from the standard curve graph.

A positive control was incorporated into the experiments by using $CuSO_4$ as an oxidant – 0.5mL of the Ham's F-10 medium (containing 100µg/mL LDL) was placed into a well (containing no cells) and sterile $CuSO_4$ solution was added at a final working concentration of 60µM.

In-Cell ELISA

An in-cell ELISA colorimetric system was optimised *de novo* for specific antibodies, for the quantification of intracellular proteins in whole cells (Figure 2.4). This method is both cost- and time-efficient. The protocol was modelled on the 'In-Cell ELISA Colorimetric Detection Kit' (Thermoscientific). Cells were plated at a density of 1 X 10^4/well in a 96 well culture plate. At the end of the experiment, the culture medium was removed and 100µL of 4% formaldehyde was added to each well for fixation and the plate was incubated for 15mins in the fume hood. The formaldehyde solution was aspirated and the plate was washed twice with 100µL/well of TBS. The plate was then left at room temperature for 15mins with

100µL/well of permeabilization buffer. The plate was washed with 100µL/well of TBS before 100µL/well of quenching solution was added. The plate was left for 20mins before the plate was washed once with 100µL/well of TBS. 100µL/well of blocking buffer was then added and the plate was incubated for 30mins at room temperature. The blocking buffer was removed and 50µL/well of primary antibody was added before the plate was sealed and incubated overnight at +4°C.

The primary antibody was then removed and the plate was washed three times with 100µL/well of wash buffer. 100µL of biotinylated secondary antibodies were added at 0.002% (v/v) in blocking buffer. Incubation was carried out for 1hr at room temperature. The primary and secondary antibodies utilised in the in-cell ELISA system and optimal dilutions were as follows:

Antibody	***Manufacturer***	***Description***	***Recognition***	***Optimal Dilution***
BVR	Abcam	Rabbit polyclonal	Human	1/5000
HO-1	Abcam	Rabbit polyclonal	Human	1/10000
Akt	Cell Signalling	Rabbit polyclonal	Human	1/1000
p-Akt (S473)	Cell Signalling	Rabbit polyclonal	Human	1/500
eNOS	Cell Signalling	Rabbit polyclonal	Human	1/10000
p-eNOS (S1177)	Cell Signalling	Rabbit polyclonal	Human	1/10000
β-actin	Sigma	Mouse monoclonal	Human	1/40000
Biotinylated Anti-rabbit IgG (H+L)	Vector Labs	Goat polyclonal	Rabbit	1/500
Biotinylated Anti-mouse IgG (H+L)	Vector Labs	Horse polyclonal	Mouse	1/500

Table 2.5 ***Primary antibodies and relevant dilutions utilised for in-cell ELISAs***.

After incubation with secondary antibody, the plate was washed with wash buffer three times. 100µL/well of 0.005% (v/v) HRP conjugate was added before incubation for 30mins. The plate was washed three times with wash buffer and then 100µL/well of TMB substrate

was added. The plate was protected from light and incubated for 10mins before the reaction was stopped by adding 50µL of 1M H_2SO_4. The absorbance was measured with a microplate reader at 450nm with correction at 540nm. 'No primary antibody' controls were always incorporated into the experiment and these readings were subtracted from the results.

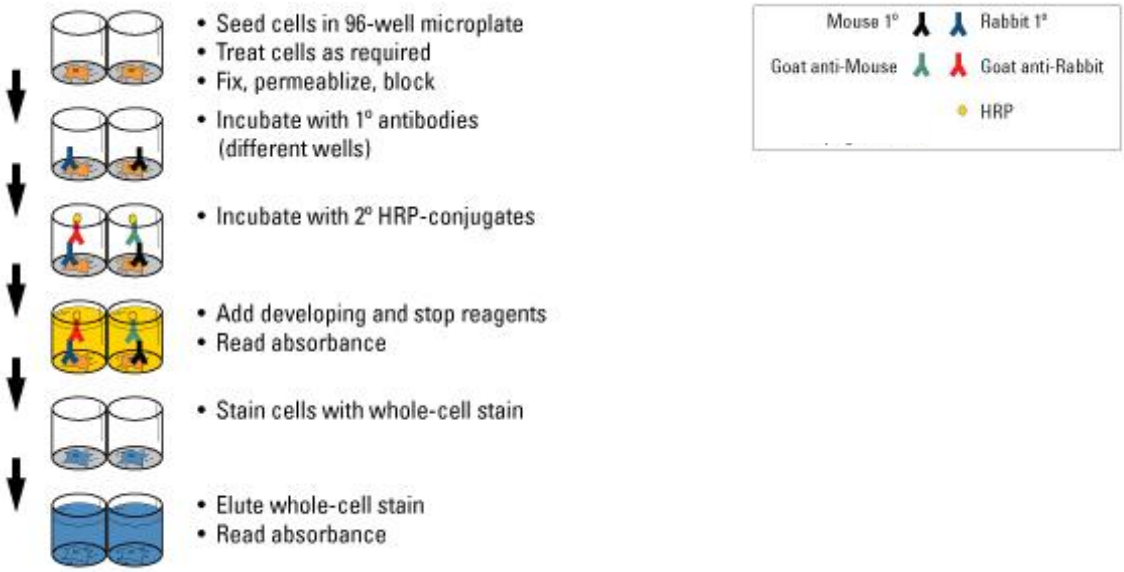

Figure 2.4 ***Schematic overview of the in-cell ELISA colorimetric detection system***. Adapted from Thermoscientific (www.piercenet.com).

In some experiments, whole-cell staining was then performed to control against varying inter- and intra-experiment cell densities. In this case, plate contents were discarded and wells were washed three times with 200µL/well of ultrapure water (filtered at 18.2 MOhm.cm). Water was removed and 50µl/well of Janus green whole-cell stain was added and incubated for 10mins at room temperature. The stain was discarded and the plate was washed 3-6 times with 200µL/well of ultrapure water until all excess stain had been

removed. 100µL/well of elution buffer (i.e. 0.5M HCL) was then added, the plate was incubated for 10mins and the absorbance was measured at 615nm.

Pharmacological Inhibitors

Several pharmacological inhibitors were utilised during the study. The table below shows working concentrations of all inhibitors used (Table 2.6). The inhibitors were pre-incubated with cells for one hour (unless stated otherwise) before addition of TNFα as required.

Inhibitor	***Manufacturer***	***Description***	***Working Concentration***
Tin protoporphyrin-IX (SnPP)	Alexis biochemicals	HO competitive inhibitor	20µM
LY294002	Calbiochem	PI3K competitive inhibitor	10µM
N^G-Nitro-L-arginine (L-NNA)	Alexis biochemicals	NOS competitive inhibitor	500µM
Ro-31-8220	Calbiochem	PKC competitive inhibitor	1µM
6-Amino-4-(4-phenoxyphenylethylamino) quinazoline	Calbiochem	NFκB Activation Inhibitor	10µM
Diphenyleneiodonium (DPI)	Sigma	Flavoenzyme competitive inhibitor	10µM
SP600125	Calbiochem	JNK competitive inhibitor	10µM
PD98059	Calbiochem	MEK competitive inhibitor	10µM

Table 2.6 ***Pharmacological inhibitors utilised during the study and relevant working concentrations***.

Statistical Analyses

Data were analysed and graphed using GraphPad Prism 4 software. Generally, a one-way ANOVA was performed followed by a *post-hoc* Newmann-Keuls multiple comparison test to evaluate statistical significance. A *t*-test was performed when comparing just two groups.

RESULTS

Validation

Optimal Adenoviral MOIs

Our study utilised biliverdin reductase adenovirus (AdBVR), as a strategy to elucidate the intracellular functions of the protein via its overexpression. Our preliminary experiments sought to ask two fundamental questions; ***1***, does AdBVR transduction correlate with protein expression and ***2***, what multiplicity of infection (MOI) should be utilised in experiments. In asking our two fundamental questions, we confirmed that the protein *is* overexpressed using this method and that our chosen MOI – the lowest possible MOI that confers mild, reproducible protein overexpression – is not cytotoxic to the cells. Similarly, a number of early studies involved the use of a HO-1 adenovirus (AdHO-1). The AdHO-1 is a well-established construct and its optimal MOI, for HUVECs, had been determined by previous studies conducted in our lab (Cudmore *et al*, 2007). However, we thought it prudent to revaluate its terms of usage.

Before using these adenoviruses in experiments, we sought to confirm protein expression. HUVECs were transduced at varying MOIs in cell culture experiments and cell-lysate was collected and analysed by Western blotting for BVR or HO-1. This experiment was repeated a number of times during the course of the study to ensure that different batches of adenovirus were consistent in their protein expression. The MOI administered to the cells correlated with protein expression; in such a way that MOI is proportional, *prima facie* at least, to its protein expression (Figure 3.1). Importantly, BVR protein was not detected in none-transduced HUVECs (Figure 3.1, *A*). We inferred that an MOI of 50 (i.e. 50 viral particles/cell) for both constructs would yield sufficient protein overexpression, would not

be cytotoxic (or cause changes in visible phenotype), and would be practical and reproducible.

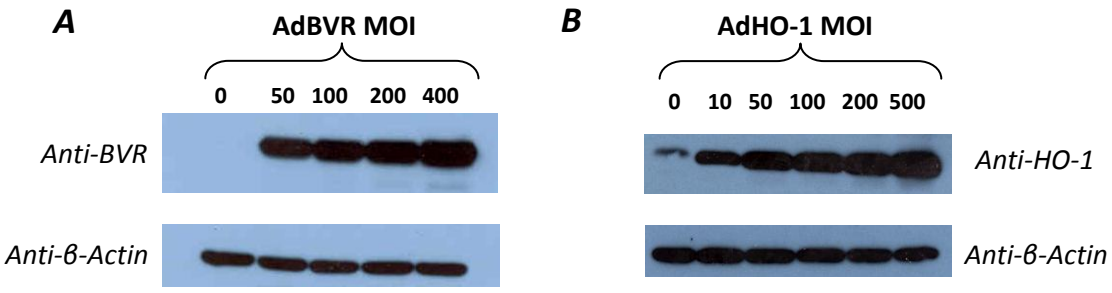

Figure 3.1 C***orrelation between MOI and protein expression in HUVECs***. Cells were plated into 6 well dishes in complete M199 medium and allowed to adhere overnight. The following afternoon, the HUVECs were transduced in complete M199 medium. After 24hrs, cell lysates were collected and analysed via Western blotting. Autoradiographic exposure time was no longer than 1min. (***A***), Of particular interest is the clear absence of BVR expression in non-infected cells. (***B***), In contrast, HO-1 is detectable in none-infected cells.

In addition to allowing us to determine optimal MOIs for these constructs, we also confirmed that BVR protein expression in HUVECs is undetectable. Importantly, we substantially increased autoradiographic exposure time and BVR remained undetectable (not shown).

In-Cell ELISA

An in-cell enzyme-linked immunosorbent assay (ELISA) was developed and optimal conditions were determined. Although cell density is controlled for when cells are plated – i.e. because approximately equal numbers of cells are dispensed into each well – we thought it prudent to use a Janus green whole-cell stain. Indeed, although the cells are fixed

using formaldehyde, cells may become detached during the numerous washing steps and hence, whole-cell staining can control for such phenomena. As expected, the greater the number of cells plated, the greater the optical density read-out (Figure 3.2). A Newman-Keuls multiple comparison test was performed in order to determine the sensitivity of this methodology that is, the degree to which the stain can significantly detect small differences in HUVEC density. We inferred that the Janus green whole-cell stain is only suitable for detecting differences of >2500 HUVECs.

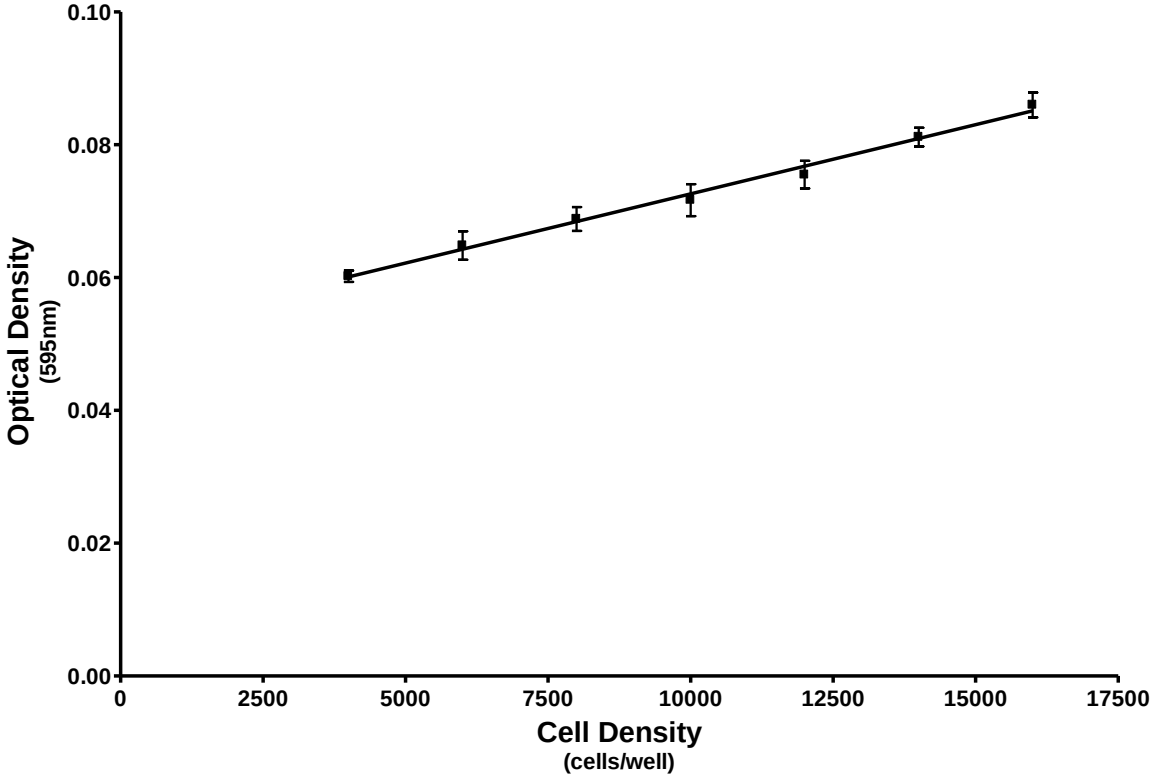

Figure 3.2 ***HUVEC density validation using Janus green whole-cell stain in an in-cell ELISA***. Early passage HUVECs were plated at the indicated densities and allowed to adhere overnight in M199 complete medium. Staining was performed using the Thermoscientific Janus green whole-cell stain. The results represent the mean of 6 wells ± SEM in one experiment. A one-way ANOVA was performed to assess the variance between the means vs. the variance within the samples. There is a statistically significant difference ($p<0.0001$), F ratio = 22.04, R^2 = 0.992. A Newman-Keuls multiple comparison test was used to assess the difference in the means.

Next, we sought to determine the sensitivity of our new assay, because our primary antibodies had been previously used only for Western blotting. We were therefore conscious that there would be differences in the ability of these antibodies to recognise reduced and denatured proteins, compared to proteins in native form. Hence, we first determined the optimal concentrations of the BVR and HO-1 primary antibodies (Figure 3.3). This is important in terms of maximising the sensitivity of the assay whilst ensuring that it is cost-effective. The optimal concentrations of other primary antibodies used in our analyses had been previously determined by another member of our lab.

The small increase in HO-1 protein due to BVR overexpression *is* detectable at a dilution factor of 1/10000 (Figure 3.3, *A*). Hence, because the antibody was primarily used to evaluate increases in HO-1 due to AdBVR, we were satisfied that 1/10000 would be optimal. We decided to use an anti-BVR concentration of 1/3000 (Figure 3.3, *B*). This is because this antibody was primarily going to be used to confirm BVR overexpression. We were unlikely to encounter a situation where BVR protein levels would be higher than those elicited by 50 MOI of AdBVR.

We proceeded to evaluate whether our chosen antibody concentrations could detect changes in protein expression associated with varying MOIs of Adβ-Gal, AdHO-1 and AdBVR (Figure 3.4). We expected that the Adβ-Gal construct would not affect HO-1 or BVR expression (Figure 3.4, *A*). However, there is a statistically significant difference between 50 and 100 MOI as indicated, in terms of HO-1 expression. This may be an artifact of the in-cell ELISA methodology. The sensitivity of the anti-HO-1 antibody is low because the signal saturates at 50 MOI AdHO-1 – i.e. there is not a statistically significant difference between 50 and 100 MOI, in terms of HO-1 protein expression (Figure 3.4 *B*). HO-1 overexpression

does not appear to alter BVR protein expression. The sensitivity of the anti-BVR antibody is also low – the signal appears to saturate at 50 MOI (Figure 3.4, *C*). In this regard, there is no statistically significant difference in BVR (or indeed HO-1) expression between 50 and 100 MOI.

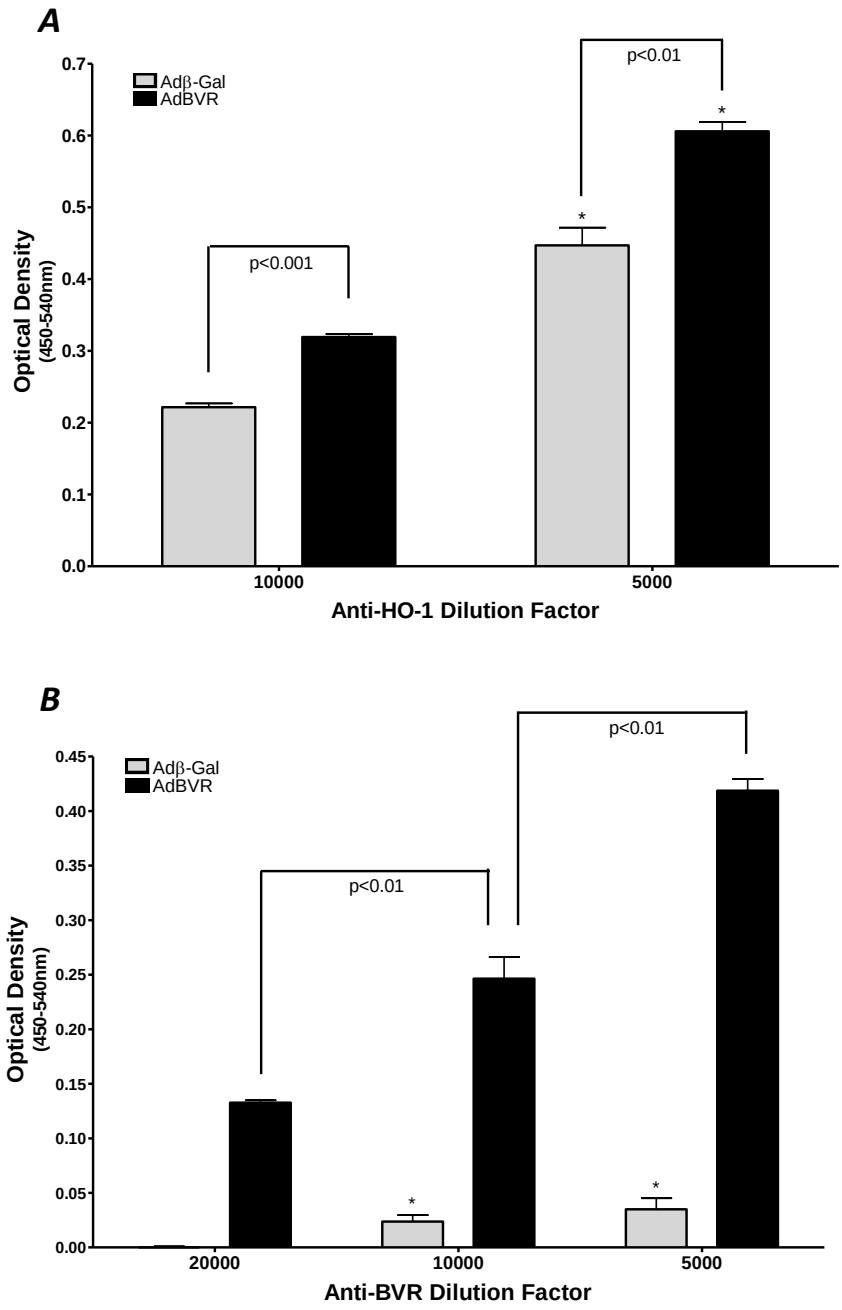

Figure 3.3 In-cell ELISA to determine the optimal concentrations of the anti-BVR and anti-HO-1 antibodies. (***A***), ***A dilution factor of 10000 is optimal for the anti-HO-1 antibody***. The optimal concentration of the anti-HO-1 antibody is 1/10000. (***B***), ***The anti-BVR antibody must be present at a dilution factor of less than 5000 for optimality***. We decided that a concentration of 1/3000 for the Anti-BVR antibody would be optimal. * p<0.001 vs. *lowest* concentration of antibody. These data represent the mean ± SEM of 1 experiment performed in triplicate.

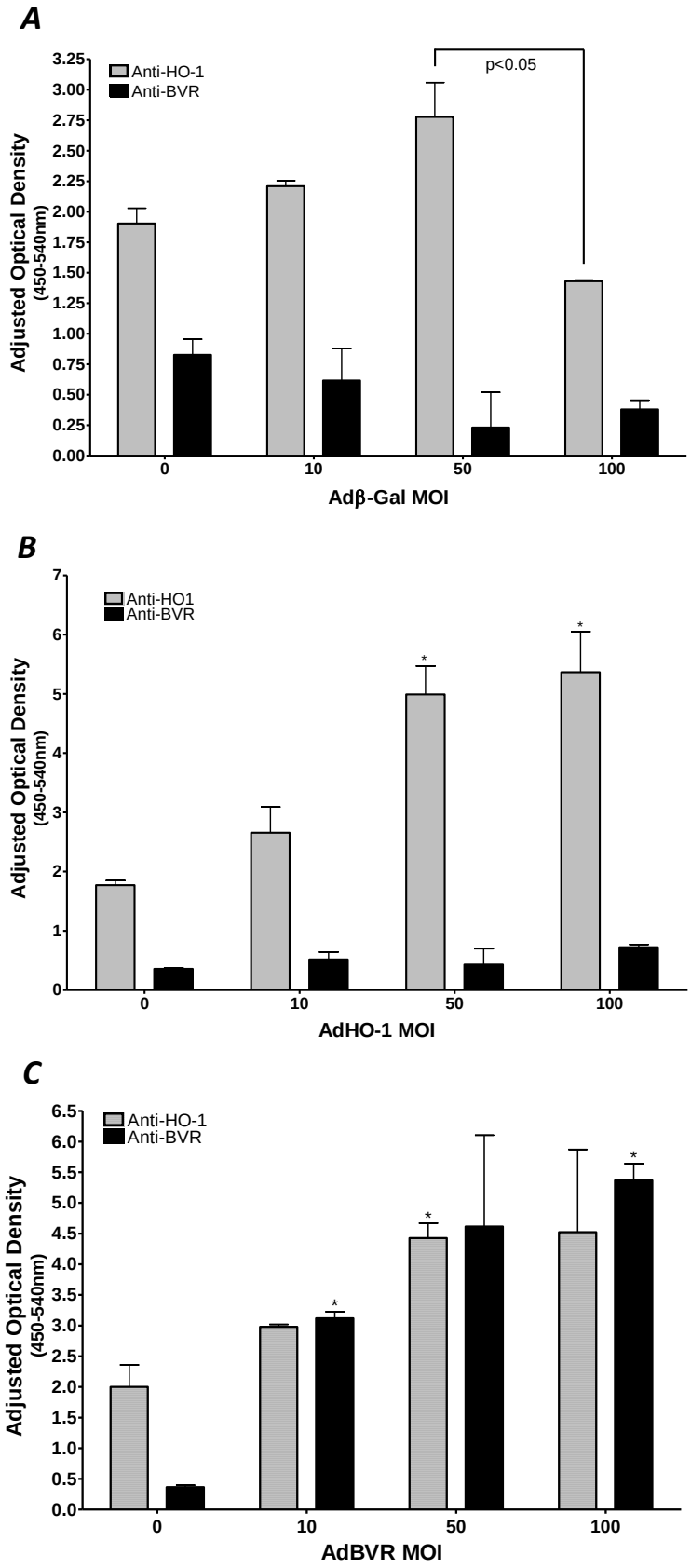

Figure 3.4 Protein Expression of HO-1 and BVR in Adβ-Gal- AdHO-1- and AdBVR-infected cells. HUVECs were plated in 96 well plates and allowed to adhere overnight in M199 complete medium. The following day, the cells were transduced at the indicated MOIs. Approximately 24hrs later, levels of HO-1 and BVR protein were assessed in an in-cell ELISA. (***A***), ***BVR and HO-1 protein expression in Adβ-Gal-infected HUVECs.*** In any case, an MOI of 50 was used for the Adβ-Gal construct. (***B***), ***BVR and HO-1 protein expression in AdHO-1-infected HUVECs.*** As expected, higher MOIs of the AdHO-1 construct led to higher protein expression of HO-1. (***C***), ***BVR and HO-1 protein expression in AdBVR-infected HUVECs.*** Interestingly however, we see that BVR overexpression appears to increase HO-1 protein levels. * p<0.05 vs. 0 MOI. OD was adjusted for cell-density. These data represent the mean ± SEM of 1 experiment performed in duplicate.

SnPP inhibits Bilirubin Generation

In order to distinguish between the effect of the reductase activity (i.e. bilirubin) and other non-canonical activities of BVR in an inflammatory context, we utilized SnPP to block bilirubin production. We sought to ensure that the inhibitor was having the desired effect on bilirubin production in both control and AdBVR-transduced cells. Prof Libor Vitek (Charles University, Czech Republic) kindly analyzed our samples for intracellular unconjugated bilirubin concentration using high-performance liquid chromatography (Figure 3.5).

We asked a number of questions; ***1***, does BVR overexpression alter intracellular bilirubin concentration, ***2***, what is the effect, if any, of TNFα on bilirubin production, and ***3***, what effect does SnPP have in these different contexts. We measured bilirubin at two different time-points; 1hr, and 6hrs (excluding 1hr pre-treatment). This is because our assays pre-incubated with SnPP for 1hr followed by addition of TNFα for a further 6hrs as appropriate.

After the 1hr pre-treatment phase, the levels of bilirubin are marginally lower in the SnPP group compared to the control (Figure 3.5, *A*). Interestingly, we also see that bilirubin levels are slightly lower in the BVR overexpressing cells as compared to the control (CMV) cells. After 6hrs however, we see that the BVR overexpressing cells have substantially reduced (>50%) bilirubin levels as compared to the control (Figure 3.5, *B*). In the presence of TNFα only, this is reversed – CMV and AdBVR treatment groups have similar bilirubin levels. However when HO-1 is inhibited in the presence of TNFα, AdBVR-infected cells have 50% lower bilirubin levels compared to CMV-transduced cells. In the presence of HO-1 inhibitor only, bilirubin levels are substantially reduced compared to control.

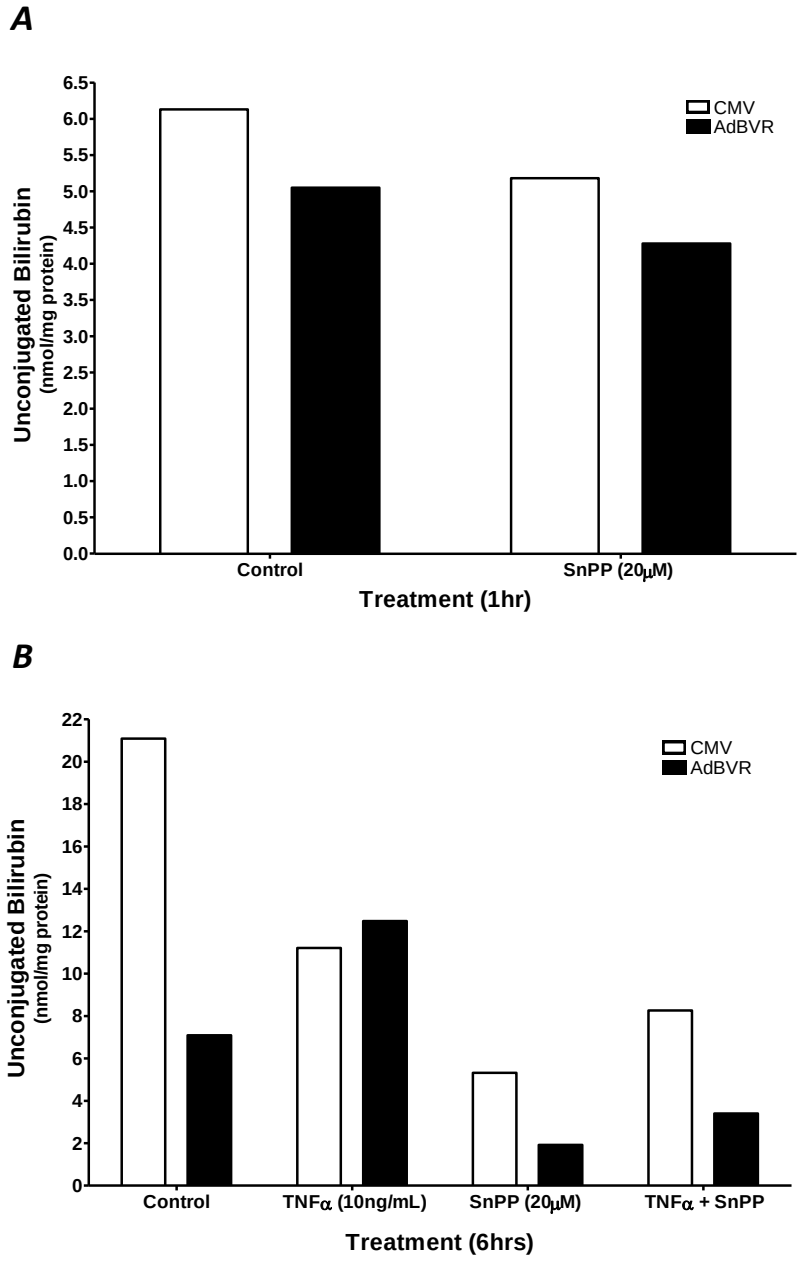

Figure 3.5 HPLC analysis of intracellular unconjugated bilirubin levels in CMV- and AdBVR-infected HUVECs. (***A***), ***BVR overexpression reduces intracellular bilirubin in HO-1-inhibited HUVECs***. At 1hr, bilirubin levels are lower with BVR overexpression, in both control and SnPP groups. (***B***), ***HO-1-inhibition reduces intracellular bilirubin in BVR overexpressing HUVECs***. After 6hrs, the unstimulated treatment groups (i.e. 'control' and 'SnPP') have lower bilirubin levels when BVR is being overexpressed. The experiment was performed in single wells and hence this precluded statistical analysis, although we are assured of the accuracy of the results. Samples were collected and then sent to Prof Libor Vitek for the HPLC analysis.

In summary, these data have allowed us to confirm that SnPP is effective in suppressing intracellular bilirubin levels, including in the presence of TNFα. Surprisingly and importantly however, overexpression of BVR is *not* associated with increases in intracellular bilirubin. In control cells, TNFα reduces bilirubin levels whilst the opposite effect is seen in AdBVR-infected cells.

Results

BVR Activates Akt

Akt is a downstream effector of PI3K and is involved in various cellular processes including for example, the promotion of cell survival. In endothelial cells, Akt is part of the PI3K/Akt/eNOS/NO pathway (Fulton *et al*, 1999). This pathway is important in atherosclerosis – its downregulation is implicated in diabetes-related vascular dysfunction and atherosclerosis (Du *et al*, 2001 and Okon *et al*, 2005). The importance of the PI3K/Akt/eNOS/NO pathway in atherosclerosis is further demonstrated by the finding that ellagic acid attenuates ox-LDL-induced cytotoxicity in HUVECs via this pathway (Ou *et al*, 2010).

BVR has been shown to activate Akt in H9c2 and HK-2 cells (Pachori *et al*, 2007 and Zeng *et al*, 2008). However, this has not been demonstrated in endothelial cells. We therefore evaluated this in HUVECs using an adenoviral-mediated overexpression strategy (Figure 4.1).

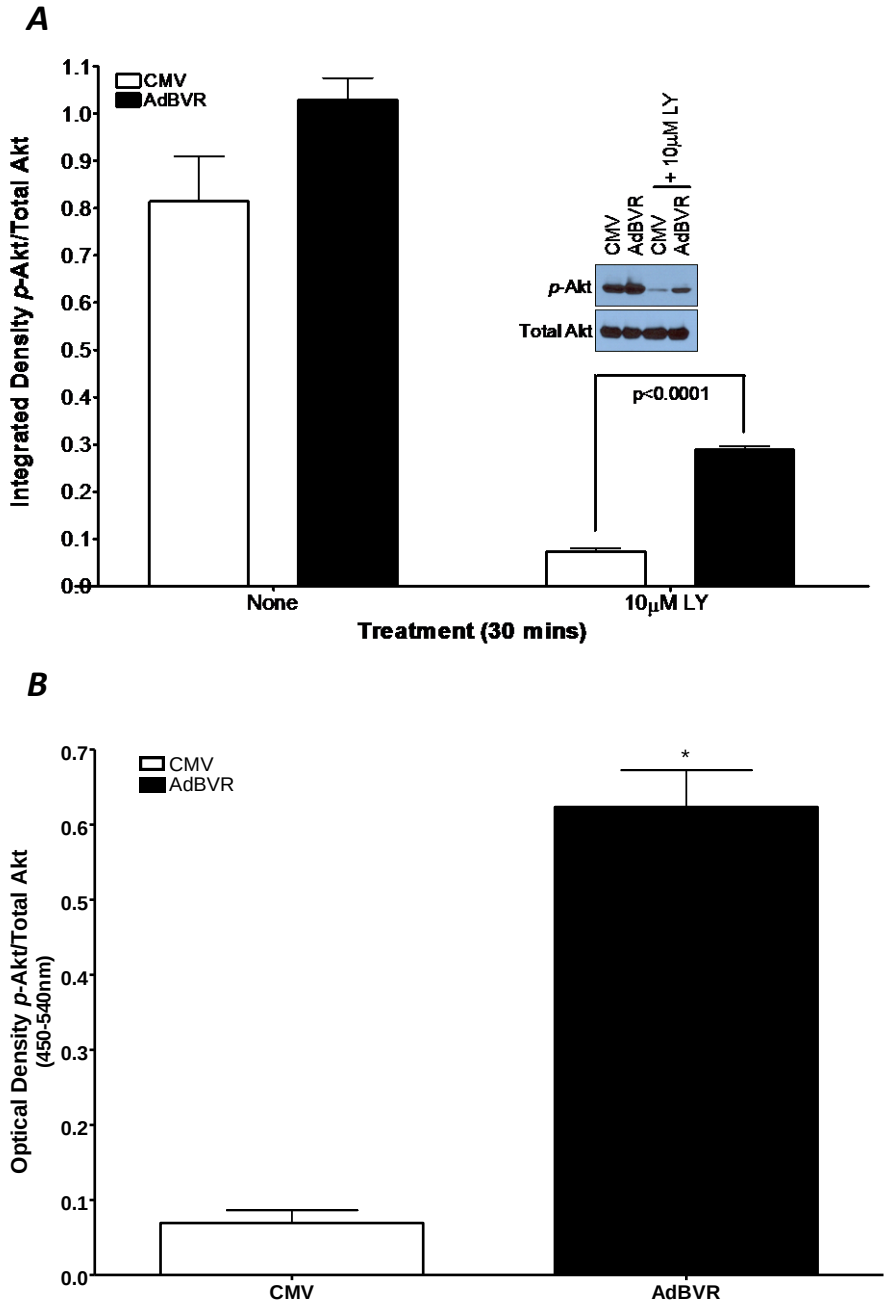

Figure 4.1 BVR activates Akt in HUVECs. The experiment was conducted 24hrs post-infection in HUVEC starvation medium. P-Akt levels were normalized to total Akt levels. (***A***), ***BVR induces Akt S473 phosphorylation in a Western blot densitometric analysis***. PI3K inhibition with an inhibitor (i.e. LY294002) precipitates BVR-induced Akt activation. (***B***), ***BVR overexpression induces Akt S473 phosphorylation in HUVECs in an in-cell ELISA***. BVR activates Akt under basal conditions. * $p < 0.0001$ vs. CMV control. These data represent the mean ± SEM of three independent experiments, conducted in at least duplicate wells.

Our Western blot analyses show that under conditions of PI3K inhibition, BVR overexpression substantially increases Akt activation. There is no difference in Akt activation between CMV and BVR infected cells under basal conditions (Figure 4.1, *A*). However in the in-cell ELISA (Figure 4.1, *B*), BVR overexpression does indeed increase Akt activation under basal conditions (i.e. in the absence of PI3K inhibition). These findings are novel, suggesting that BVR is a strong activator of Akt in endothelial cells.

BVR Activates eNOS & Induces NO Release

Encouraged by our early finding that BVR activates Akt in endothelial cells, we proceeded to evaluate the next downstream component in the BVR/PI3K/Akt/eNOS/NO pathway; eNOS (Figure 4.2).

Our highly novel findings clearly demonstrate that BVR induces eNOS activation via S1177 phosphorylation in HUVECs. As this effect was lost in the presence of the PI3K inhibitor, LY294002, BVR activates eNOS via PI3K. Published studies have not yet demonstrated BVR-induced eNOS activation in any cell type.

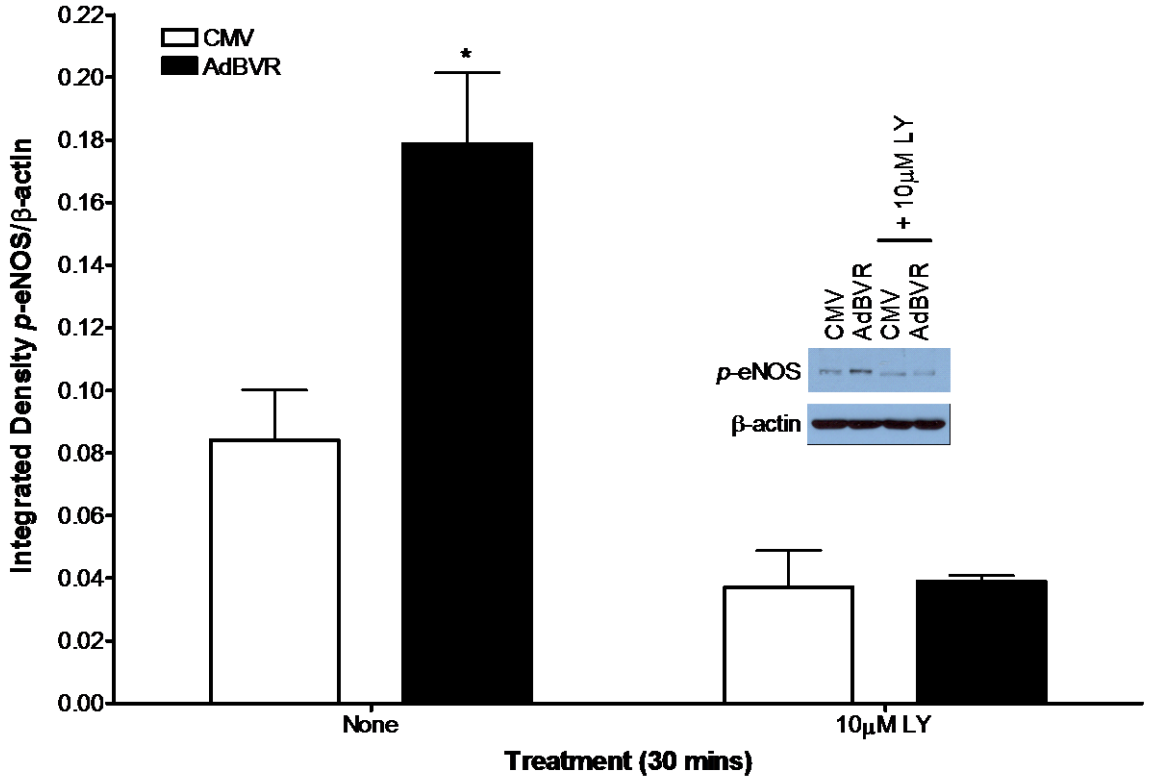

Figure 4.2 ***BVR induces eNOS S1177 phosphorylation in a PI3K-dependent manner in a Western blot densitometric analysis***. HUVECs were infected as indicated and the experiment was conducted 24hrs later in HUVEC starvation medium. Due to the unavailability of a total eNOS antibody, p-eNOS levels were normalized to β-actin. * $p < 0.05$ vs. CMV. These data represent the mean ± SEM of three independent experiments conducted in duplicate wells.

Given that eNOS S1177 phosphorylation is associated with activation of the enzyme and NO release, we sought to demonstrate that BVR overexpression induces NO release (Figure 4.3). Our preliminary experiments with HUVECs were inconclusive. Undeterred, we decided to conduct the same experiment in another related cell type, porcine aortic endothelial cells (PAECs). Given the aortic (vs. umbilical) origins of these cells, we reasoned that the 'eNOS/NO system' would be of greater similarity to endothelial cells from atherosclerotic-susceptible arteries.

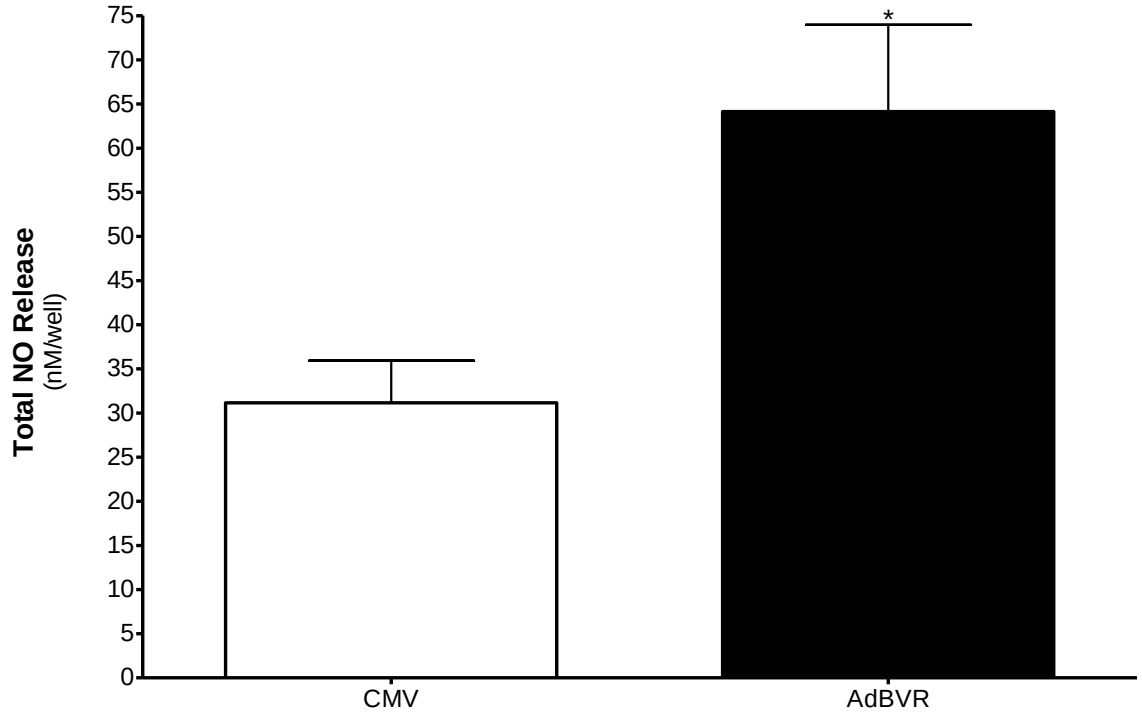

Figure 4.3 ***BVR doubles nitric oxide release in PAECs during a 30min stimulation***. Cell-free medium was incubated alongside the samples to correct for NO indigenous to the medium itself. PAECs were infected as indicated in RPMI 1640 (+ 0.2% BSA) medium. Approximately 24hrs later, fresh RPMI 1640 medium was gently added to each well, being careful to avoid shear stress. The cells were incubated for 30mins before medium was removed into tubes and frozen at -80°C until analysis. * $p < 0.01$ vs. CMV. These data represent the mean ± SEM of three independent experiments conducted in at least duplicate wells.

BVR overexpression induces NO release in PAECs (Figure 4.3). This is a highly novel finding, especially in regard to our previous finding that BVR activates eNOS via S1177 phosphorylation.

BVR Induces HO-1 Expression

Given the well-documented protective actions of HO-1 in atherosclerosis (Hoekstra *et al*, 2004), we sought to determine whether BVR can induce HO-1 expression in endothelial cells (Figure 4.4). We utilised both Western blotting and the in-cell ELISA.

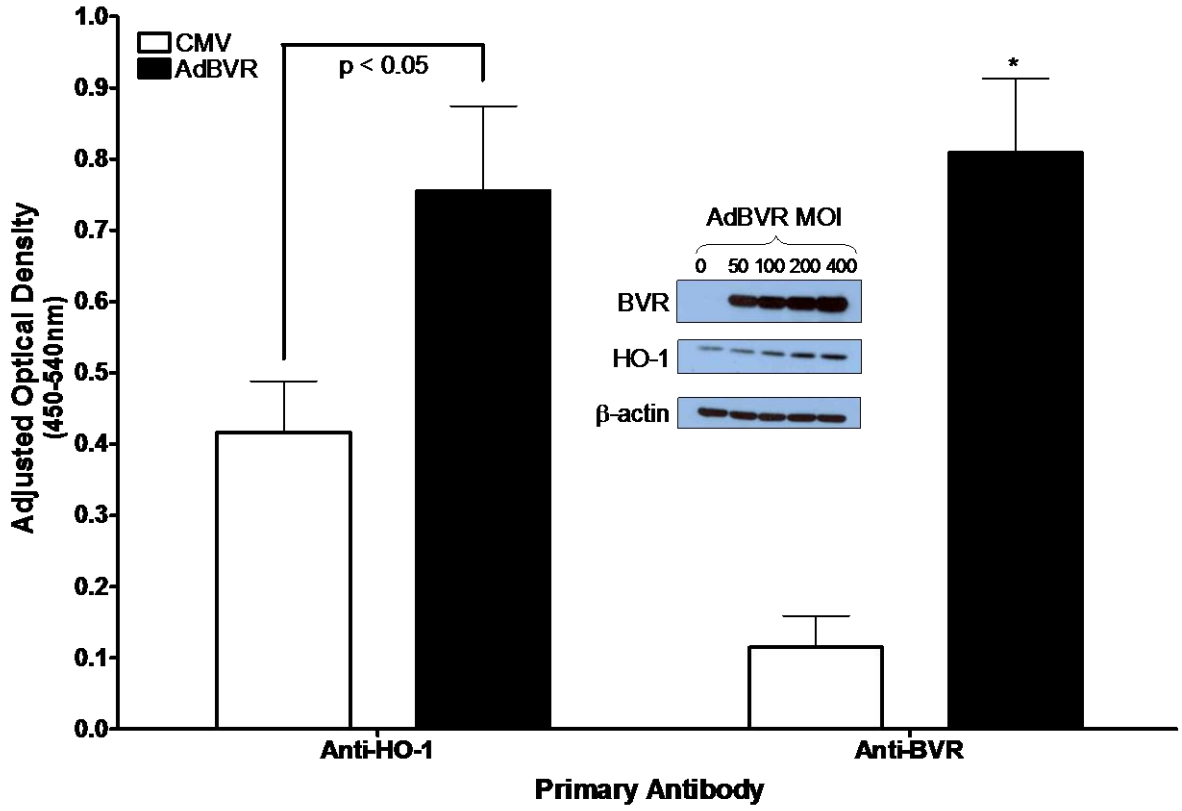

Figure 4.4 ***BVR induces HO-1 protein expression in HUVECs in an in-cell ELISA***. HUVECs were infected in HUVEC complete medium as indicated and the experiment commenced 24hrs later. *Inset*, a representative Western blot demonstrating that the magnitude of BVR overexpression (i.e. AdBVR MOI) correlates with HO-1 protein expression. * $p < 0.01$ vs. CMV with same antibody. These data represent the mean ± SEM of three independent experiments conducted in at least duplicate wells.

BVR overexpression almost doubles HO-1 protein expression in HUVECs. Furthermore, the extent to which HO-1 expression is increased appears to correlate linearly with the degree to which BVR is overexpressed (Figure 4.4, *inset*). Published studies have not yet demonstrated this effect in endothelial cells.

LDL Oxidation

We examined whether BVR overexpression would have any effect on LDL oxidation independent of its bilirubin-producing capacity (Figure 4.5), especially given that the enzyme appears to induce NO release (Figure 4.3). We also examined the effect of HO-1 overexpression on LDL oxidation; this enzyme is upregulated in response to ox-LDL (Siow *et al*, 199) and so may participate in a defence mechanism against LDL oxidation. However CO, a product of HO-1, is known to increase ROS generation (Piantadosi, 2008) and Fe^{2+}, also a HO-1 product, is a potent oxidising agent capable of oxidising LDL (Kapiotis *et al*, 2005).

The results show that BVR overexpression in HUVECs does not significantly reduce LDL oxidation. It is curious that HO-1 overexpression has a significantly opposite effect on LDL oxidation than BVR, not least because BVR induces HO-1 expression. Possible explanations for this are discussed later.

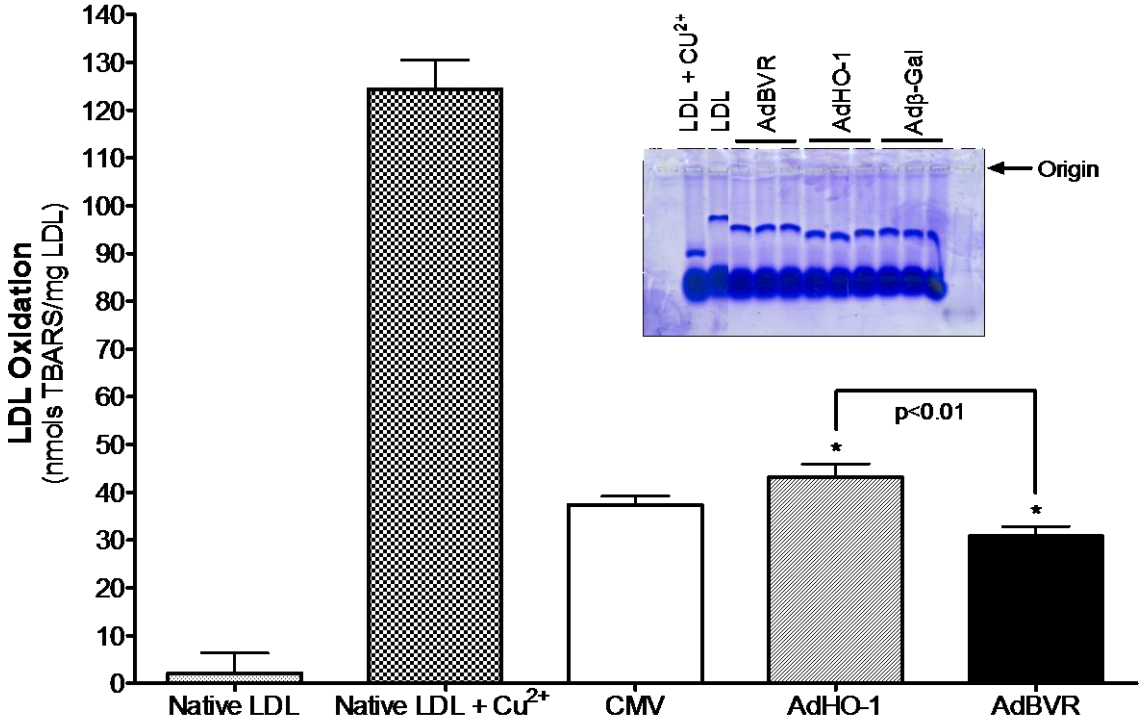

Figure 4.5 ***BVR and HO-1 have opposite effects on LDL oxidation in a TBARs Assay***. A TBARs assay and *inset*, a representative electrophoretic mobility shift assay (EMSA). HUVECs were infected as stated. 100µg/mL of LDL was exogenously applied to fresh cell culture medium (Ham's F-10) and the stimulation was conducted for 18hrs before the medium was assayed for TBARs. Cell-free controls were incorporated – i.e. a negative control consisting of native LDL and, a positive control consisting of native LDL in the presence of 60µM $CuSO_4$, which acts as an oxidizing agent. Whilst HO-1 overexpression appears to increase LDL oxidation (none-significantly), BVR appears to reduce LDL oxidation (none-significantly). This is also demonstrated in the EMSA – the *upper bands* represent LDL. Oxidised LDL migrates quicker across the gel compared to none-oxidised LDL. These data represent the mean ± SEM of 3 independent experiments conducted in at least duplicate. * $p > 0.05$ compared to CMV control.

BVR Attenuates TNFα-Induced MCP-1 Release

Our experiments aimed to address the apparent discrepancy between the canonical (i.e. bilirubin production) and non-canonical activities of BVR in terms of inflammation. We evaluated the effect of adenoviral-mediated BVR overexpression on TNFα-induced NFκB pro-inflammatory gene expression (i.e. MCP-1 and adhesion molecules) in HUVECs. We were therefore keen to evaluate the relative contributions of the reductase and kinase activities of BVR to these end-points.

We initially assessed the effect of BVR overexpression in HUVECs on TNFα-induced MCP-1 release (Figure 4.6). As discussed previously, MCP-1 is a chemokine involved in leukocyte recruitment and has an important role in atherosclerosis.

Our findings are highly novel, demonstrating that BVR inhibits TNFα-induced MCP-1 release in endothelial cells. When HO-1 is inhibited, BVR overexpression continues to suppress MCP-1 release, suggesting that its mechanism of action is independent of bilirubin production. In control (CMV) cells, we see that HO-1 inhibition reduces MCP-1 release. The NFκB activation inhibitor (NAI) reduces TNFα-induced MCP-1 release by a small extent in control cells. BVR overexpression continues to inhibit MCP-1 release by the same amount in the presence of the NAI, as compared to without the NAI.

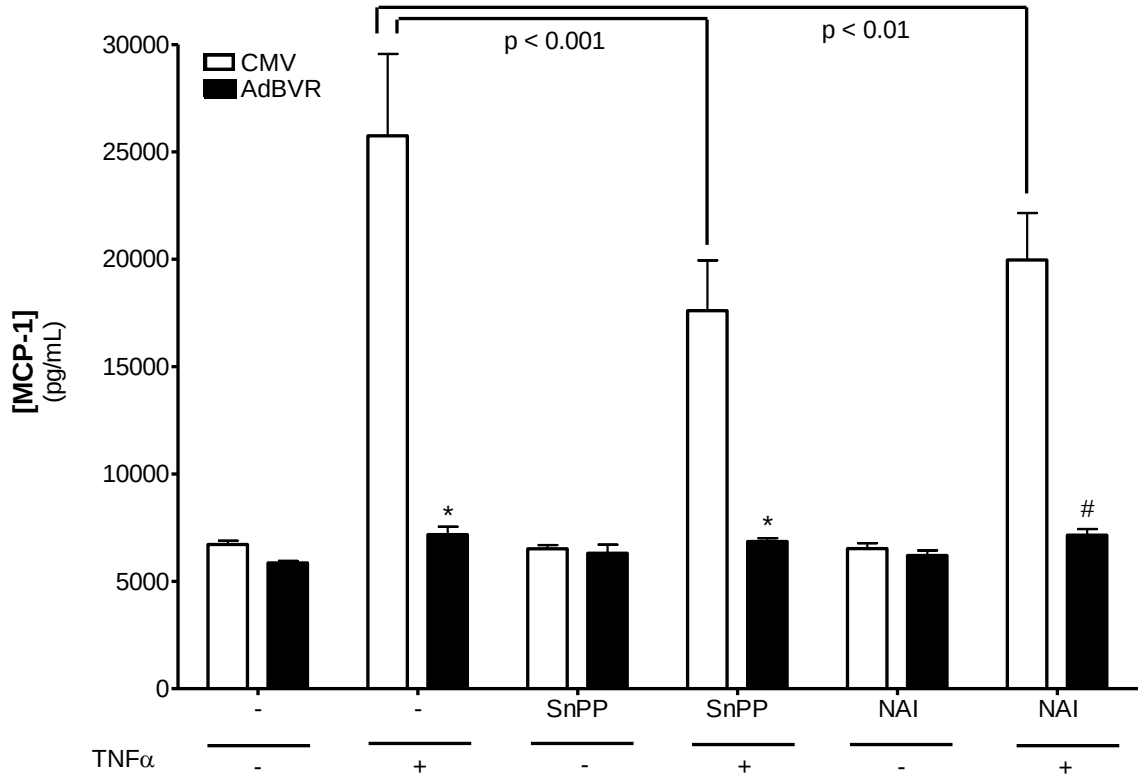

Figure 4.6 ***BVR attenuates TNFα-induced MCP-1 release in a bilirubin-independent manner in HUVECs***. An ELISA for MCP-1 released into cell culture medium by HUVECs, following a 24hr stimulation with TNFα. HUVECs were treated with two different inhibitors as indicated – 20μM SnPP (a HO-1 inhibitor) and 10μM NAI (NFκB activation inhibitor). TNFα was applied at a concentration of 10ng/mL, in HUVEC complete medium. The NAI was incorporated in order to assess the component of TNFα-induced MCP-1 release that is NFκB-dependent. * $p < 0.001$ vs. CMV with same treatment . # $p < 0.01$ vs. CMV with same treatment. These data represent the mean ± SEM of three independent experiments conducted in duplicate wells.

BVR Attenuates TNFα-Induced Leukocyte-Endothelium Adherence

Given that adhesion molecule expression is broadly regulated by the same intracellular signaling pathways as MCP-1 expression in endothelial cells (i.e. NFκB, JNK and p38), we proceeded to evaluate the effect of BVR overexpression on adhesion molecule expression.

As previously discussed, endothelial expression of adhesion molecules is an early marker of endothelial dysfunction. Adhesion molecules function to recruit leukocytes from the circulation across the endothelium. We decided to assay for ICAM-1, VCAM-1 and E-selectin expression using flow cytometry. These adhesion molecules have subtlety distinct functions in the process of leukocyte recruitment. Hence assaying for all three of these adhesion molecules is advantageous because, collectively, the adhesion molecule expression data is likely to correlate with functional (i.e. monocyte binding) data.

In tandem with our flow cytometric analyses, we decided to conduct monocyte adhesion assays to ascertain the functional relevance of changes in cell-surface expression levels of ICAM-1, VCAM-1 and E-selectin. The monocyte adhesion assay consisted of applying monocytes to a HUVEC monolayer in the presence/absence of TNFα (and any inhibitors) and then subsequently counting the adhered monocytes. Although initial, preliminary experiments were conducted with THP-1 cells (supplementary results); we decided to use freshly isolated monocytes from human blood for our subsequent experiments.

Mazzone *et al* showed that bilirubin, in its unconjugated form, could attenuate TNFα-induced adhesion molecule expression in HUVECs (Mazzone *et al*, 2009). Furthermore, the authors demonstrated that bilirubin exerts its effects on adhesion molecule expression via inhibition of TNFα-induced NFκB activation. Although we had previously established that BVR overexpression is not associated with bilirubin generation (Figure 3.5), indeed at the same time-point and with the same stimulation (TNFα) as in our adhesion molecule experiments, we were keen to rule out any bilirubin-dependent effect. This was especially important because we had only analysed a single set of samples for bilirubin. In addition to this, we have previously shown that BVR overexpression induces HO-1 protein expression

(Figure 4.4). For this reason, it was important to distinguish between BVR-mediated effects and HO-1-mediated effects. Our early experiments therefore incorporated SnPP, a HO-1 inhibitor (Figures 4.7 and 4.8).

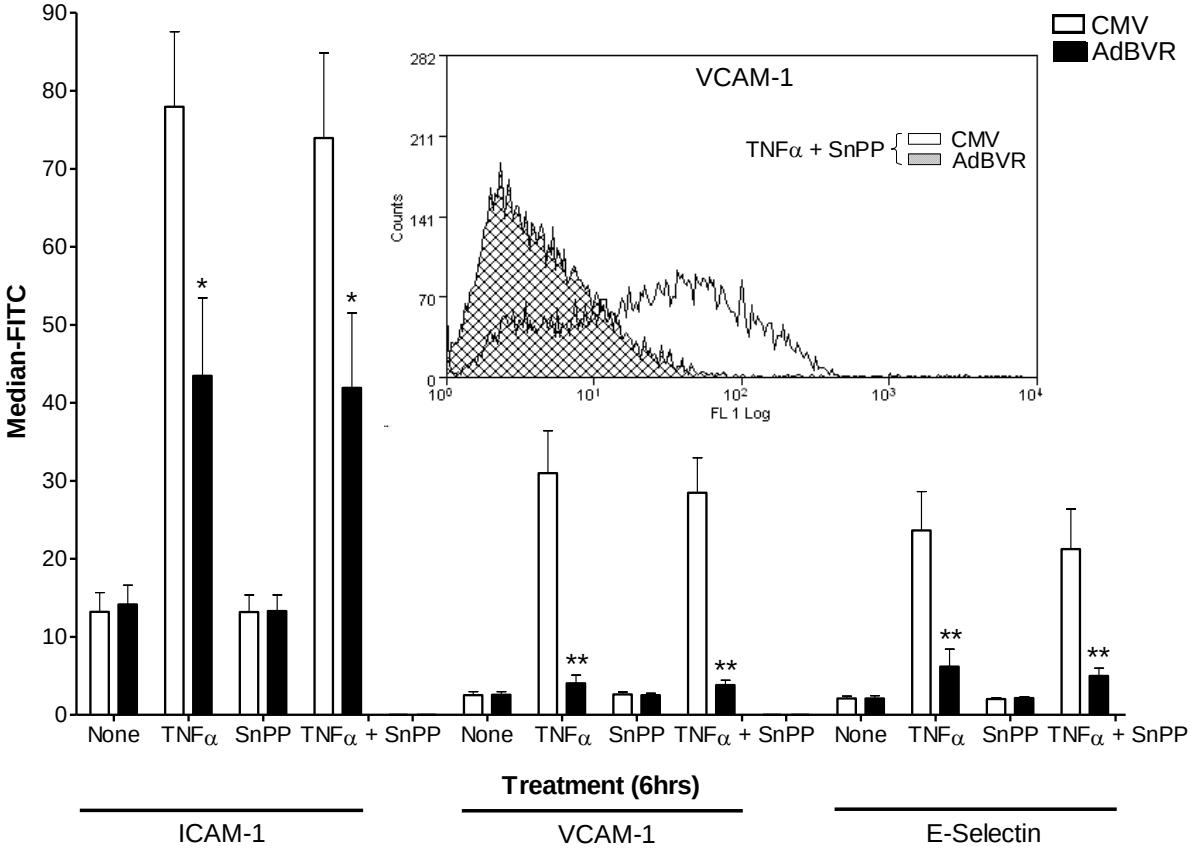

Figure 4.7 ***BVR attenuates TNFα-induced cell-surface adhesion molecule expression in a bilirubin-independent manner***. Flow cytometric analyses utilizing anti-ICAM-1, anti-VCAM-1 and anti-E-Selectin antibodies and, *inset*, a representative overlay. HUVECs were grown in 12-well plates and infected as indicated. Approximately 24hrs later, HUVECs were pre-treated as indicated with SnPP for 1hr in HUVEC starvation medium. Then, TNFα was applied for 6hrs in fresh medium as indicated. The cells were then harvested and subsequently analyzed. The results clearly demonstrate that inhibition of bilirubin production (via inhibition of HO-1 with SnPP) does not affect the ability of BVR to attenuate TNFα-induced ICAM-1, VCAM-1 and E-Selectin expression. * $p < 0.01$ vs. CMV with identical treatment. ** $p < 0.001$ vs. CMV with identical treatment. These results represent the mean ± SEM of three independent experiments performed in duplicate.

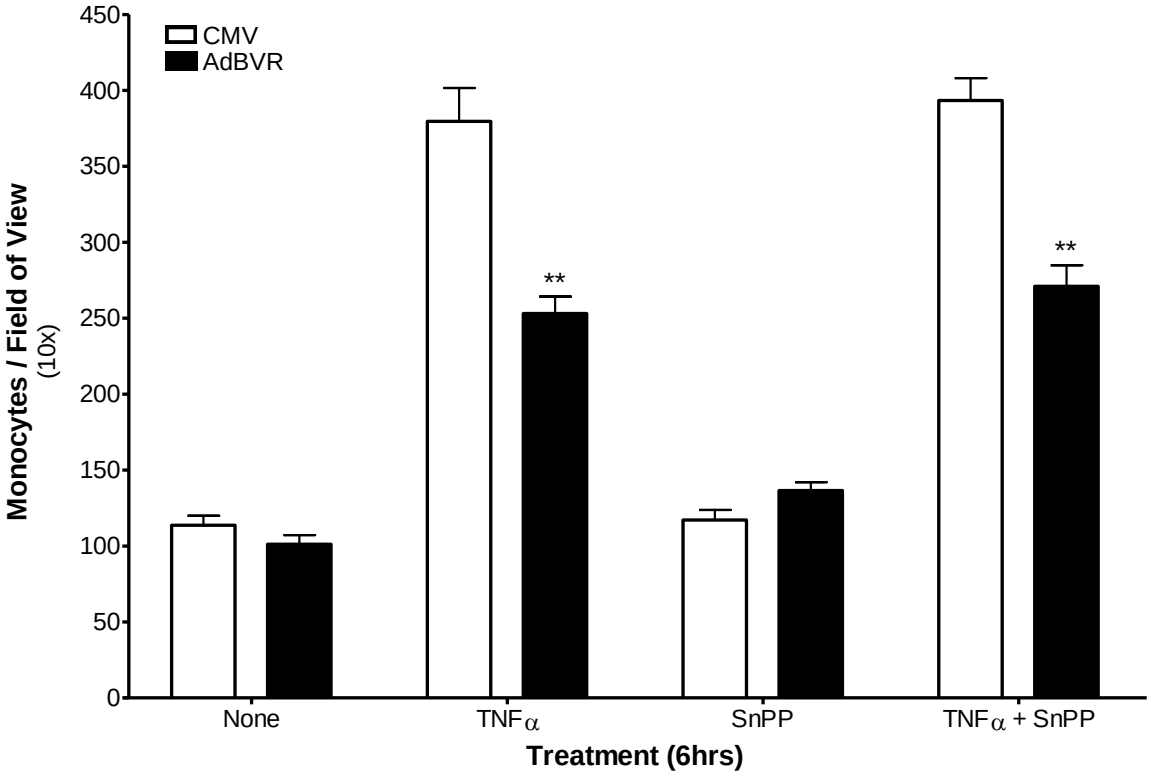

Figure 4.8 ***BVR attenuates TNFα-induced monocyte adhesion in a bilirubin-independent manner***. HUVECs were grown in 24 well plates and infected. Approximately 24hrs later, the cells were pre-treated for 1hr with 20μM SnPP in HUVEC starvation medium as indicated. 10ng/mL TNFα was then applied as indicated for 6hrs. Then, freshly isolated human monocytes were applied to each well (2 X 10^5/well) and allowed to adhere for 1hr. The HUVEC monolayer was then washed, fixed and analysed. Inhibition of bilirubin production (with SnPP) has no effect on the ability of BVR to attenuate TNFα-induced monocyte adhesion. ** $p < 0.001$ vs. CMV with identical treatment. These results represent the mean ± SEM of four independent experiments performed in singlet or duplicate. A minimum of five randomly chosen fields of view per well were analysed.

Taken together, our highly novel flow cytometric and monocyte adhesion data show that BVR is capable of attenuating TNFα-induced monocyte-endothelium adherence independently of its bilirubin generating capacity. This is in agreement with our earlier demonstration that BVR attenuates TNFα-induced MCP-1 secretion independently of bilirubin production.

As Figure 4.7 shows, BVR attenuates TNFα-induced leukocyte-endothelium interactions via, at least in part, downregulation of cell-surface ICAM-1, VCAM-1 and E-selectin. Our flow cytometric experiments also suggest that BVR is most potent in attenuating TNFα-induced VCAM-1 cell-surface expression and least potent in regard to ICAM-1. This flow cytometric data is in concordance with our monocyte adhesion data (Figure 4.8) in that addition of SnPP does not affect BVR-mediated attenuation of TNFα-induced leukocyte-endothelium interaction.

Next, we sought to determine the relevance of BVR's ability to activate Akt via PI3K, to its capacity to inhibit TNFα-induced leukocyte-endothelium adherence. Our rationale stemmed from the fact that the PI3K/Akt axis has multilateral effects in atherosclerosis. On the one hand, Akt activates eNOS and this correlates with NO production in endothelial cells (Figure 3.8). NO inhibits adhesion molecule expression (Park *et al*, 2005). NO also inhibits NFκB activation (Zeiher *et al*, 1995). A recent *in vivo* study showed that upregulation of the PI3K/Akt pathway, with angiotensin-converting enzyme II, has anti-atherosclerotic effects (Zhang *et al*, 2010). On the other hand, there is strong evidence that Akt activates IKK, and consequently NFκB, in various cell types (Meng *et al*, 2002; Narayan *et al*, 2006). Akt activation has also been shown to be increased in atherosclerotic lesions in humans and animal models (Miyauchi *et al*, 2004).

In order to investigate the role of the BVR/PI3K/Akt pathway in monocyte-endothelium adherence we utilized LY294002 (LY), a PI3K inhibitor (Figures 4.9 and 4.10).

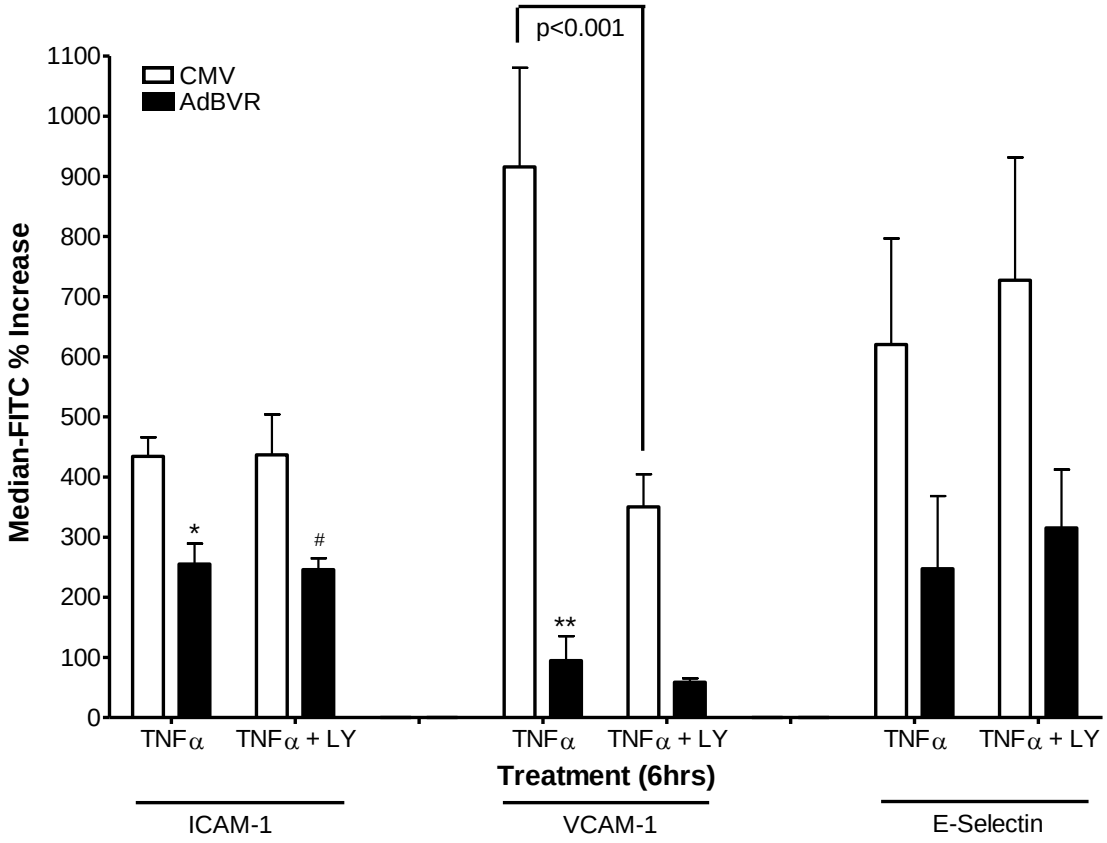

Figure 4.9 ***BVR attenuates TNFα-induced cell-surface adhesion molecule expression in a PI3K-independent manner***. Flow cytometric analyses utilizing anti-ICAM-1, anti-VCAM-1 and anti-E-Selectin antibodies. HUVECs were grown in 12 well plates and infected as indicated. Approximately 24hrs later, HUVECs were pre-treated as indicated with 10μM LY294002 (LY) for 1hr in HUVEC starvation medium. Then, TNFα was applied for 6hrs in fresh medium as indicated. The cells were then harvested and subsequently analyzed. The results indicate that BVR attenuates TNFα-induced adhesion molecule expression in a manner that is independent of the BVR/PI3K/Akt/eNOS/NO pathway. # $p < 0.05$ vs. CMV with identical treatment. * $p < 0.01$ vs. CMV with identical treatment. ** $p < 0.001$ vs. CMV with identical treatment. These results represent the mean ± SEM of three independent experiments performed in duplicate.

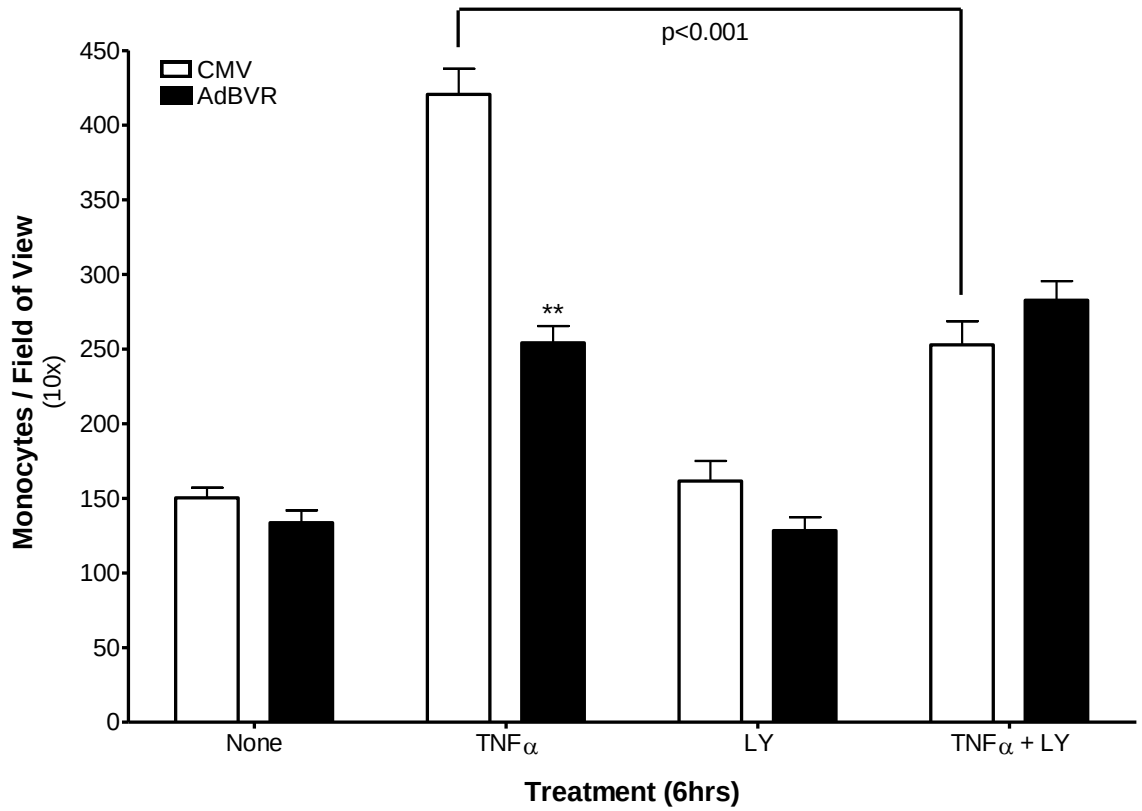

Figure 4.10 ***BVR attenuates TNFα-induced monocyte adhesion in a PI3K-independent manner***. HUVECs were grown in 24 well plates and infected. Approximately 24hrs later, the cells were pre-treated for 1hr with 10μM LY294002 (LY) in HUVEC starvation medium as indicated. 10ng/mL TNFα was then applied as indicated for 6hrs. Then, freshly isolated human monocytes were applied to each well (2 X 10^5/well) and allowed to adhere for 1hr. The HUVEC monolayer was then washed, fixed and analysed. Inhibition of PI3K in has no effect on the ability of BVR to attenuate TNFα-induced monocyte adhesion. ** $p < 0.001$ vs. CMV with identical treatment. These results represent the mean ± SEM of three independent experiments performed in singlet or duplicate. A minimum of five randomly chosen fields of view per well were analyzed.

Taken together, these results suggest that the BVR/PI3K/Akt pathway has no functional net effect in terms of monocyte adhesion. As shown in Figure 4.10, inhibition of PI3K reduces TNFα-induced monocyte adhesion in CMV control cells. This indicates that the net effect of the PI3K/Akt pathway is to *increase* TNFα-induced adhesion. Importantly, Figure 4.9 would

suggest that this is specifically due to upregulation of VCAM-1, as opposed to the other adhesion molecules.

Next, we sought to examine the role of NFκB activation in relation to BVR's ability to attenuate adhesion molecule expression (Figure 4.11). Previous analyses of TNFα-induced MCP-1 release (Figure 4.6) showed that whilst our NFκB activation inhibitor (NAI) significantly reduced MCP-1 release, it did not do so substantially. A number of considerations are relevant; ***1***, that both BVR's kinase and reductase activities are increased by TNFα (Lerner-Marmarosh *et al*, 2007), ***2***, that bilirubin may attenuate adhesion molecule expression via inhibition of NFκB activation (Mazzone *et al*, 2007), ***3***, that BVR may increase NFκB activation via PKCζ (Lerner-Marmarosh *et al*, 2007), ***4***, that BVR may activate IKK via Akt (i.e. BVR/PI3K/Akt/IKK/NFκB pathway) and ***5***, that BVR may attenuate NFκB activation via the BVR/PI3K/Akt/eNOS/NO pathway.

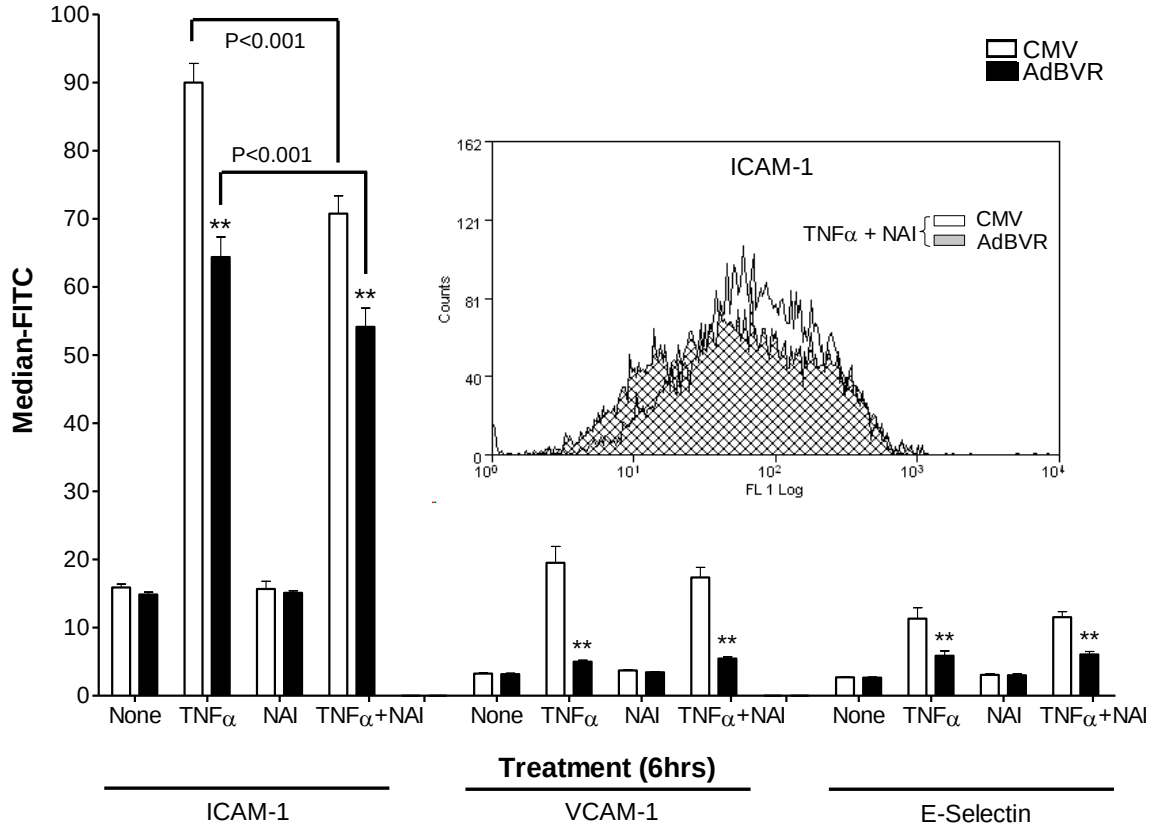

Figure 4.11 ***BVR additively attenuates TNFα-induced cell-surface ICAM-1 expression in the presence of NFκB activation inhibitor***. Flow cytometric analyses utilizing anti-ICAM-1, anti-VCAM-1 and anti-E-Selectin antibodies and, *inset*, a representative overlay. HUVECs were grown in 12-well plates and infected as indicated. Approximately 24hrs later, HUVECs were pre-treated as indicated with 10μM NFκB Activation Inhibitor (NAI) for 1hr in HUVEC starvation medium. Then, TNFα was applied for 6hrs in fresh medium as indicated. The cells were then harvested and subsequently analyzed. The results indicate that BVR and NAI, additively, attenuate ICAM-1 expression. ** $p < 0.001$ vs. CMV with identical treatment. These results represent the mean ± SEM of three independent experiments performed in duplicate.

Our results are in broad agreement with Mazzone *et al*, 2009. In their study, Mazzone *et al* showed that exogenously applied bilirubin, together with an NFκB activation inhibitor, could suppress adhesion molecule expression – i.e. E-Selectin – in endothelial cells to a greater extent than the inhibitor alone (i.e. without bilirubin). Our results show that this additive

effect is only evident in regard to ICAM-1. Importantly however, our experiments utilize a method of BVR overexpression (as opposed to application of bilirubin) and we have previously shown that AdBVR is not associated with increased intracellular bilirubin. The NAI attenuates only TNFα-induced ICAM-1 expression by a small degree, and does not seem to attenuate TNFα-induced VCAM-1 or E-Selectin expression.

Next, we sought to probe the role of the BVR/PKCζ axis in leukocyte-endothelium adherence (Figures 4.12 and 4.13). A number of considerations are important; ***1***, that both BVR's kinase and reductase activities are increased by TNFα (Lerner-Marmarosh *et al*, 2007), ***2***, that both biliverdin and bilirubin are potent inhibitors of PKCs (biliverdin to a greater extent than bilirubin), ***3***, that BVR increases PKCζ activity and *vice versa* (Lerner-Marmarosh *et al*, 2007), and ***4***, that PKCζ has been shown to be essential in TNFα-induced NFκB activation (Nigro *et al*, 2010). Our experiments utilized RO-31-8220 (RO31), a pan-PKC inhibitor with well-established efficacy in the inhibition of the atypical PKCζ.

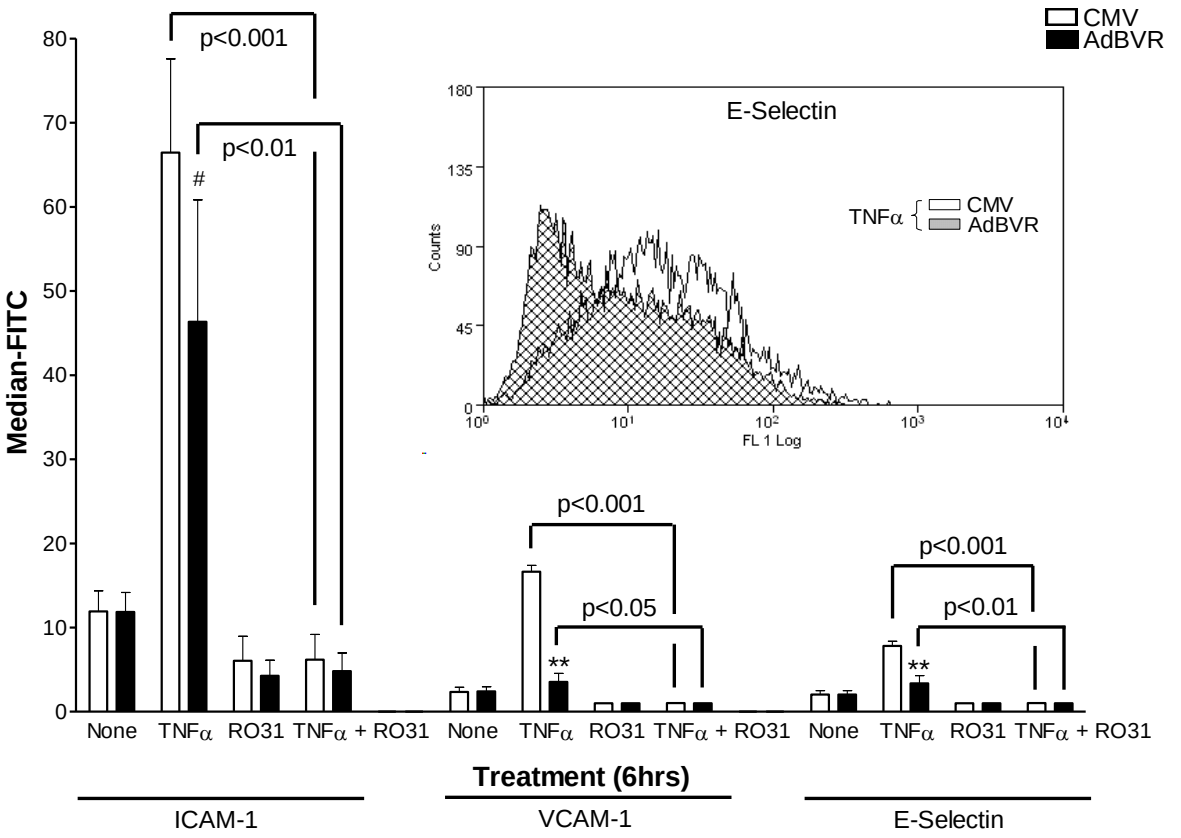

Figure 4.12 ***BVR has a limited role in inducing adhesion molecule expression via the TNFα/BVR/PKCζ/NFκB pathway***. Flow cytometric analyses utilizing anti-ICAM-1, anti-VCAM-1 and anti-E-Selectin antibodies and, *inset*, a representative overlay. HUVECs were grown in 12-well plates and infected as indicated. Approximately 24hrs later, HUVECs were pre-treated as indicated with *5μM* RO-31-8220 (RO31) for 1hr in HUVEC starvation medium. Then, TNFα was applied for 6hrs in fresh medium as indicated. The cells were then harvested and subsequently analyzed. The results indicate that BVR does not increase adhesion molecule expression via PKCζ. # $p < 0.05$. ** $p < 0.001$ vs. CMV with identical treatment. These results represent the mean ± SEM of three independent experiments performed in duplicate.

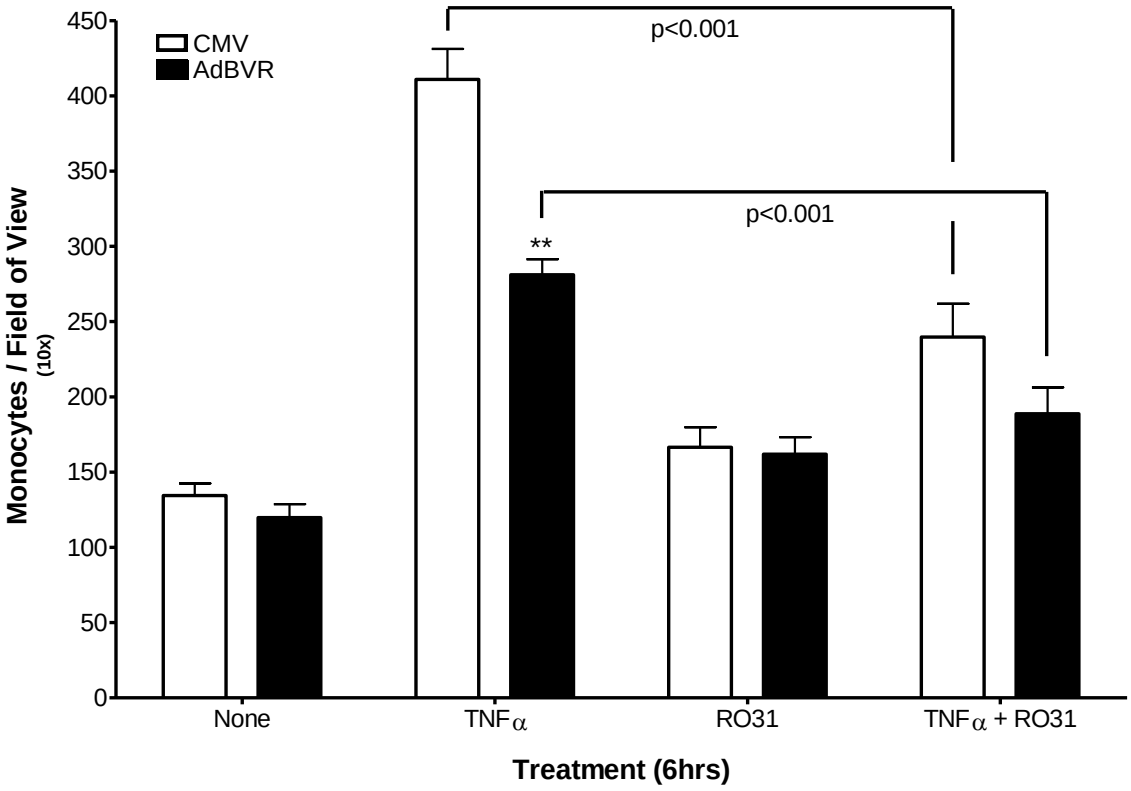

Figure 4.13 ***BVR does not increase monocyte adhesion via the TNFα/BVR/PKCζ/NFκB pathway***. HUVECs were grown in 24 well plates and infected. Approximately 24hrs later, the cells were pre-treated for 1hr with *1μM* RO-31-8220 (RO31) in HUVEC starvation medium as indicated. 10ng/mL TNFα was then applied as indicated for 6hrs. Then, freshly isolated human monocytes were applied to each well (2 X 10^5/well) and allowed to adhere for 1hr. The HUVEC monolayer was then washed, fixed and analysed. BVR overexpression attenuates TNFα-induced monocyte adhesion. Inhibition of PKCζ reduces this adhesion to the same level in both CMV control and AdBVR cells. ** $p < 0.001$ vs. CMV with identical treatment. These results represent the mean ± SEM of three independent experiments performed in singlet or duplicate. A minimum of five randomly chosen fields of view per well were analyzed.

The results indicate that, in our system, BVR does not increase adhesion molecule expression via PKCζ. It is important to note that whilst RO-31-8220 was used at a concentration of 5μM in flow cytometric analyses, only 1μM was used in the monocyte adhesion assays. This is because 5μM of the compound reduced TNFα-induced adhesion molecule expression to below basal, unstimulated levels and indeed to a level that was

almost undetectable – particularly with regard to VCAM-1 and E-Selectin. We therefore decided to utilize 1μM of the compound in the monocyte adhesion analyses because we felt that 5μM would inhibit PKCζ to such an extent that it would be impossible for BVR to activate NFκB via this pathway.

It was our aim to test the notion that BVR may activate PKCζ and therefore increase adhesion molecule expression via this pathway. In a sense, we utilized the same strategy as for our earlier demonstration that BVR activates Akt via PI3K (cf. Figure 4.1, *A*) – an inhibitor was used in both experiments to try and precipitate a particular downstream event (i.e. Akt activation or adhesion molecule expression/monocyte adherence). Our results demonstrate that, even under conditions of PKCζ inhibition, BVR does not increase monocyte adherence via this pathway. This is an important finding that gives credence to our view that modulation of BVR activity *in vivo* may have therapeutic potential in chronic inflammatory diseases such as atherosclerosis.

Supplementary Results

Leukocyte-Endothelium Adherence

The flavin enzymes include the nitric oxide synthases, such as eNOS, and also the NADPH oxidases (NOXs). The different flavin enzymes have different effects on adhesion molecule expression; eNOS produces NO which has the effect of reducing monocyte adhesion whilst NOXs generate superoxide which increases adhesion molecule expression via NFκB in response to TNFα stimulation (Ray and Shah, 2005). BVR produces bilirubin which inhibits NOX, and also activates eNOS. Biliverdin also inhibits NOX (Fujii *et al*, 2010). As previously demonstrated BVR activates eNOS and increases NO generation (Figure 4.3). In an early experiment utilising THP-1 cells, we were keen to study the interplay between BVR, flavin enzymes and monocyte adhesion, with a view to establish the mechanism by which the reductase inhibits monocyte adhesion (Figure 5.1). We utilised diphenyliodonium (DPI), an established inhibitor of flavin enzymes.

BVR overexpression is associated with atennuation of TNFα-induced monocyte (i.e. THP-1) adherence. When flavin enzymes are inhibited in the presence of TNFα, BVR overexpression continues to suppress monocyte adherence, indeed to a greater extent than with TNFα alone. In control (CMV) cells, we also see that TNFα-induced monocyte adherence is lower with flavin enzyme inhibition.

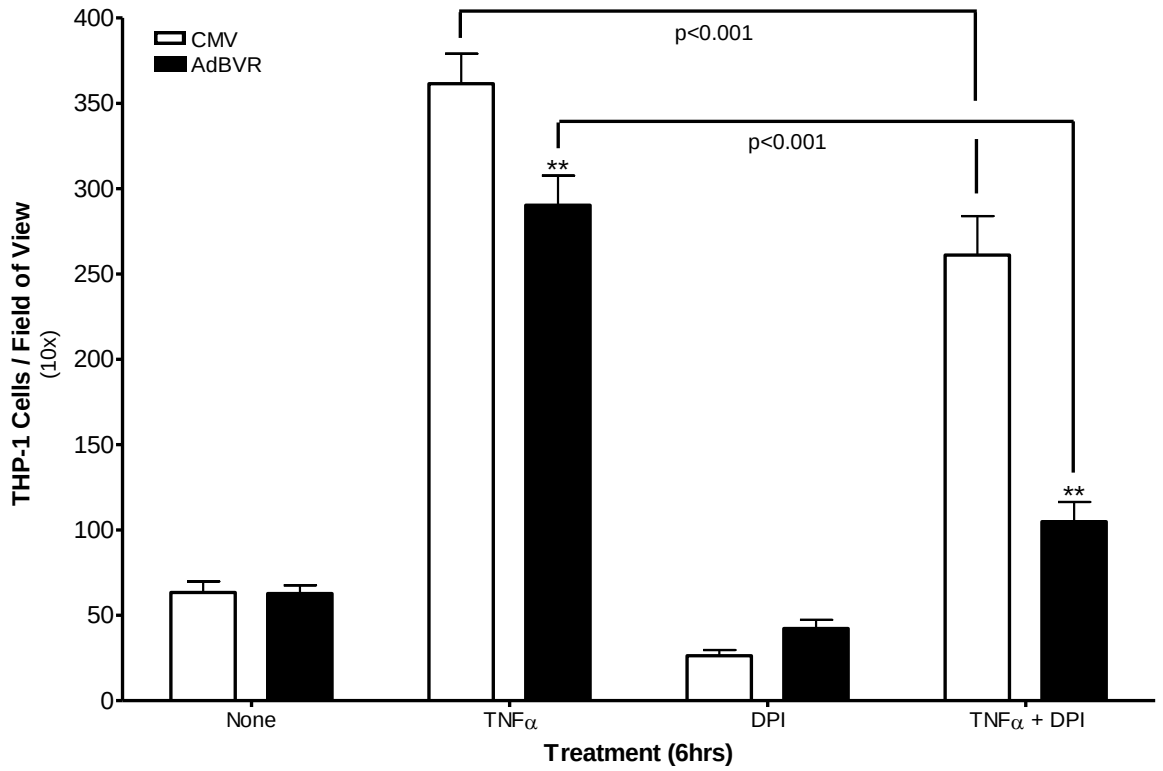

Figure 5.1 ***BVR inhibits TNFα-induced monocyte adhesion independently of flavin enzymes***. HUVECs were grown in 24 well plates and infected. Approximately 24hrs later, the cells were pre-treated for 1hr with 10μM diphenyliodonium (DPI) in HUVEC starvation medium as indicated. 10ng/mL TNFα was then applied as indicated for 6hrs. Then, THP-1 cells were applied to each well (2 X 10^5/well) and allowed to adhere for 1hr. The HUVEC monolayer was then washed, fixed and analysed. ** $p < 0.001$ vs. CMV with identical treatment. These results represent the mean ± SEM of one experiment performed in triplicate. Six randomly chosen fields of view per well were analyzed.

Another one of our early experiments incorporated SnPP (a HO-1 inhibitor) in order to determine whether BVR reduces monocyte (THP-1) adhesion via bilirubin generation (Figure 5.2).

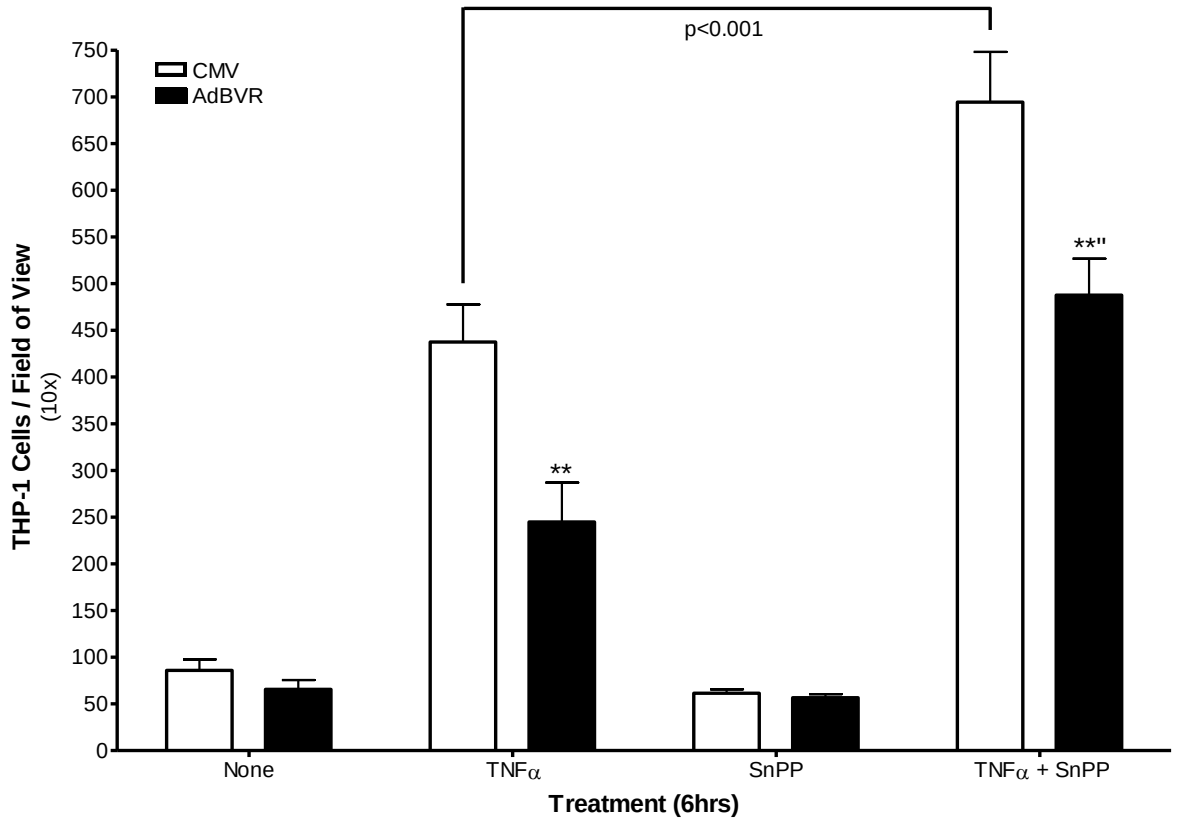

Figure 5.2 ***BVR inhibits TNFα-induced monocyte adhesion independently of bilirubin production***. HUVECs were grown in 24 well plates and infected. Approximately 24hrs later, the cells were pre-treated for 1hr with 20μM SnPP in HUVEC starvation medium as indicated. 10ng/mL TNFα was then applied as indicated for 6hrs. Then, THP-1 cells were applied to each well (2 X 10^5/well) and allowed to adhere for 1hr. The HUVEC monolayer was then washed, fixed and analysed. ** $p < 0.001$ vs. CMV with identical treatment. " $p < 0.001$ vs. AdBVR with TNFα treatment only. These results represent the mean ± SEM of one experiment performed in triplicate. Five randomly chosen fields of view per well were analyzed.

The results indicate that BVR is able to inhibit TNFα-induced monocyte adhesion independently of bilirubin generation. Interestingly, TNFα-induced monocyte adhesion appeared to increase in the presence of HO-1 inhibitor.

Before repeating this experiment with monocytes, we conducted a number of experiments with peripheral blood mononuclear cells (PBMCs). This allowed us to perfect and optimize our isolation method (Figure 5.3). PBMCs include lymphocytes in addition to monocytes.

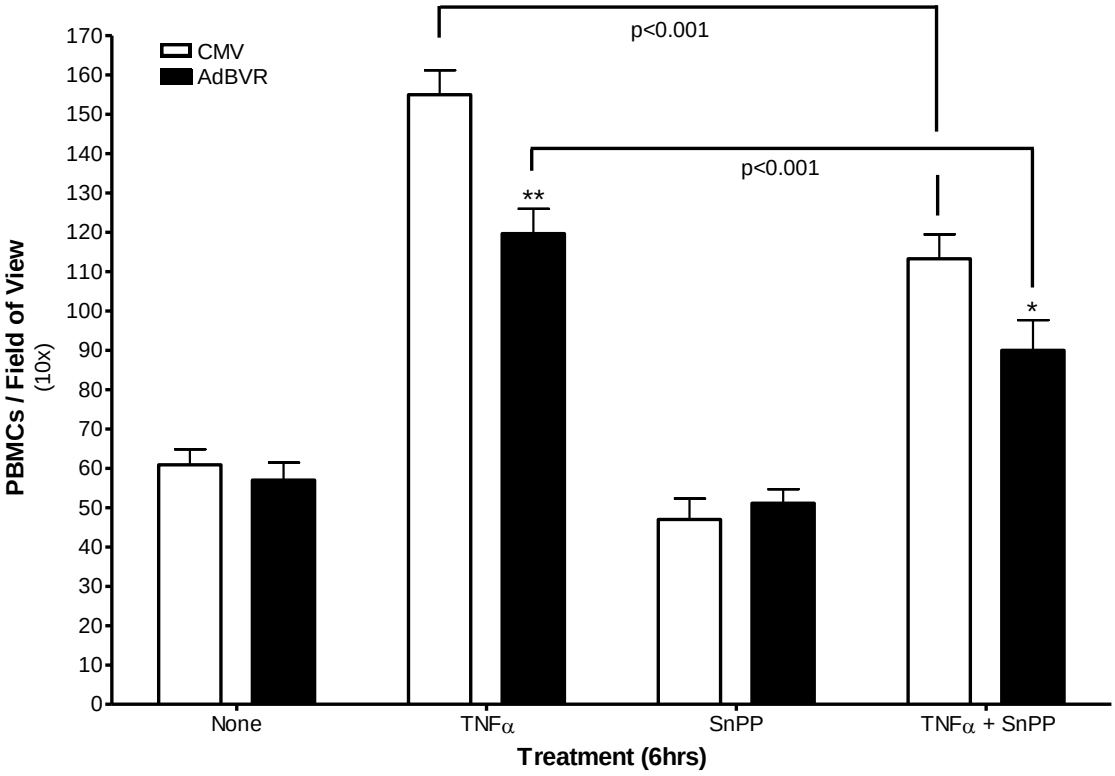

Figure 5.3 ***BVR inhibits TNFα-induced monocyte adhesion independently of bilirubin production***. HUVECs were grown in 24 well plates and infected. Approximately 24hrs later, the cells were pre-treated for 1hr with 20μM SnPP in HUVEC starvation medium as indicated. 10ng/mL TNFα was then applied as indicated for 6hrs. Then, THP-1 cells were applied to each well (2 X 10^5/well) and allowed to adhere for 1hr. The HUVEC monolayer was then washed, fixed and analysed. ** $p < 0.001$ vs. CMV with identical treatment.* $p < 0.01$ vs. CMV with same identical treatment. These results represent the mean ± SEM of three independent experiments performed in duplicate. Five randomly chosen fields of view per well were analyzed.

As with THP-1 cells, the results are consistent with a bilirubin-independent mechanism of action. Interestingly, HO-1 inhibition consistently resulted in lower TNFα-induced monocyte adhesion (Figure 5.3). This is in contrast to our earlier experiment with THP-1 cells which demonstrated the opposite effect (Figure 5.2).

THP-1 cells were also utilized in our initial experiments examining the role of the PI3K/Akt axis in the ability of BVR to attenuate TNFα-induced monocyte adhesion (Figure 5.4). The PI3K/Akt axis has an important role in atherosclerosis. For example, PI3K/Akt activation correlates with eNOS activation and NO production, and NO inhibits adhesion molecule expression.

The results of this experiment suggest that BVR does not inhibit TNFα-induced monocyte adhesion via the PI3K/Akt/eNOS/NO pathway. Moreover, we actually see a decrease in TNFα-induced monocyte adhesion with PI3K inhibition in both control and BVR overexpressing cells, suggesting that the PI3K/Akt axis is pro-inflammatory in our system.

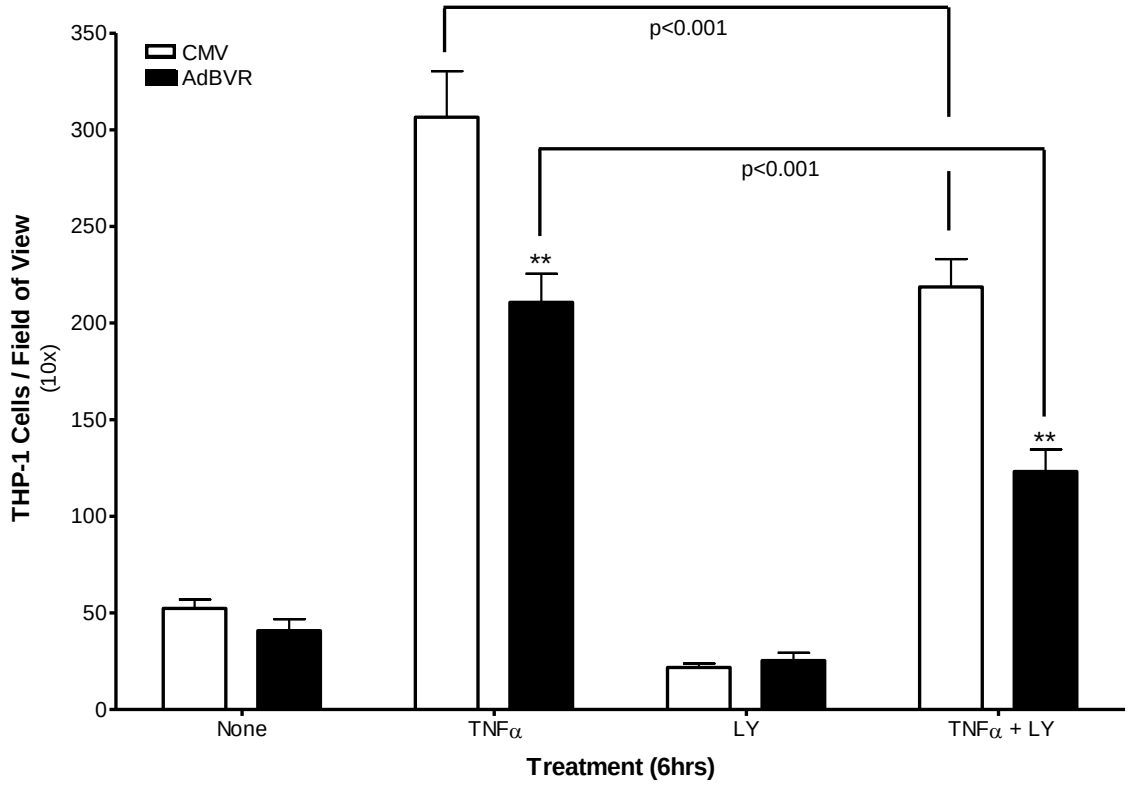

Figure 5.4 ***BVR inhibits TNFα-induced monocyte adhesion independently of PI3K/Akt activation***. HUVECs were grown in 24 well plates and infected. Approximately 24hrs later, the cells were pre-treated for 1hr with 10μM LY294002 (LY) in HUVEC starvation medium as indicated. 10ng/mL TNFα was then applied as indicated for 6hrs. Then, THP-1 cells were applied to each well (2 X 10^5/well) and allowed to adhere for 1hr. The HUVEC monolayer was then washed, fixed and analysed. ** $p < 0.001$ vs. CMV with identical treatment. These results represent the mean ± SEM of one experiment performed in triplicate. Five randomly chosen fields of view per well were analyzed.

We evaluated the roles of the p38 MAPK, ERK1/2 and JNK pathways in the modulation of TNFα-induced monocyte adhesion by BVR (Figures 5.5, 5.6 and 5.7 respectively). Indeed, previous studies have suggested that BVR activates these pathways (Kapitulnik and Maines, 2009). A number of studies have shown that these three pathways, in addition to the NFκB pathway, are activated by TNFα and are involved in adhesion molecule expression (Paul *et al*, 1997 and Schmitz *et al*, 2001). We therefore wondered whether BVR was exerting its effects

on adhesion molecule expression by inhibiting one, or a combination of these pathways, or indeed whether these pathways made any contribution to adhesion molecule expression. We utilized a pharmacological strategy; SB203580 (SB) to inhibit p38, SP600125 (SP) to inhibit JNK and PD98059 (PD) to inhibit MEK1 (and therefore ERK1/2).

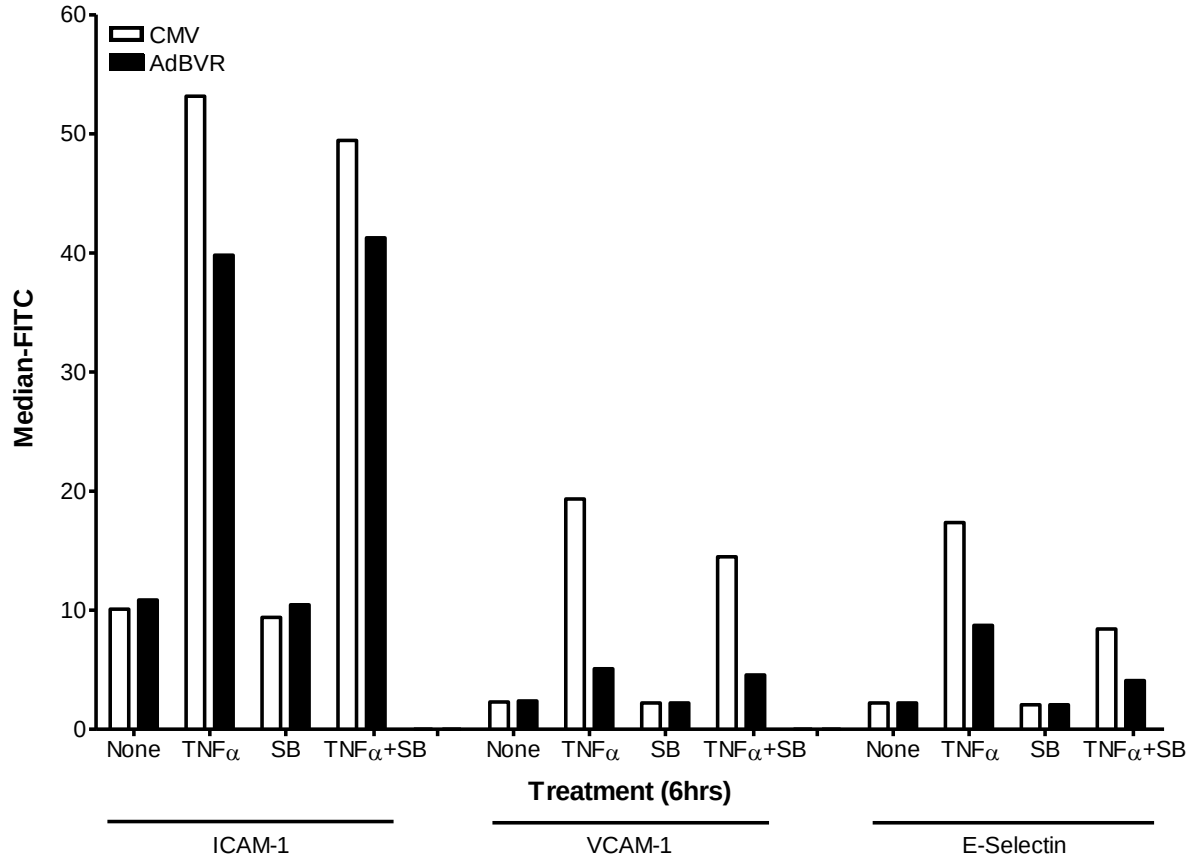

Figure 5.5 ***BVR inhibits TNFα-induced adhesion molecule expression independently of the p38 pathway***. Flow cytometric analyses utilizing anti-ICAM-1, anti-VCAM-1 and anti-E-Selectin antibodies. HUVECs were grown in 12-well plates and infected as indicated. Approximately 24hrs later, HUVECs were pre-treated as indicated with 5μM SB203580 (SB) for 1hr in HUVEC starvation medium. Then, TNFα was applied for 6hrs in fresh medium as indicated. The cells were then harvested and subsequently analyzed. The results indicate that the p38 pathway has a limited role in TNFα-induced adhesion molecule expression in our system. These results represent the mean ± SEM of one experiment performed in single wells.

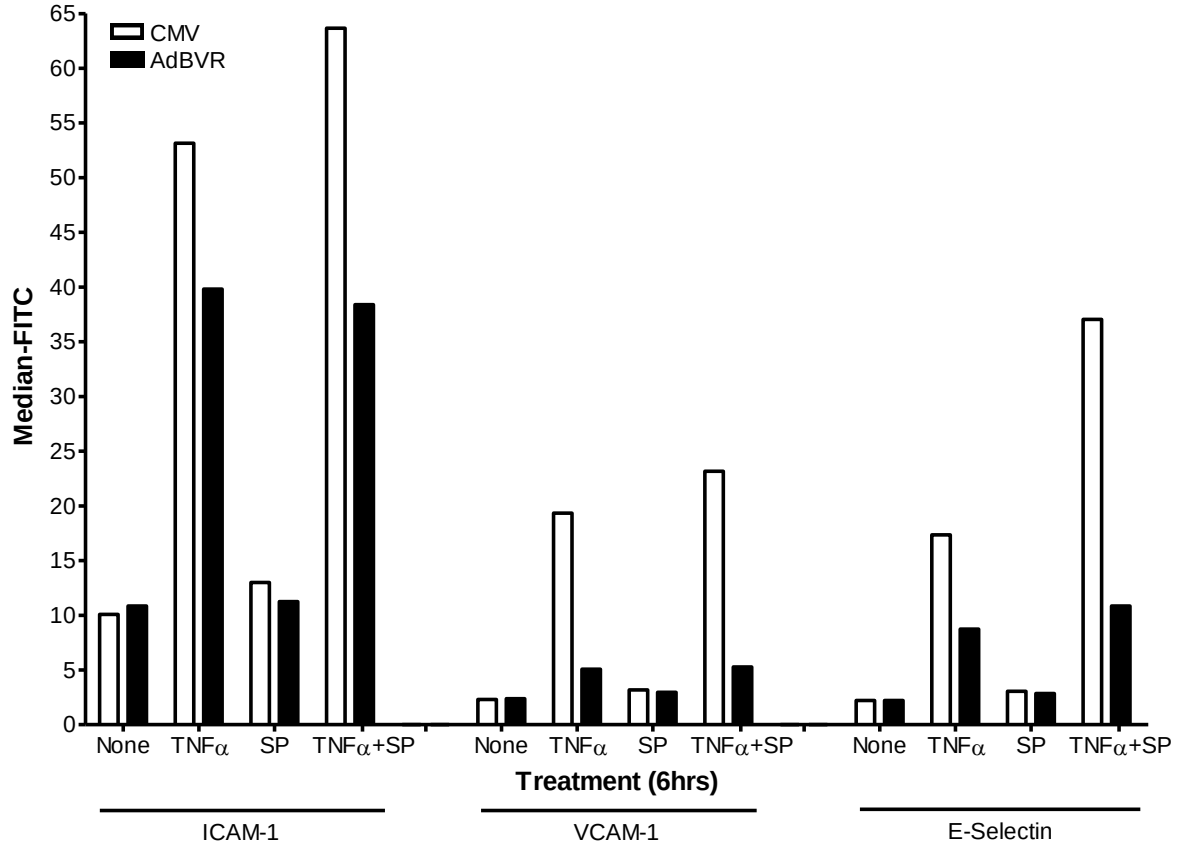

Figure 5.6 ***BVR inhibits TNFα-induced adhesion molecule expression independently of the JNK pathway***. Flow cytometric analyses utilizing anti-ICAM-1, anti-VCAM-1 and anti-E-Selectin antibodies. HUVECs were grown in 12-well plates and infected as indicated. Approximately 24hrs later, HUVECs were pre-treated as indicated with 30μM SP600125 (SP) for 1hr in HUVEC starvation medium. Then, TNFα was applied for 6hrs in fresh medium as indicated. The cells were then harvested and subsequently analyzed. The results indicate that the JNK pathway has a limited role in TNFα-induced adhesion molecule expression in our system. These results represent the mean ± SEM of one experiment performed in single wells.

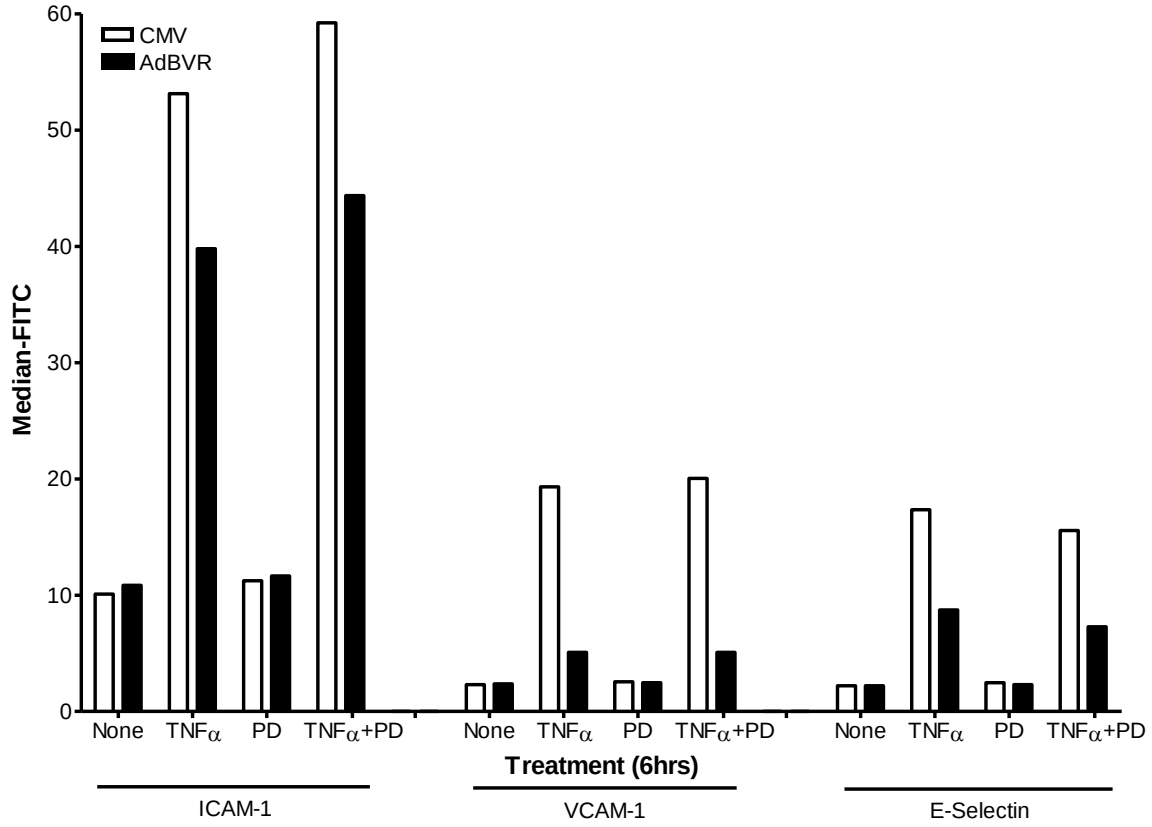

Figure 5.7 ***BVR inhibits TNFα-induced adhesion molecule expression independently of ERK1/2***. Flow cytometric analyses utilizing anti-ICAM-1, anti-VCAM-1 and anti-E-Selectin antibodies. HUVECs were grown in 12-well plates and infected as indicated. Approximately 24hrs later, HUVECs were pre-treated as indicated with 30μM PD98059 (PD) for 1hr in HUVEC starvation medium. Then, TNFα was applied for 6hrs in fresh medium as indicated. The cells were then harvested and subsequently analyzed. The results indicate that ERK1/2 is not involved in TNFα-induced adhesion molecule expression in our system. These results represent the mean ± SEM of one experiment performed in single wells.

The results indicate that p38, JNK and ERK1/2 are not involved in TNFα-induced ICAM-1 and VCAM-1 expression in our system. To a small extent, p38 appears to contribute to TNFα-induced E-Selectin expression. However, we can safely conclude that BVR does not inhibit adhesion molecule expression by inhibiting these pathways.

Cytotoxicity

We sought to determine whether BVR could protect HUVECs against oxidative stress – as associated with hydrogen peroxide and ox-LDL (Figures 5.8, 5.9 and 5.10). BVR produces bilirubin which protects against oxidative stress, possibly via a biliverdin-bilirubin redox cycle (Sedlak and Snyder, 2009). Furthermore, we have demonstrated that BVR increases NO production (Figure 4.3), and NO is involved in protection against oxidative stress (Napoli *et al*, 2006).

We incorporated hemin, the substrate for biliverdin (and hence bilirubin) synthesis. Ox-LDL was generated from native LDL using a well-established method of $CuSO_4$-mediated oxidation (Esterbauer *et al*, 1992). A TBARs assay was then conducted to ensure that the LDL had indeed been oxidized (not shown).

We conducted MTT assays to assess HUVEC viability under these conditions, and at various time-points, with or without BVR overexpression.

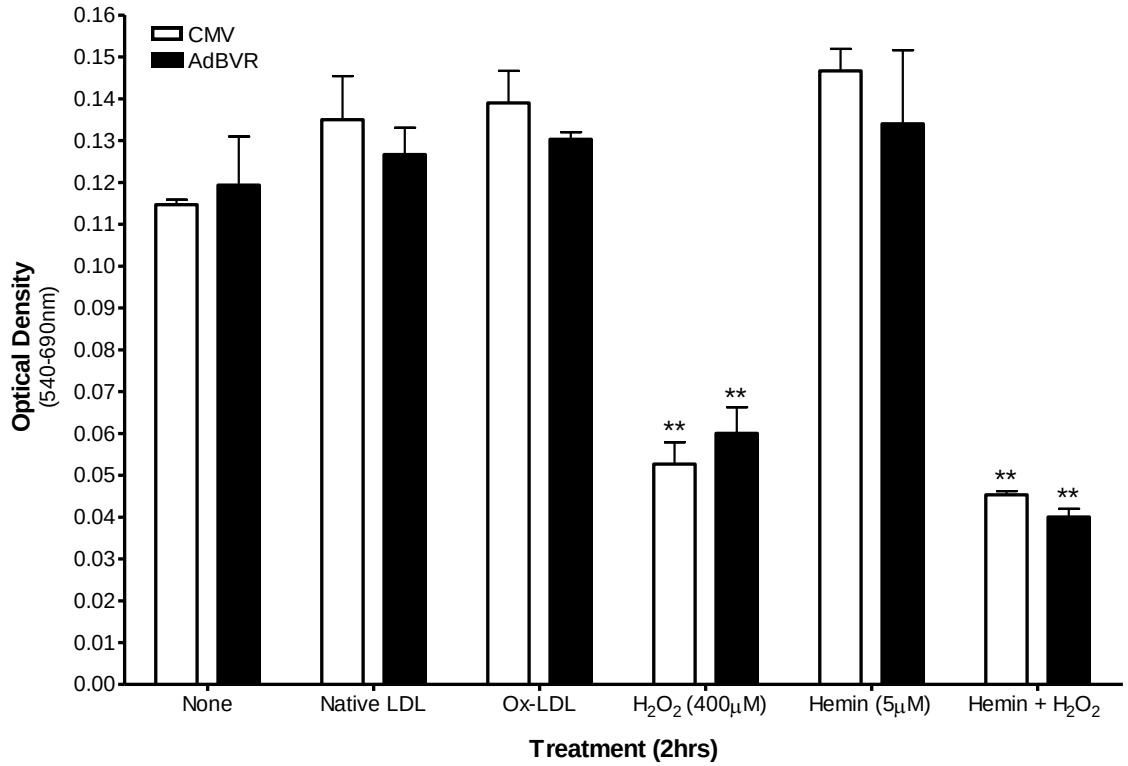

Figure 5.8 ***BVR is not cytoprotective against oxidative stresss in a MTT assay***. MTT assay conducted following 2hrs exposure to cytotoxic agents. HUVECs were grown in 96-well plates and infected as indicated. Approximately 24hrs later, HUVECs were pre-treated with 5μM hemin for 1hr. Then, treatments were applied as indicated in HUVEC starvation medium for 2hrs. MTT was then added in serum-free medium and incubated for 4hrs, after which the solution was aspirated and DMSO applied. The results indicate that BVR overexpression does not protect against cytotoxicity associated with oxidative stress. ** $p < 0.05$ vs. same virus, no treatment control. These results represent the mean ± SEM of one experiment performed in duplicate wells.

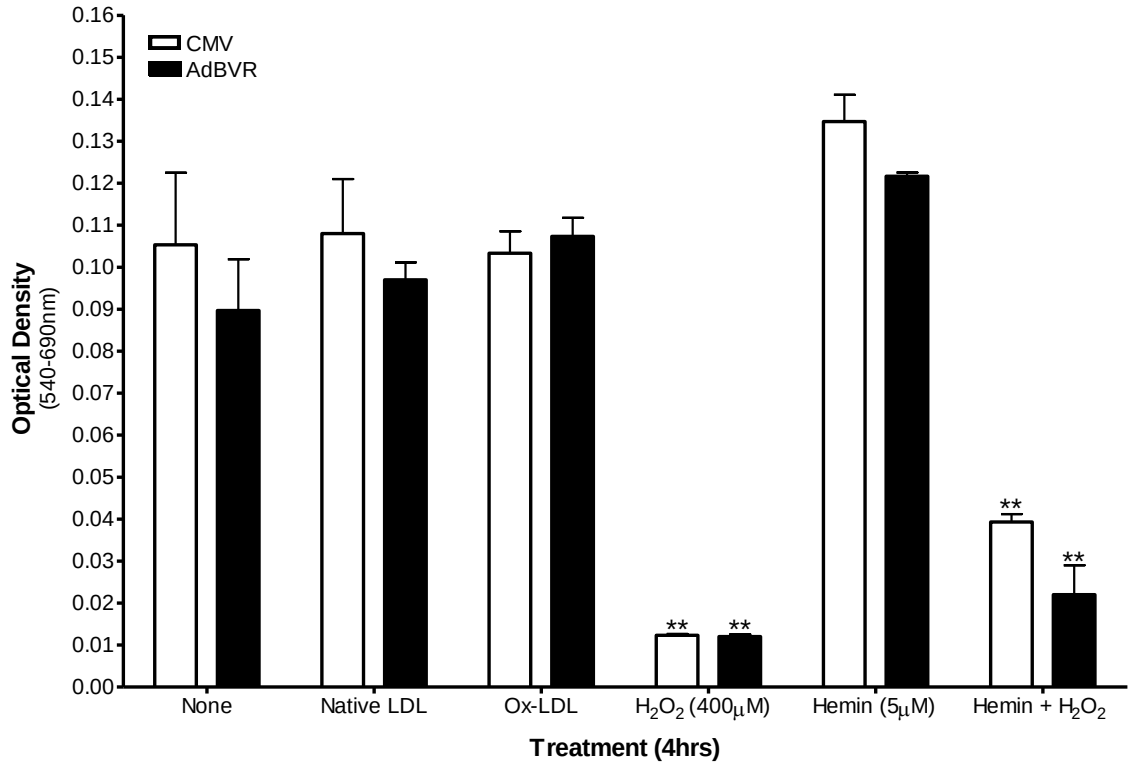

Figure 5.9 ***BVR is not cytoprotective against oxidative stress in a MTT assay***. MTT assay conducted following 4hrs exposure to cytotoxic agents. HUVECs were grown in 96-well plates and infected as indicated. Approximately 24hrs later, HUVECs were pre-treated with 5μM hemin for 1hr. Then, treatments were applied as indicated in HUVEC starvation medium for 4hrs. MTT was then added in serum-free medium and incubated for 4hrs, after which the solution was aspirated and DMSO applied. The results indicate that BVR overexpression does not protect against cytotoxicity associated with oxidative stress. ** $p < 0.05$ vs. same virus, no treatment control. These results represent the mean ± SEM of one experiment performed in duplicate wells.

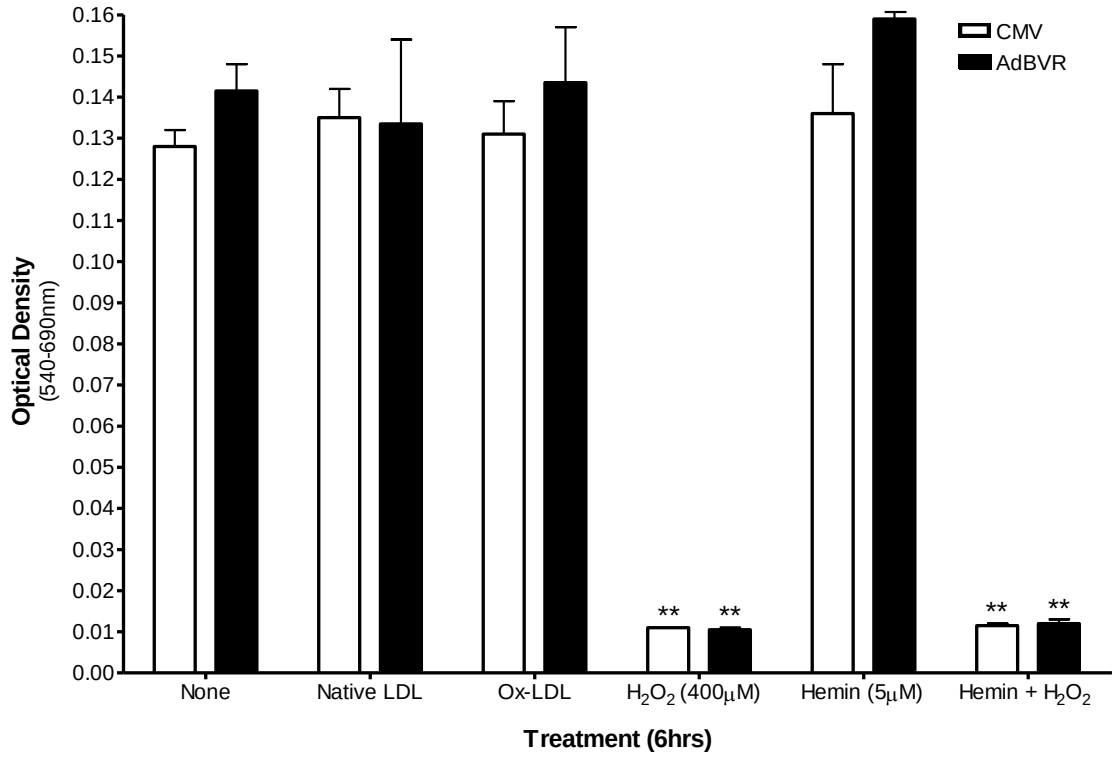

Figure 5.10 ***BVR is not cytoprotective against oxidative stress in a MTT assay***. MTT assay conducted following 6hrs exposure to cytotoxic agents. HUVECs were grown in 96-well plates and infected as indicated. Approximately 24hrs later, HUVECs were pre-treated with 5μM hemin for 1hr. Then, treatments were applied as indicated in HUVEC starvation medium for 6hrs. MTT was then added in serum-free medium and incubated for 4hrs, after which the solution was aspirated and DMSO applied. The results indicate that BVR overexpression does not protect against cytotoxicity associated with oxidative stress. ** $p < 0.05$ vs. same virus, no treatment control. These results represent the mean ± SEM of one experiment performed in duplicate wells.

The results suggest that BVR overexpression in HUVECs does not protect against H_2O_2-associated oxidative stress. We found that although the LDL had been significantly oxidized, the ox-LDL was not cytotoxic to the HUVECs in our system. Hemin was generally ineffective in protecting against H_2O_2-associated cytotoxicity and had only a small (insignificant) effect on increasing viability at the 4hr time-point.

Nitric Oxide

We examined the effect of BVR overexpression on NO release in a number of different cell-types. Amongst these, we tested human aortic endothelial cells (HAECs). Due to the aortic origin of this cell line, the 'eNOS/NO system' is of greater similarity to endothelial cells from atherosclerosis-susceptible arteries (Figure 5.11).

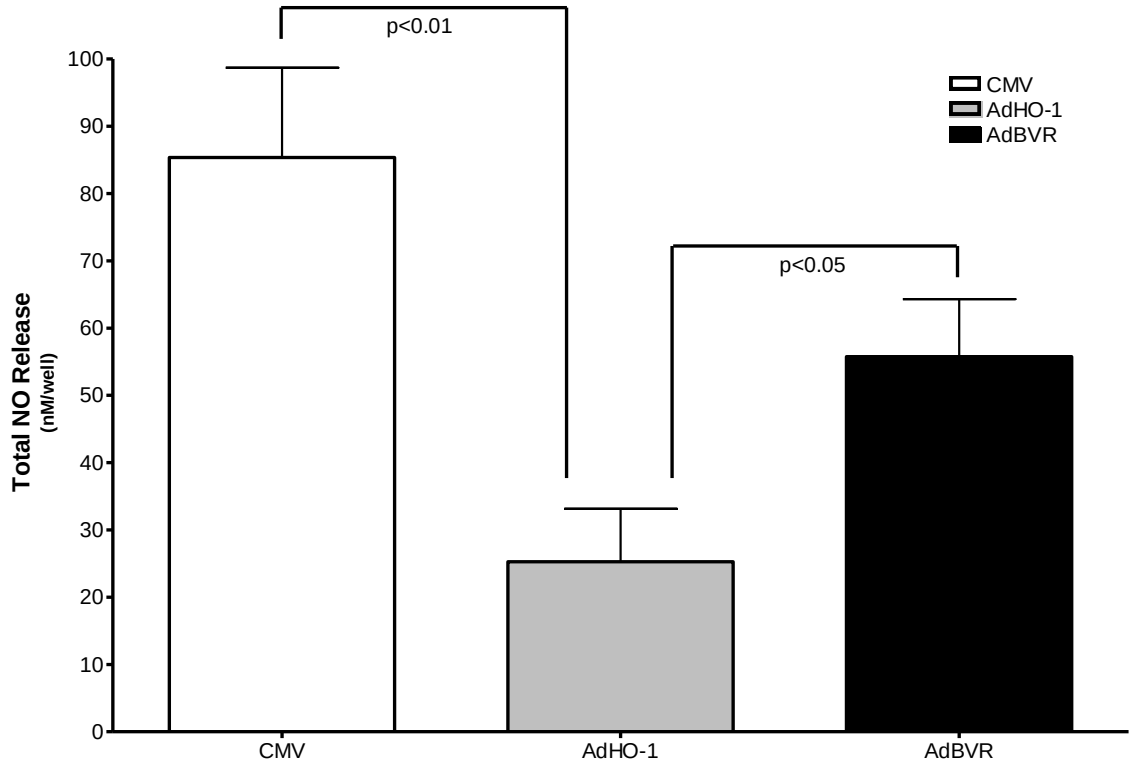

Figure 5.11 ***BVR and HO-1 have opposing effects on nitric oxide release in HAECs during a 30min stimulation***. Cell-free medium was incubated alongside the samples to correct for NO indigenous to the medium itself. HAECs were infected as indicated in RPMI 1640 (+ 0.2% BSA) medium. Approximately 24hrs later, fresh RPMI 1640 medium was gently added to each well, being careful to avoid shear stress. The cells were incubated for 30mins before medium was removed into tubes and frozen at -80°C until analysis. These data represent the mean ± SEM of one experiment conducted in triplicate wells.

The results from this experiment were not conclusive. BVR overexpression did not significantly alter NO release (compared to CMV control), whilst HO-1 overexpression reduced NO release. Interestingly, BVR overexpression had a significantly opposite effect to HO-1 overexpression.

In another experiment, we attempted to evaluate the optimal duration of stimulation for NO release in HUVECs, the time-point at which BVR overexpression would have the largest impact on NO generation (Figure 5.12). We tested three different time-points; 30mins, 60mins and 90mins.

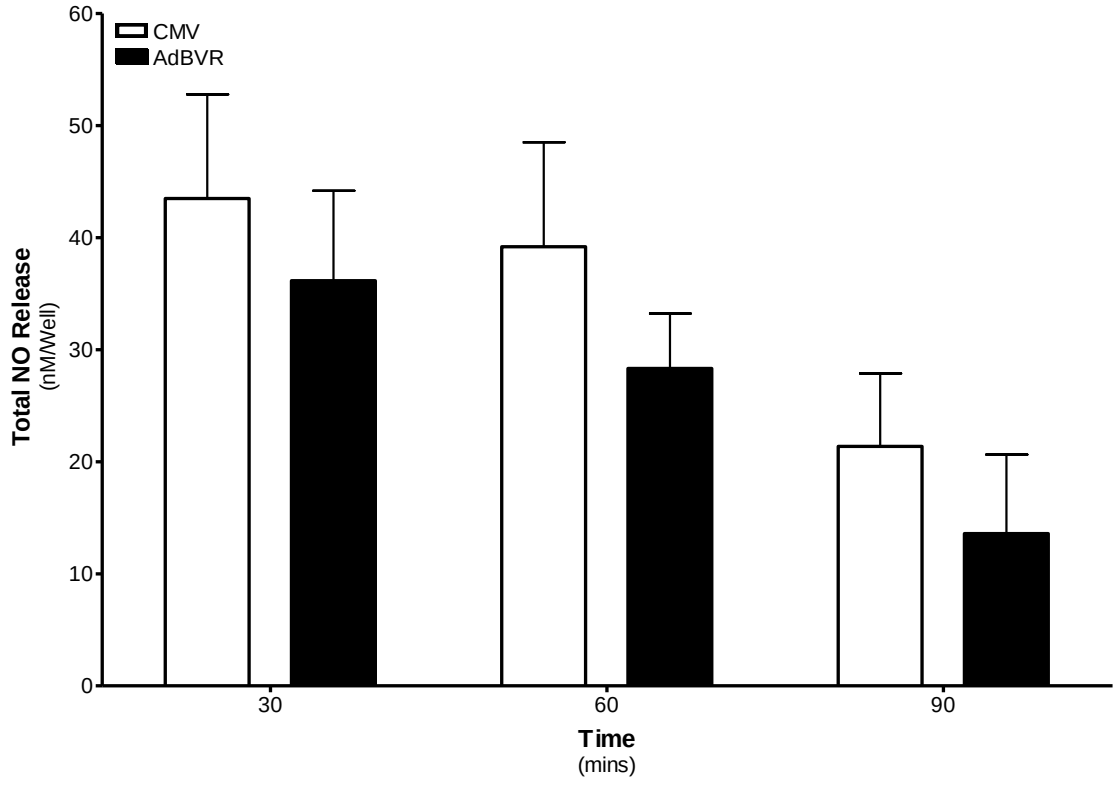

Figure 5.12 ***Measured NO release decreases with duration of stimulation in HUVECs***. Cell-free medium was incubated alongside the samples to correct for NO indigenous to the medium itself. HUVECs were infected as indicated in RPMI 1640 (+ 0.2% BSA) medium. Approximately 24hrs later, fresh RPMI 1640 medium was gently added to each well, being careful to avoid shear stress. The cells were incubated for 30, 60 and 90mins before medium was removed into tubes and frozen at -80°C until analysis. These data represent the mean ± SEM of one experiment conducted in triplicate wells.

The results from this experiment were inconclusive. We found that BVR overexpression actually slightly (insignificantly) decreased NO release at all three time-points, the opposite of what we expected. Interestingly, the measured NO release decreased with the duration of stimulation.

NFκB Activation

Many of our experiments centered on evaluating the ability of BVR to suppress the TNFα-induced expression of (largely) NFκB-dependent genes (i.e. adhesion molecules and MCP-1). NFκB activation is dependent on the degradation of IκBα (Figure 1.13). IκBα effectively sequesters inactive NFκB in the cytoplasm. Upon stimulation (i.e. TNFα), IKK phosphorylates IκBα thus marking it for degradation via the ubiquitin-proteasome pathway. IκBα levels can therefore indicate the extent of NFκB activation. We decided to conduct a Western blot for intracellular IκBα levels in the presence/absence of AdBVR, TNFα, and various inhibitors, at two different time-points (Figure 5.13).

The first lane for each treatment represents CMV-infected cells whilst the second lane for each treatment represents AdBVR-infected cells (Figure 5.13). If we consider just the TNFα treatment, we see that BVR overexpression decreases IκBα degradation 1hr post TNFα stimulation. Surprisingly however, BVR overexpression is associated with *increased* IκBα degradation at 6hrs post-stimulation. SnPP appears to inhibit TNFα-induced IκBα degradation. At 1hr and 6hrs post-stimulation (with TNFα and SnPP) however, BVR still appears to marginally inhibit IκBα degradation.

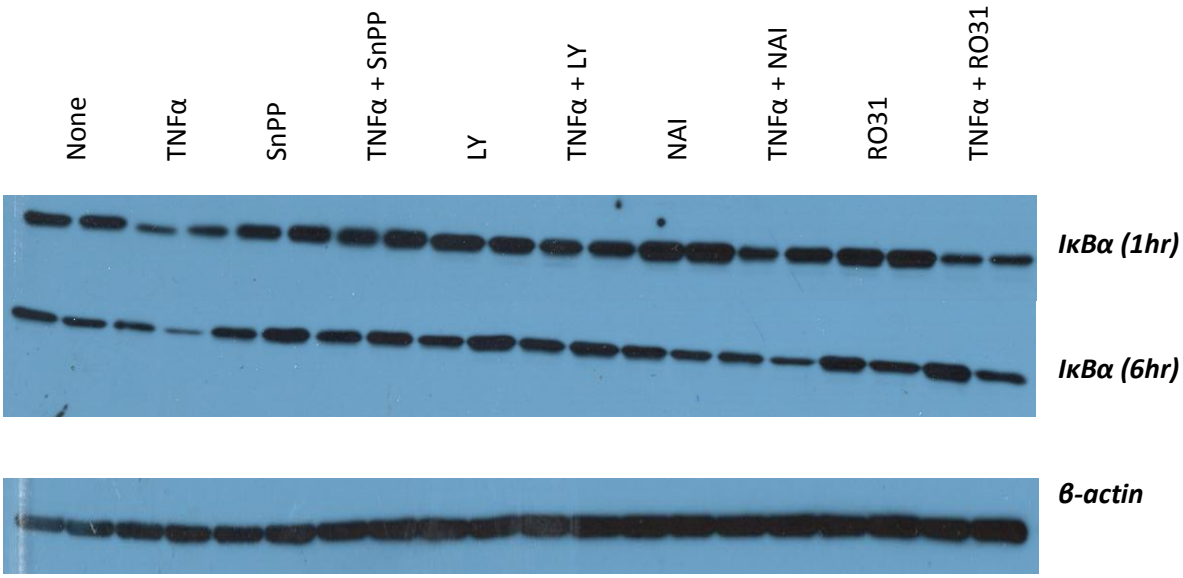

Figure 5.13 ***Western blots for IκBα at 1- and 6hrs post-stimulation in the presence/absence of various inhibitors and AdBVR in HUVECs***. Importantly, the first lane for each treatment is CMV-infected cells whilst the second lane for each treatment represents AdBVR-infected cells. HUVECs were grown in 12 well plates and infected. Approximately 24hrs later, the cells were pre-treated for 1hr with inhibitors (i.e. 20μM SnPP, 10μM LY, 10μM NAI and 1μM RO31) in HUVEC starvation medium as indicated. 10ng/mL TNFα was then applied as indicated for 1hr (*top*) or 6hrs (*bottom*). Cell lysates were then harvested and analyzed via SDS-PAGE. Unfortunately, the poor quality of the β-actin blot precluded quantification. These results are representative of one experiment.

PI3K inhibition appears to substantially reduce TNFα-induced IκBα degradation at both time-points. BVR overexpression in the presence of TNFα and LY appears to slightly increase IκBα levels at both time-points.

Although some of our experiments suggested that the NFκB activation inhibitor (NAI) was ineffectual, it clearly inhibits IκBα degradation at both 1hr and 6hrs post-stimulation. The

RO31 inhibitor was utilized at a concentration of 1μM. It does not appear to completely attenuate TNFα-induced IκBα degradation at either time-point. In comparison to TNFα treatment only however, RO31 does appear to reduce TNFα-induced IκBα degradation, particularly at the 6hr time-point. In the presence of RO31, BVR overexpression is associated with *greater* TNFα-induced IκBα degradation at the 6hr time-point – as is the case at the 6hr time-point with TNFα only.

The results from this experiment are of great significance, and highly relevant to many of our earlier experiments, and therefore certainly merit repetition to ensure accuracy and reliability, and to allow quantification.

Below, representative monocyte adhesion assay images are shown:

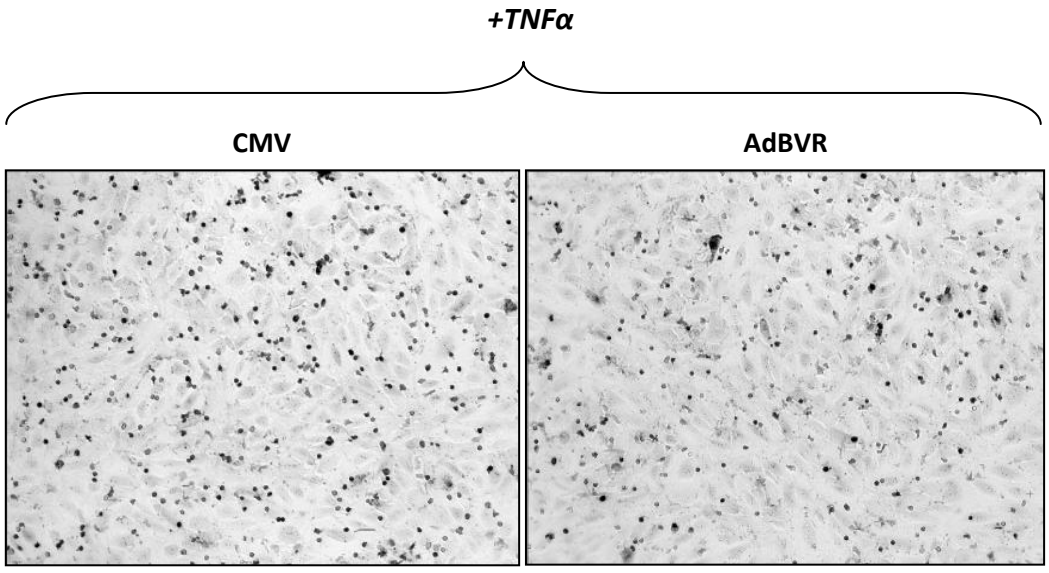

Figure 5.14 ***Representative 10X monocyte adhesion assay images***. HUVECs were grown in 24 well plates and infected. 24hrs later, pre-treatments with inhibitors were carried out as required for 1hr in HUVEC starvation medium. Then, 10ng/mL TNFα was applied for 6hrs before the monolayer was washed fixed and stained. Monocytes (small dark circles) were counted using Image-Pro Plus software.

DISCUSSION

Validation

Although previous studies have transduced AdBVR constructs into HEK293A cells, and therefore independently validated that BVR overexpression is a suitable method in terms of characterising the enzyme (Kravets *et al*, 2004), investigators have not yet published findings involving AdBVR-transduced endothelial cells.

In our preliminary experiments, very high MOIs (i.e. >400) of AdBVR were found to induce cell death – as evidenced by microscopic examination of cell structure and, the substantially lower protein yields from these wells. In addition to allowing us to determine optimal MOIs for these constructs, these experiments also confirmed that native BVR protein expression in endothelial cells (i.e. in HUVECs) is undetectable (Figure 3.1, *A*). Importantly, we substantially increased autoradiographic exposure time (1hr) and BVR remained undetectable.

An in-cell ELISA system was optimised for the present study. This required optimal antibody concentrations to be detertmined (Figure 3.3). Although we found the in-cell ELISA system to be more time-efficient and more economical than Western blotting, the sensitivity of this method was low. Hence, when BVR was overexpressed using AdBVR, the signal increased by approximately sevenfold only, in comparison to non-transduced cells (Figure 3.3, *B*). However, Western blotting reveals a much larger (essentially unquantifiable) discrepancy between BVR protein levels in non-transduced and transduced cells, also at 50 MOI (Figure 3.1, *A*). The different spatial expression profile of different proteins is one factor likely to affect the sensitivity of this assay – i.e. because the proteins are fixed *in situ*. Hence, whilst this assay is preferable to traditional Western blotting when large differences in expression

are expected and require confirmation; it is not suitable for detecting small changes in expression. However, higher sensitivities may have been achieved with other antibodies.

Many of our experiments utilised SnPP, a HO-1 inhibitor, to inhibit bilirubin production such that the reductase properties of BVR could be distinguished from its other non-canonical functions. HO-1 inhibition deprives BVR of its substrate, biliverdin. This has the effect of reducing bilirubin production because HO-1 is rate-limiting for its formation. However TNFα, an important mediator of the chronic inflammatory milieu, has the effect of increasing both the reductase and kinase activities of BVR (Lerner-Marmarosh *et al*, 2007). We were therefore keen to evaluate the effects of our inhibitor on intracellular unconjugated bilirubin levels under various experimental conditions (Figure 3.5).

Although HO-1 activity (i.e. rate of bilirubin production) has been measured for a number of decades, the HPLC methodology used to analyse levels of intracellular unconjugated bilirubin in our samples was only recently developed (Zelenka *et al*, 2008). Unfortunately therefore, comparative data are not available. It is advantageous to measure intracellular unconjugated bilirubin because this is the active version of bilirubin (Mazzone *et al*, 2009). HO-1 activity assays on the other hand measure both conjugated (no relevant biological activity) and unconjugated bilirubin. Samples were collected and then sent to Prof Libor Vitek (Charles University, Czech Republic) to be assayed for intracellular bilirubin using HPLC.

A number of considerations are important before our results (Figure 3.5) can be interpreted. First, HO-1 activity in HUVECs is approximately 0.6nmol bilirubin produced/mg protein/hr (Wagener *et al*, 1999) and unconjugated bilirubin concentration in tissues is approximately 10nM (Malik *et al*, 2010). Second, we must remember that BVR is known to induce expression of the rate-limiting enzyme for bilirubin formation, HO-1 (Figure 4.4 and Tudor *et*

al, 2008). Third, that HO-1 substrate (i.e. heme) depletion may be occurring as a result of BVR overexpression (Sedlak and Snyder, 2009). In this regard, one could imagine that BVR overexpression depletes heme before the experiment has begun. This would lead to lower unconjugated bilirubin levels in AdBVR-transduced cells. Finally, that the experiment begins with a change of medium – from 20% FCS HUVEC complete medium to 5% HUVEC starvation medium. This could potentially affect HO-1 activity.

Given that HO-1 activity in HUVECs under basal conditions is approximately 0.6nmol *bilirubin* produced/mg protein/hr (Wagener *et al*, 1999 and others), it is dubious that *unconjugated bilirubin* levels increase from approximately 6nmol/mg protein to 21nmol/mg protein in CMV-infected cells, in just 6hrs. It would have been useful to compare this to a none-infected control, in order to rule out a CMV non-specific effect.

The reduced bilirubin levels seen for TNFα-treated (Figure 3.5, *B*), CMV-infected cells may be due to ROS-mediated oxidation of bilirubin (to species other than biliverdin). It is well established that TNFα induces intracellular ROS generation in HUVECs (Lee *et al*, 2010). It is also known that TNFα induces HO-1 gene expression (Terry *et al*, 1999). Interestingly, the opposite effect is seen for TNFα-treated, AdBVR-infected cells – bilirubin increases compared to the control. This may be due to the increased reductase activity of BVR in response to TNFα (Lerner-Marmarosh *et al*, 2007). It is also likely due to the higher HO-1 activity in the AdBVR-infected cells (because BVR upregulates HO-1 expression) and this would explain the relatively large reduction in bilirubin seen when SnPP is added.

It is important to note that SnPP is a widely used inhibitor of bilirubin production (i.e. HO-1 activity). Indeed Pae *et al* utilised the same concentration (20μM) of SnPP, and found that a 6hr incubation reduced bilirubin production in HUVECs to below basal levels, even in the

presence of a compound which induces HO-1 activity (Pae *et al*, 2005). This is therefore compelling evidence that our methodology – i.e. using SnPP to attenuate the reductase activity of BVR – is indeed valid. Also, given that the investigators demonstrate a nearly 5-fold increase in bilirubin production following pharmacological induction of HO-1 (i.e. increased HO-1 protein expression) over 6hrs; it is unlikely that heme depletion is occurring at this time point.

In summary, we have validated our utilisation of SnPP to prevent increases in bilirubin production associated with BVR overexpression; even in the presence of TNFα, which increases the reductase activity of BVR. Athough we would have ideally repeated our SnPP validation experiment at least three times, we can be confident of our methodology because SnPP is a ubiquitously used inhibitor of bilirubin production.

Results

BVR Activates the PI3K/Akt/eNOS/NO Pathway

BVR possesses a dual-specificity kinase activity and several studies have already examined the contributions of the enzyme to inflammatory signaling. However, no such study has addressed this issue in endothelial cells, the site at which atherosclerosis first develops in the form of endothelial dysfunction. Whilst the protein expression levels of BVR in endothelial cells is known to be very low, knockdown studies have confirmed the significance of this low-level expression in such cells (Jansen *et al*, 2010). Furthermore TNFα, an important cytokine involved in atherosclerosis, upregulates both the reductase and kinase activities of BVR (Lerner-Marmarosh *et al*, 2007), further increasing the significance

of any cell signaling contribution. Previous studies have shown that BVR activates Akt in HEK293, HK-2 and H9c2 cells (Zeng *et al*, 2008 and Pachori *et al*, 2007); there is no published evidence demonstrating this in endothelial cells.

We utilised a PI3K inhibitor to precipitate the phenomena of BVR-induced Akt activation (Figure 4.1, *A*). The Western blot analysis reveals that in the presence of PI3K inhibition, BVR activates Akt. However, we do not see higher Akt activation in the BVR overexpressing cells under basal conditions (i.e. in the absence of the PI3K inhibitor), perhaps because Akt activation is already high under these conditions. However the in-cell ELISA reveals that even under basal conditions, BVR overexpression is associated with increased Akt activation (Figure 4.1, *B*).

Although our focus was to demonstrate BVR-mediated Akt activation and downstream eNOS activation, we must also remember that Akt serves numerous other functions in endothelial cells unrelated to eNOS activation. For example Akt promotes cell survival and angiogenesis, and in this regard is important in protecting against atherosclerosis and consequences thereof (Shiojima and Walsh, 2002). Our experiments have demonstrated that BVR strongly activates Akt in endothelial cells (i.e. HUVECs). We can be particularly confident of this finding because we utilized two different methods; traditional Western blotting and an in-cell ELISA.

Given the association of Akt activation with eNOS activation in endothelial cells (Fulton *et al*, 1999), we also sought to demonstrate that BVR could induce NO release via this pathway. This is important because deficiency of NO is characteristic of endothelial dysfunction and, numerous therapies for atherosclerosis (either already in use or in development) act to increase NO bioavailability (Li and Forstermann, 2009). We demonstrated that BVR

overexpression was associated with eNOS S1177 phosphorylation (Figure 4.2). Phosphorylation of this residue is a marker of eNOS activation and is indicative of downstream NO release.

Unfortunately, we were unable to demonstrate increased NO release in AdBVR-infected HUVECs. We believe that the reasons for this are technical, and related to the abnormal temperature-regulation of our Sievers NOA machine. Although we were aware of other methods by which NO could be analyzed in cell culture medium, we decided that the costs involved in changing strategy were prohibitive. We therefore improvised a cooling mechanism for our machine and proceeded to use PAECs instead of HUVECs. As a stable cell line, we felt that the PAECs would give us consistent and reproducible results and that their aortic origin (as opposed to umbilical) would be conducive to the extrapolation of our findings to *in vivo* atherosclerotic scenarios. We demonstrated that BVR overexpression was associated with an approximately two-fold increase in NO release over 30mins (Figure 4.3).

However, we cannot decipher whether the NO released into the medium is eNOS-derived or iNOS-derived. This is of relevance because BVR has been shown to induce iNOS gene expression in HEK293A cells via NFκB activation (Gibbs and Maines, 2007). Incorporation of an eNOS selective inhibitor (e.g. L-NNA) into our experiments would have allowed us to determine the relative contributions of eNOS and iNOS to BVR-mediated NO release. Importantly, iNOS is implicated in pathological inflammatory processes. For example, Detmers *et al* found that $ApoE^{-/-}$ $iNOS^{-/-}$ mice had substantially reduced atherosclerotic lesion sizes compared to $ApoE^{-/-}$ $iNOS^{+/+}$ mice (Detmers *et al*, 2000). However given the strong degree of BVR-induced eNOS activation (i.e. S1177 phosphorylation), it is likely that at least some of the NO release is attributable to eNOS.

In summary, we have demonstrated the existence of a BVR/PI3K/Akt/eNOS/NO pathway in endothelial cells. This finding is highly novel and published studies have not yet demonstrated the existence of this pathway in any cell type. The importance of NO in suppressing the initiation and progression of atherosclerosis is well established. Given that TNFα, a prominent cytokine in atherosclerosis, increases both the reductase and kinase activities of BVR, it is tempting to speculate the existence of an anti-atherosclerotic defense mechanism in which TNFα induces NO release via BVR. However, knockout/knockdown studies are required to elucidate the pathophysiological significance of such a mechanism. We believe that the signaling activities of BVR in endothelial cells, which are as yet wholly unaddressed by published studies, are likely to be of significance in atherosclerosis (and other chronic inflammatory diseases). Positive modulators of BVR activity in the endothelium may be found and developed, in addition to gene therapy approaches.

BVR Induces HO-1 Expression

HO-1 is the rate-limiting enzyme in bilirubin production and for this reason, increased BVR activity may not correlate with increased bilirubin production. However if BVR were to increase HO-1 activity (i.e. by increasing its protein expression) we could then assume that BVR overexpression does indeed increase bilirubin production if substrate availability is not limiting.

That BVR is directly involved in gene expression, as a transcription factor, is suggested by its possession of a bZip domain. Indeed the association of BVR with induction of HO-1 expression is certainly not novel. Ahmad *et al* first demonstrated that BVR was involved in oxidative stress-induced HO-1 expression in COS cells (Ahmad *et al*, 2002). Subsequently,

the ability of the reductase to induce HO-1 expression in HEK293A cells was demonstrated (Kravets *et al*, 2004). BVR binds as a homodimer to various regulatory elements in the HO-1 promoter, including for example the antioxidant response element (Tudor *et al*, 2008). Aside from its own transcription factor capacity, BVR influences the activities of transcription factors involved in HO-1 expression. Most notable amongst these is NFκB; BVR increases NFκB activation (Gibbs and Maines, 2007) and this, theoretically at least, leads to HO-1 expression. This is because the link between NFκB activation and HO-1 gene expression is well-established, in numerous cell-types (Alam and Cook, 2007).

We have shown that BVR does indeed increase HO-1 protein expression in HUVECs (Figure 4.3). However, our findings do not reveal the mechanism by which BVR induces HO-1 expression. This may occur directly via BVR's transcription factor activity or indirectly, for example through BVR-mediated NFκB activation and subsequent HO-1 expression.

In summary, we have demonstrated that therapeutic strategies aiming to upregulate BVR in the endothelium will have the secondary benefit of increasing HO-1 expression. This confers greater substrate flux through the HO-1/BVR axis and also therefore increases levels of CO, a powerful anti-inflammatory molecule which protects against atherosclerosis (Durante *et al*, 2006). However our experiments do not reveal the mechanism by which BVR induces HO-1 gene expression; whether via direct DNA binding via its transcription factor capacity or, via modulation of NFκB activity. Nonetheless, this finding has important implications in terms of determining flux through the HO-1/BVR axis, because HO-1 is rate-limiting. In this regard, it might have been argued that therapeutic strategies aiming to induce BVR in the endothelium will *not* lead to bilirubin production, because HO-1 is rate-limiting. Our finding suggests that this is not the case because BVR induces HO-1 protein expression.

BVR & Ox-LDL

Our preliminary studies suggested that BVR overexpression in HUVECs does *not* result in increased bilirubin levels (Figure 3.5). As discussed previously, bilirubin has a well-established antioxidant effect, which protects against LDL oxidation in Gilbert's syndrome patients. However, our earlier experiments had demonstrated that BVR could phosphorylate eNOS S1177 and in so doing increase NO production (Figure 4.3). Reduced NO bioavailability is a characteristic feature of atherosclerosis and previous studies conducted in our lab have demonstrated that increased NO release is the mechanism by which angiopoietin-2 confers reduced LDL oxidation in the atherosclerotic plaques of $apoE^{-/-}$ mice. This was shown to correlate with reduced atherosclerotic plaque size (Ahmed *et al*, 2009).

Our findings indicate that BVR overexpression is not significantly associated with reduced LDL oxidation (Figure 4.5), independently of bilirubin production via the BVR/PI3K/Akt/eNOS/NO pathway, or otherwise. In our preliminary experiments, we showed that BVR overexpression was not associated with increased unconjugated bilirubin production (Figure 3.5). This may, in part, explain why BVR overexpression does not reduce LDL oxidation in our system. Given that increased bilirubin is associated with reduced LDL oxidation, we could have incorporated heme (the ultimate substrate for bilirubin production) into the experiment. However this would have confounded the experiment because heme strongly induces HO-1. That bilirubin production by BVR is important in protection against oxidative stress was demonstrated in a recent study utilising a siRNA-mediated BVR knockdown strategy (Jansen *et al*, 2010).

HO-1 overexpression had a significantly opposite effect to BVR overexpression, and was therefore associated (non-significantly) with increased LDL oxidation relative to the CMV controls. This may be attributable to increased Fe^{2+} (although this would induce ferritin synthesis and sequestration) or increased CO, which may be acting in a pro-oxidant manner (Piantadosi, 2008). Also, heme depletion (in AdHO-1 cells) may reduce flux through the HO-1 pathway such that the reduction in bile pigment generation results in increased LDL oxidation in AdHO-1 cells.

In summary, BVR does not appear to significantly reduce LDL oxidation via the BVR/PI3K/Akt/eNOS/NO pathway. Given that BVR induces HO-1 protein synthesis, it may be the case that BVR overexpression does increase bilirubin production if substrate availability is not limiting and this may or may not correlate with reduced LDL oxidation.

BVR Attenuates TNFα-Induced Leukocyte-Endothelium Adherence

In short, we have shown that BVR substantially attenuates endothelial TNFα-induced MCP-1 release, adhesion molecule expression (i.e. ICAM-1, VCAM-1 and E-Selectin) and monocyte adherence. These findings are highly novel and indeed highly surprising in regard to a previous study by Lerner-Marmarosh *et al* (Lerner-Marmarosh *et al*, 2007). In this study, the authors demonstrated that BVR *induces* the TNFα/PKCζ/NFκB pathway in HEK293 cells – suggesting that BVR increases TNFα-induced NFκB activation. Our experiments, in endothelial cells, are not in agreement with this model.

TNFα is an inflammatory cytokine and serves a critical role in chronic inflammatory diseases such as atherosclerosis (Figure 1.16). Most relevantly to our studies, the cytokine induces

ROS generation and also various pro-inflammatory genes, including MCP-1 and adhesion molecules, via NFκB activation (Zhang *et al*, 2009). The current consensus in the literature is that the dual-specificity kinase activities of BVR are almost completely associated with induction of inflammation, especially via NFκB (and to a lesser extent, JNK and p38) activation and subsequent pro-inflammatory gene expression (Kapitulnik and Maines, 2009). Indeed, BVR potentiates TNFα-induced inflammatory gene induction, via PKCζ activation in HEK293 cells (Lerner-Marmarosh *et al*, 2007). This would suggest that BVR is in fact pro-inflammatory. On the other hand, BVR generates bilirubin which is a potent antioxidant, and anti-inflammatory molecule. Bilirubin has been shown to inhibit NFκB activation (Liu *et al*, 2008) and in this regard, low nanomolar concentrations can attenuate TNFα-induced adhesion molecule expression (Mazzone *et al*, 2009). Bilirubin also attenuates increases in ROS levels associated with TNFα stimulation (Basuroy *et al*, 2009).

Our experiments suggest that BVR attenuates TNFα-induced MCP-1 release, adhesion molecule expression and monocyte adherence independently of bilirubin production. Bilirubin production was inhibited using SnPP. A recent study showed that SnPP (used at the same concentration and over the same time-point as in our experiments) does indeed attenuate bilirubin production to below basal levels in HUVECs (Pae *et al*, 2006). In addition we had previously shown that BVR overexpression in our system was not associated with increased intracellular unconjugated bilirubin levels (Figure 3.5). Taken together therefore, our experiments suggest that BVR is capable of attenuating TNFα-induced leukocyte-endothelium adherence independently of its bilirubin-generating capacity.

The results of our MCP-1 ELISA (Figure 4.6) are in agreement with our previous finding that BVR overexpression does not increase intracellular bilirubin levels. Inhibition of NFκB

activation does not appear to completely suppress TNFα-induced MCP-1 release in the control. This may indicate that our inhibitor is ineffective.

The MCP-1 ELISA results are remarkable for two reasons; ***1***, BVR continues to inhibit MCP-1 when bilirubin production is blocked with SnPP and ***2***, the aforementioned (Figure 1.15) TNFα/PKCζ/NFκB activation pathway – of which BVR is a potentiator – is not evident, or at least does not dominate, in our system. With regard to the former, bilirubin has been associated with attenuation of NFκB activation, and consequently reduced pro-inflammatory gene expression (Mazzone *et al*, 2009). In regard to the latter, BVR is either not a significant participant in this pathway in our system or, some component of MCP-1 release occurs via a mechanism not involving NFκB (e.g. p38 pathway).

We also examined the role of the BVR/PI3K/Akt axis in TNFα-induced leukocyte-endothelium adherence. Whilst we have demonstrated that this pathway may lead to NO generation (Figure 4.2), which may in turn inhibit NFκB activation (Zeiher *et al*, 1995), there is also strong evidence that Akt activates IKK, and consequently NFκB (Meng *et al*, 2002). Taken together, our results show that the BVR/PI3K/Akt/eNOS/NO pathway has no dominant effect (positive or negative) on TNFα-induced monocyte adherence. We can therefore conclude that BVR does not reduce adhesion molecule expression or monocyte adherence via this pathway. However, inhibition of PI3K reduces TNFα-induced monocyte adhesion in CMV control cells (Figure 4.10). This indicates that the net effect of the PI3K/Akt pathway is to *increase* TNFα-induced monocyte adhesion, possibly via the PI3K/Akt/IKK/NFκB pathway. Specifically this appears to be attributable, at least in part, to VCAM-1 upregulation (Figure 4.9). The upregulation of VCAM-1 may occur via the aforementioned PI3K/Akt/IKK/NFκB pathway.

In this set of experiments (utilising LY), our flow cytometric analyses show that BVR does not significantly attenuate TNFα-induced E-Selectin expression (Figure 4.9). However, the other sets of flow cytometric analyses prove otherwise and we conclude that this is due to experimental variability. Experimental variability is also likely responsible for the none-significant difference between TNFα-induced, PI3K-inhibited, VCAM-1 expression in CMV vs. AdBVR cells.

Our studies on leukocyte-endothelium adherence incorporated an NFκB Activation Inhibitor (NAI). We expected that this inhibitor would completely attenuate TNFα-induced increases in MCP-1 and adhesion molecule expression. However, the NAI appeared to have little or no effect. It reduced TNFα-induced MCP-1 release by less than 30% (Figure 4.6) and had no effect on VCAM-1 or E-Selectin expression (Figure 4.11). TNFα-induced ICAM-1 was reduced by less than 25%. This may indicate that our inhibitor is ineffective or that TNFα-induced expression of these adhesion molecules occurs, to some extent, independently of NFκB activation or indeed independently of transcription altogether, in this system. However, we also examined the roles of the p38, JNK and ERK1/2 in TNFα-induced adhesion molecule expression and found these pathways to make little or no contribution (supplementary results). It is therefore tempting to conclude that our inhibitor is ineffective however, our Western blots for IκBα show that the NAI does indeed have some effect (supplementary results).

We also examined the role of the BVR/PKCζ axis in leukocyte-endothelium adherence. Both the kinase and reductase activities of BVR are increased by TNFα, and PKCζ is essential in TNFα-induced NFκB activation (Nigro *et al*, 2010). Importantly, BVR increases PKCζ activity and *vice versa*. One could therefore postulate the existence of a TNFα/BVR/PKCζ/NFκB

pathway in which BVR is acting in a *pro*-inflammatory manner (Lerner-Marmarosh *et al*, 2007). Our flow cytometric analyses utilised RO31, an inhibitor of PKCζ, and confirmed the essentiality of PKCζ in TNFα-induced adhesion molecule expression. More importantly, we demonstrated that BVR does not increase monocyte adhesion via the TNFα/BVR/PKCζ/NFκB pathway.

In summary, we have demonstrated that positive modulation of BVR activity is likely associated with attenuation of leukocyte-endothelium adherence in the inflammatory milleu of atherosclerosis. Specifically, BVR was found to reduce TNFα-induced expression of endothelial MCP-1 and adhesion molecules (i.e. VCAM-1, ICAM-1 and E-selectin), in a manner that is independent of bilirubin production and the PI3K/Akt axis. Although previous studies (Lerner-Marmarosh *et al*, 2007 and Gibbs and Maines, 2007) have suggested that BVR increases NFκB activation, partly via increased PKCζ activation, our study strongly suggests that in endothelial cells at least, BVR has an anti-inflammatory effect.

Supplemetary Results

Leukocyte-Endothelium Adherence

Our preliminary experiments examining how BVR overexpression affects leukocyte-endothelium adherence utilised both THP-1 and PBMCs. PBMCs include both lymphocytes and monocytes whilst THP-1 cells are derived from a monocytic cell line.

BVR has multilateral effects on the flavin enzymes (e.g. the NOSs and NOXs) and we therefore utilised DPI, an inhibitor of flavin enzymes, to clarify the interplay between BVR,

the flavin enzymes and THP-1 adherence in HUVECs (Figure 5.1). DPI reduces TNFα-induced THP-1 adherence in both CMV and AdBVR infected cells. The results therefore indicate that the net, combined effect of flavin enzymes (including for example eNOS and NOXs) is to *increase* monocyte adhesion. Also, we can infer that the BVR/PI3K/Akt/eNOS/NO pathway is not responsible for the attenuation of TNFα-induced THP-1 adherence in BVR overexpressing cells.

We utilised both THP-1 and PBMCs in preliminary experiments to examine how SnPP affects BVR's ability to attenuate TNFα-induced adherence. Whilst SnPP significantly increased TNFα-induced THP-1 adherence (Figure 5.2), the opposite effect was observed with PBMCs – SnPP significantly reduced PBMC adherence (Figure 5.3). The former is consistent with the notion that HO-1-derived products (e.g. bilirubin) inhibit monocyte adhesion whilst the latter indicates that HO-1 has some pro-inflammatory component. However neither effect was observed when the same experiment was conducted with pure human monocytes (Figure 4.8).

PI3K inhibition reduced TNFα-induced THP-1 adhesion in both control and BVR overexpressing cells (Figure 5.4). However, when this experiment was repeated with monocytes isolated from human whole blood, we found that PI3K inhibition was only associated with reduced TNFα-induced monocyte adhesion in the control cells (Figure 4.10). It is likely that this is reflective of experimental variability – the experiment which utilised THP-1 cells was only conducted once. The results are consistent with the notion that the PI3K/Akt axis is pro-inflammatory in our system.

We used flow cytometry to assess TNFα-induced adhesion molecule expression in the presence of various pharmacological inhibitors – i.e. inhibitors of p38 MAPK, JNK and MEK1

(Figures 5.5, 5.6 and 5.7 respectively). The results indicate that BVR has little, if any effect on these pathways, positive or negative. However, previous studies have shown that BVR activates p38 MAPK, JNK and ERK1/2 (Kapitulnik and Maines, 2009). The results would therefore suggest that BVR does not activate these pathways in our system – we would expect to observe a decrease in TNFα-induced adhesion molecule expression in the BVR overexpressing cells in the presence of inhibitor if this were the case. To a small extent, p38 does appear to contribute to TNFα-induced E-selectin expression (Figure 5.5).

Cytotoxicity

Our MTT assays suggest that BVR overexpression does not protect against oxidative stress, as elicited by ox-LDL and H_2O_2 (Figure 5.8, 5.9 and 5.10). This was surprising, especially given that we incorporated hemin into the experiment. An effect may have been precipitated if we had utilised a different substance to create the oxidative stress. Indeed, a previous study demonstrated the importance of BVR in protecting against arsenic-mediated oxidative stress (Miralem *et al*, 2005). However, our results are in agreement with those of Maghzal *et al.* In this study, the authors showed that BVR overexpression in HeLa fails to protect against H_2O_2-mediated cell death (despite the addition of biliverdin or bilirubin), and that BVR overexpression does not decrease H_2O_2-induced ROS levels. Furthermore, BVR knockdown in these cells did not increase susceptibility to H_2O_2-mediated cell death (Maghzal *et al*, 2009).

Nitric Oxide

We attempted to evaluate the optimal duration of stimulation for NO release in HUVECs, and therefore tested three different time-points; 30mins, 60mins and 90mins (Figure 5.12). NO release appeared to decrease as the duration of stimulation increased. One might have expected the opposite – that NO release would cumulatively increase with duration of stimulation. These results may therefore be indicative of some degree of NO degradation, and so we decided to employ the 30 mins time-point in future NO release experiments.

NFκB Activation

NFκB activation is dependent on the degradation of the cytosolic IκBα and hence protein levels of IκBα can be assessed in order to determine the extent of NFκB activation. We conducted a Western blot for intracellular IκBα levels in the presence/absence of AdBVR, TNFα and inhibitors (i.e. SnPP, LY, NAI and RO31), at two different time-points (Figure 5.13). This experiment was designed so that the results would be comparable with our other endothelial-leukocyte interaction experiments, in terms of time-points. Unfortunately, the experiment was only conducted once and the poor quality of the β-actin blot precluded quantification.

In the presence of TNFα alone, BVR overexpression *accelerates* IκBα degradation at the 6hr time-point. This is surprising and would suggest that whilst BVR overexpression reduces IκBα degradation at 1hr with TNFα (as might be expected); it increases NFκB activation at 6hrs. This may involve the BVR/PI3K/Akt/IKK and/or the TNFα/BVR/PKCζ/NFκB pathway. We must also remember that IκBα may be resynthesized during the 6hrs stimulation period.

Whilst most of the functional assays used a 6hr time-point (i.e. monocyte adhesion assays and adhesion molecule expression experiments) we must remember that our MCP-1 ELISA was performed over 24hrs – sufficient time to allow for the transcription of any MCP-1 that may arise from this additional IκBα degradation in BVR overexpressing cells.

Interestingly, SnPP appeared to inhibit TNFα-induced IκBα degradation in both CMV and AdBVR infected cells. This may suggest that some product of HO-1 accelerates IκBα degradation. Consistent with this, CO has been shown to activate NFκB via a CO/PI3K/Akt/IKK pathway in hepatocytes (Kim *et al*, 2008).

PI3K inhibition appears to substantially reduce TNFα-induced IκBα degradation in both CMV and AdBVR infected cells, at both time-points. This would indicate some involvement of the PI3K/Akt pathway in TNFα-induced IκBα degradation, possibly via the aforementioned PI3K/Akt/IKK pathway. The presence of BVR overexpression (with TNFα + LY) appears to slightly increase IκBα levels at both time-points, although the significance of this remains to be determined when this experiment is repeated.

In the presence of RO31, BVR overexpression is still associated with *greater* TNFα-induced IκBα degradation at the 6hr time-point. This would suggest that BVR accelerates TNFα-induced IκBα degradation independently of the aforementioned TNFα/BVR/PKCζ/NFκB pathway.

Limitations & Future Studies

Many of our experiments utilized a BVR overexpression strategy, conferred by AdBVR, and sought to differentiate between bilirubin-mediated and kinase-mediated functions, using SnPP to inhibit bilirubin generation. However given that the X-ray structure of BVR has been solved one could, theoretically at least, develop a variant of AdBVR that is devoid of reductase activity. Such a construct would retain its capacity to function as a dual-specificity kinase and transcription factor however; the reductase active site would have been mutated such that bilirubin cannot be produced. Alternatively, one could mutate the kinase active site to produce a BVR mutant which is capable of producing bilirubin but which does not have a kinase capacity. Such mutational methodologies are preferable to using SnPP because it is more direct and avoids off-target effects associated with pharmacological inhibitors. For example, our studies utilised RO-31-8220 (RO31) as an inhibitor of PKCζ. However, this inhibitor has been shown to also inhibit Rsk-2 and p70 S6 kinase (Alessi, 1997).

Overexpression strategies using adenoviruses also have other disadvantages. Whilst such experiments potentially provide useful information regarding situations in which BVR activity is dramatically increased, it is dubious to extend these findings to physiological settings in which BVR activity is not increased. For example, one might argue that whilst eNOS activation and NO release are indeed substantially increased with BVR overexpression, BVR does not make a significant contribution to eNOS activation and NO release under physiological conditions (where BVR levels are extremely low in comparison to those achieved with 50MOI of AdBVR). Clearly, such arguments could be addressed by knocking down BVR in cells with siRNA and then measuring eNOS activation and NO release. This method was recently used in HUVECs to demonstrate the contribution of the low-level

expression of BVR to protection against oxidative stress (Jansen *et al*, 2010). We must also remember that it is unlikely that a pharmacological modulator would be developed that would be capable of elevating BVR expression levels to those achieved with 50MOI AdBVR. In this regard, it may have been preferable to have used an even lower MOI of AdBVR. Also, many of our experiments, for reasons of cost and practicality, did not incorporate a no-virus control. Ideally, such a control would have been included in every experiment that involved an adenovirus. Although we used CMV as a control for AdBVR, it might be argued that Adβ-Gal would have been more appropriate. This is because whilst CMV controls for viral infection, it does not control for the high protein expression associated with AdBVR.

We ascertained the purity of our endothelial cell preparations (i.e. HUVECs and PAECs) by staining for the von Willebrand Factor (vWF). This is a widely used endothelial cell marker (for example, Au-Yeung *et al*, 2004). HUVEC purity was checked by staining for vWF at regular intervals and in addition to this, we ensured that the cells displayed the characteristic endothelial cobblestone phenotype before utilising these cells in experiements. With hindsight, it would have been prudent to have also utilised CD31 IgG (anti-PECAM-1) to determine the endothelial cell nature of the cells. If the purity of the isolation is not adequate, anti-CD31 magnetic beads can be used.

Our results suggested that BVR overexpression was associated with PI3K-dependent eNOS S1177 phosphoryaltion in HUVECs. Whilst we were unable to demonstrate that BVR increases NO release in HUVECs, we showed this to be the case in PAECs. To rule out the possibility that BVR overexpression does not induce NO release in HUVECs because the enzyme phosphorylates eNOS at Thr495 as well as S1177, it would have been prudent to have assessed eNOS Thr495 phosphorylation. As discussed previously, Thr495

phosphorylation is inhibitory in terms of NO production. Interestingly, this residue is phosphorylated by PKCs (Fleming, 2010). It is therefore tempting to hypothesise that BVR indirectly induces eNOS Thr495 phosphorylation via PKCζ activation. It would have also been prudent to have utilised L-NNA in our demonstration that BVR increases NO release in PAECs, to rule out an iNOS-dependent effect.

In our preliminary experiments, we showed that BVR overexpression did not result in increased intracellular unconjugated bilirubin levels. Ideally, we would have repeated our measurements and to then have conducted statistical analyses. With hindsight, it would have also been prudent to have included hemin as a substrate for bilirubin production, to rule out the possibility that AdBVR is not associated with increased bilirubin levels due to lack of substrate. This would have informed our choice about whether to incorporate hemin into our LDL oxidation experiments.

We were unable to conclude precisely how BVR inhibits TNFα-induced leukocyte-endothelium interactions (i.e. MCP-1 release, adhesion molecule expression and monocyte adhesion). To strengthen the reliability of our conclusions, it would have been prudent to have repeated our Western blots for IκBα (supplementary results) and to then have conducted densitometric and statistical analyses. Furthermore, rather than using the extent of IκBα degradation as an indirect measure of NFκB activation, it would have been better to have used a more direct method. For example, an NFκB nuclear translocation assay may have been performed. This assay compares (inactive) cytosolic and (active) nuclear levels of NFκB.

Whilst we believe that our cell culture experiments provide strong evidence that BVR is in fact anti-inflammatory in the endothelium (even independent of its bilirubin generating

capacity), it remains to be seen whether these findings will agree with *in vivo* animal models. Indeed, these cell culture studies have led us to generate a ubiquitous BVR overexpressing mouse which will be utilised in experiments. To date, there are no published studies which have utilised such an animal model. We believe that our BVR overexpressing mouse will serve to evolve the *in vivo* literature surrounding the HO-1/BVR axis from its current focus on (administration of) bile pigments to one that also addresses the *in vivo* significance of the non-canonical activities of BVR. In this regard, it would be interesting to administer UGT1A1 adenovirus to BVR overexpressing $ApoE^{-/-}$ mice and to then examine atherosclerotic lesions. The UGT1A1 adenovirus, which is very well established, would serve to conjugate and remove serum bilirubin. This would allow us to examine the *in vivo* effects of BVR, independent of its bilirubin generating capacity.

APPENDIX

Chemical Reagents & Suppliers

30% (w/v) Acrylamide solution:	National Diagnostics Protogel, UK.
PVDF:	Millipore, UK.
Paraformaldehyde:	Sigma, UK.
Percoll:	Sigma, UK.
Saran wrap:	Dow, UK.
2-Thiobarbituric acid (98%):	Sigma, UK.
Extra thick blot paper:	Bio-Rad, UK.
NaH_2PO_4:	BDH, UK.
$NaH_2PO_4.2H_2O$:	BDH, UK.
Na_2HPO_4:	BDH, UK.
$CuSO_4.5H_2O$:	Sigma, UK.
Agarose (molecular grade):	Bioline, UK.
Sodium Citrate:	Sigma, UK.
Citric Acid:	Sigma, UK.
NaOH pellets:	Sigma, UK.
EDTA:	BDH, UK.
EZ-ECL:	Geneflow, UK.

Janus green whole-cell stain:	Thermoscientific, UK.
LDL:	Sigma, UK and Sunnylab, USA.
Glacial acetic acid:	Sigma UK.
Ammonium persulphate:	Sigma, UK.
Biotin protein ladder:	Cell signaling technology, UK.
Goat Serum:	Sigma, UK.
RIPA:	Upstate, UK.
Glutaraldehyde:	Sigma, UK.
DMSO:	Sigma, UK.
M199 medium:	Sigma, UK.
H_2O_2 (30%):	Sigma, UK.
RPMI-1640:	Sigma, UK.
Gelatin:	Sigma, UK.
Ham's F-10:	Sigma, UK.
Ham' F-12:	Lonza, UK.
L-glutamine:	Sigma, UK.
Ficoll-Paque Plus:	Amersham biosciences, UK.
Trypan blue:	Sigma, UK.

Hydrocortisone:	Sigma, UK.
Anti-von Willebrand Factor:	Sigma, UK.
BSA (for ELISAs):	Sigma, UK.
BSA (for tissue culture):	Melford, UK.
Glycine:	CN Biosciences, UK.
Kaleidoscope protein ladder:	Bio-Rad, UK.
Glycerol:	Sigma, UK.
Penicillin:	GibcoBRL life technologies, Scotland
Bromophenol blue:	Sigma, UK.
Hybond ECL nitrocellulose membrane:	Amersham International, UK.
Marvel dried skimmed milk:	Sainsbury's, UK.
Sodium chloride:	Sigma, UK.
Methanol:	BDH, UK.
Bio-Rad protein estimation:	Bio-Rad, UK.
Fetal calf serum:	GibcoBRL life technologies, Scotland.
Goat serum:	Sigma, UK.
Phosphate buffered saline tablets (PBS):	Sigma, UK.
Tris:	CN Biosciences, UK.

Streptomycin:	GibcoBRL Life Technologies, Scotland.
Isopropanol:	Sigma, UK.
Mayer's Haematoxylin:	Sigma, UK.
Trypsin-EDTA:	Sigma, UK.
Sodium nitrite:	Sigma, UK.
TEMED:	Sigma, UK.
Collagenase A:	Boehringer Mannheim, UK.
Phosphatase Inhibitor Cocktail I:	Sigma, UK.
Phosphatase Inhibitor Cocktail II:	Sigma, UK.
Protease inhibitor cocktail:	Sigma, UK.
SDS:	Sigma UK.
Sodium hydroxide:	Sigma, UK.
Triton X-100:	Sigma, UK.
Potassium chloride:	Sigma, UK.
Proteinase K:	Sigma, UK.
Ethanol (99.7-100%):	BDH, UK.
DMSO:	Sigma, UK.
Kodak, Biomax MR film:	Anachem, UK.

Sodium iodide:	Sigma, UK.
Tween-20:	Sigma, UK.
β-mercaptoethanol:	Sigma, UK.
TNFα:	PeproTech, UK
16% Formaldehyde (methanol-free):	Thermoscientific, UK.
TMB substrate:	R & D systems, UK.
HRP conjugate:	R & D systems, UK.

Solutions & Buffers

PBS:	5 PBS tablets into 1L d.H_2O – pH 7.4, 10mM $NaPO_4$, 2.7mM KCl, 127mM NaCl.
TBS:	50mM Tris, 150mM NaCl, HCl – pH 7.6.
RIPA buffer:	50mM Tris HCl pH7.4, 1% IGEPAL, 0.25% Na Deoxycholate, 150nM NaCl, 1mM EGTA, 1mM PMSF, 1μg/ml Aprotinin, Pepstatin, Leupeptin, 1mM Na_3VO_4, 1mM NaF.
Running buffer:	0.05% Tris, 0.384 M Glycine, 0.1% SDS.
Sample buffer 4X:	0.04 M Tris, 4 mM EDTA, 4% SDS, 40% Glycerol, 0.02% Bromophenol Blue.
Transfer buffer:	190mM Glycine, 25mM Tris, 40% Methanol.
TTBS:	0.1M Tris, 0.3M NaCl, 0.1% Tween-20 pH 7.5.
TBARS reagent:	15% Tricholoroacetic acid, 0.09375M 2-Thiobarbituric acid, 0.25M HCl.
Antibiotics:	100 μg/ml Streptomycin, 100 μg/ml Penicillin.
10% APS:	10% (w/v) in d.H_20.
4% Formaldehyde:	2.75mL 16% formaldehyde (methanol-free), 8.25mL TBS.

Permeabilization buffer: 0.11mL Triton X-100 (10%), 11mL TBS.

Quenching solution: 0.38mL H_2O_2 (30%), 11mL TBS.

Wash buffer: 7.5mL 20X TBS, 141mL ultrapure H_2O, 1.5mL Tween-20 (10%).

Blocking buffer: 1mL goat serum, 9mL wash buffer.

Constituent	***SDS-PAG Type***	
	Stacking (5%)	***Resolving (10%)***
d.H_2O	5.6mL	11.9mL
30% Acrylamide Solution	1.7mL	10mL
1.5M Tris	2.5mL	7.5mL
10% SDS	0.1mL	0.3mL
10% APS	0.1mL	0.3mL
TEMED	10µL	30µL

Table 3.1 ***Composition of a 10% SDS-PAG for Western blotting***.

REFERENCES

References

ABRAHAM, N. G. & KAPPAS, A. 2008. Pharmacological and clinical aspects of heme oxygenase. *Pharmacol Rev,* 60**,** 79-127.

AGARWAL, A., BALLA, J., BALLA, G., CROATT, A. J., VERCELLOTTI, G. M. & NATH, K. A. 1996. Renal tubular epithelial cells mimic endothelial cells upon exposure to oxidized LDL. *Am J Physiol,* 271**,** F814-23.

AHMAD, Z., SALIM, M. & MAINES, M. D. 2002. Human biliverdin reductase is a leucine zipper-like DNA-binding protein and functions in transcriptional activation of heme oxygenase-1 by oxidative stress. *J Biol Chem,* 277**,** 9226-32.

AHMED, A., FUJISAWA, T., NIU, X. L., AHMAD, S., AL-ANI, B., CHUDASAMA, K., ABBAS, A., POTLURI, R., BHANDARI, V., FINDLEY, C. M., LAM, G. K., HUANG, J., HEWETT, P. W., CUDMORE, M. & KONTOS, C. D. 2009. Angiopoietin-2 confers Atheroprotection in apoE-/- mice by inhibiting LDL oxidation via nitric oxide. *Circ Res,* 104**,** 1333-6.

ALAM, J. & COOK, J. L. 2007. How many transcription factors does it take to turn on the heme oxygenase-1 gene? *Am J Respir Cell Mol Biol,* 36**,** 166-74.

ALESSI, D. R. 1997. The protein kinase C inhibitors Ro 318220 and GF 109203X are equally potent inhibitors of MAPKAP kinase-1beta (Rsk-2) and p70 S6 kinase. *FEBS Lett,* 402**,** 121-3.

ANTONIADES, C., SHIRODARIA, C., CRABTREE, M., RINZE, R., ALP, N., CUNNINGTON, C., DIESCH, J., TOUSOULIS, D., STEFANADIS, C., LEESON, P., RATNATUNGA, C., PILLAI, R. & CHANNON, K. M. 2007. Altered plasma versus vascular biopterins in human atherosclerosis reveal relationships between endothelial nitric oxide synthase coupling, endothelial function, and inflammation. *Circulation,* 116**,** 2851-9.

AU-YEUNG, K. K., WOO, C. W., SUNG, F. L., YIP, J. C., SIOW, Y. L. & O, K. 2004. Hyperhomocysteinemia activates nuclear factor-kappaB in endothelial cells via oxidative stress. *Circ Res,* 94**,** 28-36.

BALLA, G., JACOB, H. S., EATON, J. W., BELCHER, J. D. & VERCELLOTTI, G. M. 1991. Hemin: a possible physiological mediator of low density lipoprotein oxidation and endothelial injury. *Arterioscler Thromb,* 11**,** 1700-11.

BALLA, J., BALLA, G., JENEY, V., KAKUK, G., JACOB, H. S. & VERCELLOTTI, G. M. 2000. Ferriporphyrins and endothelium: a 2-edged sword-promotion of oxidation and induction of cytoprotectants. *Blood,* 95**,** 3442-50.

BARANANO, D. E., RAO, M., FERRIS, C. D. & SNYDER, S. H. 2002. Biliverdin reductase: a major physiologic cytoprotectant. *Proc Natl Acad Sci U S A,* 99**,** 16093-8.

BASUROY, S., BHATTACHARYA, S., LEFFLER, C. W. & PARFENOVA, H. 2009. Nox4 NADPH oxidase mediates oxidative stress and apoptosis caused by TNF-alpha in cerebral vascular endothelial cells. *Am J Physiol Cell Physiol,* 296**,** C422-32.

BEALE, S. I. & CORNEJO, J. 1984. Enzymatic heme oxygenase activity in soluble extracts of the unicellular red alga, Cyanidium caldarium. *Arch Biochem Biophys,* 235**,** 371-84.

BECKMAN, J. A., CREAGER, M. A. & LIBBY, P. 2002. Diabetes and atherosclerosis: epidemiology, pathophysiology, and management. *JAMA,* 287**,** 2570-81.

BELTMAN, J., MCCORMICK, F. & COOK, S. J. 1996. The selective protein kinase C inhibitor, Ro-31-8220, inhibits mitogen-activated protein kinase phosphatase-1 (MKP-1) expression, induces c-Jun expression, and activates Jun N-terminal kinase. *J Biol Chem,* 271**,** 27018-24.

BLANKENBERG, S., BARBAUX, S. & TIRET, L. 2003. Adhesion molecules and atherosclerosis. *Atherosclerosis,* 170**,** 191-203.

BOO, Y. C. & JO, H. 2003. Flow-dependent regulation of endothelial nitric oxide synthase: role of protein kinases. *Am J Physiol Cell Physiol,* 285**,** C499-508.

BOSMA, P. J., CHOWDHURY, J. R., BAKKER, C., GANTLA, S., DE BOER, A., OOSTRA, B. A., LINDHOUT, D., TYTGAT, G. N., JANSEN, P. L., OUDE ELFERINK, R. P. & ET AL. 1995. The genetic basis of the reduced expression of bilirubin UDP-glucuronosyltransferase 1 in Gilbert's syndrome. *N Engl J Med,* 333**,** 1171-5.

BREIMER, L. H., WANNAMETHEE, G., EBRAHIM, S. & SHAPER, A. G. 1995. Serum bilirubin and risk of ischemic heart disease in middle-aged British men. *Clin Chem,* 41**,** 1504-8.

BULMER, A. C., BLANCHFIELD, J. T., TOTH, I., FASSETT, R. G. & COOMBES, J. S. 2008. Improved resistance to serum oxidation in Gilbert's syndrome: a mechanism for cardiovascular protection. *Atherosclerosis,* 199**,** 390-6.

CARMELIET, P. 2000. Mechanisms of angiogenesis and arteriogenesis. *Nat Med,* 6**,** 389-95.

CHANNON, K. M., BLAZING, M. A., SHETTY, G. A., POTTS, K. E. & GEORGE, S. E. 1996. Adenoviral gene transfer of nitric oxide synthase: high level expression in human vascular cells. *Cardiovasc Res,* 32**,** 962-72.

CHEN, C. C., ROSENBLOOM, C. L., ANDERSON, D. C. & MANNING, A. M. 1995. Selective inhibition of E-selectin, vascular cell adhesion molecule-1, and intercellular adhesion molecule-1 expression by inhibitors of I kappa B-alpha phosphorylation. *J Immunol,* 155**,** 3538-45.

CHOWDHARY, S. & TOWNEND, J. N. 2001. Nitric oxide and hypertension: not just an endothelium derived relaxing factor! *J Hum Hypertens,* 15**,** 219-27.

CLEMENTI, M., DI GIANANTONIO, E., FABRIS, L., FORABOSCO, P., STRAZZABOSCO, M., TENCONI, R. & OKOLICSANYI, L. 2007. Inheritance of hyperbilirubinemia: evidence for a major autosomal recessive gene. *Dig Liver Dis,* 39**,** 351-5.

COOKE, J. P. 2004. Asymmetrical dimethylarginine: the Uber marker? *Circulation,* 109**,** 1813-8.

CORRADO, E., RIZZO, M., COPPOLA, G., FATTOUCH, K., NOVO, G., MARTURANA, I., FERRARA, F. & NOVO, S. 2010. An update on the role of markers of inflammation in atherosclerosis. *J Atheroscler Thromb,* 17**,** 1-11.

CUDMORE, M., AHMAD, S., AL-ANI, B., FUJISAWA, T., COXALL, H., CHUDASAMA, K., DEVEY, L. R., WIGMORE, S. J., ABBAS, A., HEWETT, P. W. & AHMED, A. 2007. Negative regulation of soluble Flt-1 and soluble endoglin release by heme oxygenase-1. *Circulation,* 115**,** 1789-97.

DEGUCHI, K., HAYASHI, T., NAGOTANI, S., SEHARA, Y., ZHANG, H., TSUCHIYA, A., OHTA, Y., TOMIYAMA, K., MORIMOTO, N., MIYAZAKI, M., HUH, N. H., NAKAO, A., KAMIYA, T. & ABE, K. 2008. Reduction of cerebral infarction in rats by biliverdin associated with amelioration of oxidative stress. *Brain Res,* 1188**,** 1-8.

DENICOLA, A., BATTHYANY, C., LISSI, E., FREEMAN, B. A., RUBBO, H. & RADI, R. 2002. Diffusion of nitric oxide into low density lipoprotein. *J Biol Chem,* 277**,** 932-6.

DETMERS, P. A., HERNANDEZ, M., MUDGETT, J., HASSING, H., BURTON, C., MUNDT, S., CHUN, S., FLETCHER, D., CARD, D. J., LISNOCK, J., WEIKEL, R., BERGSTROM, J. D., SHEVELL, D. E., HERMANOWSKI-VOSATKA, A., SPARROW, C. P., CHAO, Y. S., RADER, D. J., WRIGHT, S. D. & PURE, E. 2000. Deficiency in inducible nitric oxide synthase results in reduced atherosclerosis in apolipoprotein E-deficient mice. *J Immunol,* 165**,** 3430-5.

DIMMELER, S., FLEMING, I., FISSLTHALER, B., HERMANN, C., BUSSE, R. & ZEIHER, A. M. 1999. Activation of nitric oxide synthase in endothelial cells by Akt-dependent phosphorylation. *Nature,* 399**,** 601-5.

DORE, S. & SNYDER, S. H. 1999. Neuroprotective action of bilirubin against oxidative stress in primary hippocampal cultures. *Ann N Y Acad Sci,* 890**,** 167-72.

DORE, S., TAKAHASHI, M., FERRIS, C. D., ZAKHARY, R., HESTER, L. D., GUASTELLA, D. & SNYDER, S. H. 1999. Bilirubin, formed by activation of heme oxygenase-2, protects neurons against oxidative stress injury. *Proc Natl Acad Sci U S A,* 96**,** 2445-50.

DU, X. L., EDELSTEIN, D., DIMMELER, S., JU, Q., SUI, C. & BROWNLEE, M. 2001. Hyperglycemia inhibits endothelial nitric oxide synthase activity by posttranslational modification at the Akt site. *J Clin Invest,* 108**,** 1341-8.

DUDNIK, L. B., TSYUPKO, A. N., KHRENOV, A. V. & ALESSENKO, A. V. 2001. Effect of bilirubin on lipid peroxidation, sphingomyelinase activity, and apoptosis induced by sphingosine and UV irradiation. *Biochemistry (Mosc),* 66**,** 1019-27.

DURANTE, W., JOHNSON, F. K. & JOHNSON, R. A. 2006. Role of carbon monoxide in cardiovascular function. *J Cell Mol Med,* 10**,** 672-86.

FLEMING, I. 2010. Molecular mechanisms underlying the activation of eNOS. *Pflugers Arch,* 459**,** 793-806.

FLORCZYK, U. M., JOZKOWICZ, A. & DULAK, J. 2008. Biliverdin reductase: new features of an old enzyme and its potential therapeutic significance. *Pharmacol Rep,* 60**,** 38-48.

FONDEVILA, C., SHEN, X. D., TSUCHIYASHI, S., YAMASHITA, K., CSIZMADIA, E., LASSMAN, C., BUSUTTIL, R. W., KUPIEC-WEGLINSKI, J. W. & BACH, F. H. 2004. Biliverdin therapy protects rat livers from ischemia and reperfusion injury. *Hepatology,* 40**,** 1333-41.

FREY, R. S., USHIO-FUKAI, M. & MALIK, A. B. 2009. NADPH oxidase-dependent signaling in endothelial cells: role in physiology and pathophysiology. *Antioxid Redox Signal,* 11**,** 791-810.

FUJII, M., INOGUCHI, T., SASAKI, S., MAEDA, Y., ZHENG, J., KOBAYASHI, K. & TAKAYANAGI, R. 2010. Bilirubin and biliverdin protect rodents against diabetic nephropathy by downregulating NAD(P)H oxidase. *Kidney Int,* 78**,** 905-19.

FULTON, D., GRATTON, J. P., MCCABE, T. J., FONTANA, J., FUJIO, Y., WALSH, K., FRANKE, T. F., PAPAPETROPOULOS, A. & SESSA, W. C. 1999. Regulation of endothelium-derived nitric oxide production by the protein kinase Akt. *Nature,* 399**,** 597-601.

GIBBS, P. E. & MAINES, M. D. 2007. Biliverdin inhibits activation of NF-kappaB: reversal of inhibition by human biliverdin reductase. *Int J Cancer,* 121**,** 2567-74.

GORIN, Y., BLOCK, K., HERNANDEZ, J., BHANDARI, B., WAGNER, B., BARNES, J. L. & ABBOUD, H. E. 2005. Nox4 NAD(P)H oxidase mediates hypertrophy and fibronectin expression in the diabetic kidney. *J Biol Chem,* 280**,** 39616-26.

GULLU, H., ERDOGAN, D., TOK, D., TOPCU, S., CALISKAN, M., ULUS, T. & MUDERRISOGLU, H. 2005. High serum bilirubin concentrations preserve coronary flow reserve and coronary microvascular functions. *Arterioscler Thromb Vasc Biol,* 25**,** 2289-94.

HANSEN, T. W., MATHIESEN, S. B. & WALAAS, S. I. 1996. Bilirubin has widespread inhibitory effects on protein phosphorylation. *Pediatr Res,* 39**,** 1072-7.

HAYASHI, S., TAKAMIYA, R., YAMAGUCHI, T., MATSUMOTO, K., TOJO, S. J., TAMATANI, T., KITAJIMA, M., MAKINO, N., ISHIMURA, Y. & SUEMATSU, M. 1999. Induction of heme oxygenase-1 suppresses venular leukocyte adhesion elicited by oxidative stress: role of bilirubin generated by the enzyme. *Circ Res,* 85**,** 663-71.

HENNIG, B. & CHOW, C. K. 1988. Lipid peroxidation and endothelial cell injury: implications in atherosclerosis. *Free Radic Biol Med,* 4**,** 99-106.

HOEFEN, R. J. & BERK, B. C. 2002. The role of MAP kinases in endothelial activation. *Vascul Pharmacol,* 38**,** 271-3.

HOEKSTRA, K. A., GODIN, D. V. & CHENG, K. M. 2004. Protective role of heme oxygenase in the blood vessel wall during atherogenesis. *Biochem Cell Biol,* 82**,** 351-9.

HUFFMAN, C., CHILLAG, S., PAULMAN, L. & MCMAHON, C. 2009. It's not easy bein' green. *Am J Med,* 122**,** 820-2.

HUNTER, T. & COOPER, J. A. 1985. Protein-tyrosine kinases. *Annu Rev Biochem,* 54**,** 897-930.

IGNARRO, L. J., CIRINO, G., CASINI, A. & NAPOLI, C. 1999. Nitric oxide as a signaling molecule in the vascular system: an overview. *J Cardiovasc Pharmacol,* 34**,** 879-86.

INOGUCHI, T., SASAKI, S., KOBAYASHI, K., TAKAYANAGI, R. & YAMADA, T. 2007. Relationship between Gilbert syndrome and prevalence of vascular complications in patients with diabetes. *JAMA,* 298**,** 1398-400.

ISHIKAWA, K., NAVAB, M., LEITINGER, N., FOGELMAN, A. M. & LUSIS, A. J. 1997. Induction of heme oxygenase-1 inhibits the monocyte transmigration induced by mildly oxidized LDL. *J Clin Invest,* 100**,** 1209-16.

ISHIKAWA, K., SUGAWARA, D., GOTO, J., WATANABE, Y., KAWAMURA, K., SHIOMI, M., ITABE, H. & MARUYAMA, Y. 2001. Heme oxygenase-1 inhibits atherogenesis in Watanabe heritable hyperlipidemic rabbits. *Circulation,* 104**,** 1831-6.

JANSEN, T., HORTMANN, M., OELZE, M., OPITZ, B., STEVEN, S., SCHELL, R., KNORR, M., KARBACH, S., SCHUHMACHER, S., WENZEL, P., MUNZEL, T. & DAIBER, A. 2010. Conversion of biliverdin to bilirubin by biliverdin reductase contributes to endothelial cell protection by heme oxygenase-1-evidence for direct and indirect antioxidant actions of bilirubin. *J Mol Cell Cardiol,* 49**,** 186-95.

JENEY, V., BALLA, J., YACHIE, A., VARGA, Z., VERCELLOTTI, G. M., EATON, J. W. & BALLA, G. 2002. Pro-oxidant and cytotoxic effects of circulating heme. *Blood,* 100**,** 879-87.

KADL, A., PONTILLER, J., EXNER, M. & LEITINGER, N. 2007. Single bolus injection of bilirubin improves the clinical outcome in a mouse model of endotoxemia. *Shock,* 28**,** 582-8.

KAMISAKO, T., KOBAYASHI, Y., TAKEUCHI, K., ISHIHARA, T., HIGUCHI, K., TANAKA, Y., GABAZZA, E. C. & ADACHI, Y. 2000. Recent advances in bilirubin metabolism research: the molecular mechanism of hepatocyte bilirubin transport and its clinical relevance. *J Gastroenterol,* 35**,** 659-64.

KAPIOTIS, S., HERMANN, M., EXNER, M., STURM, B. N., SCHEIBER-MOJDEHKAR, B., GOLDENBERG, H., KOPP, S., CHIBA, P. & GMEINER, B. M. 2005. Aluminum ions stimulate the oxidizability of low density lipoprotein by Fe2+: implication in hemodialysis mediated atherogenic LDL modification. *Free Radic Res,* 39**,** 1225-31.

KAPITULNIK, J. & MAINES, M. D. 2009. Pleiotropic functions of biliverdin reductase: cellular signaling and generation of cytoprotective and cytotoxic bilirubin. *Trends Pharmacol Sci,* 30**,** 129-37.

KAUR, H., HUGHES, M. N., GREEN, C. J., NAUGHTON, P., FORESTI, R. & MOTTERLINI, R. 2003. Interaction of bilirubin and biliverdin with reactive nitrogen species. *FEBS Lett,* 543**,** 113-9.

KAWAMURA, K., ISHIKAWA, K., WADA, Y., KIMURA, S., MATSUMOTO, H., KOHRO, T., ITABE, H., KODAMA, T. & MARUYAMA, Y. 2005. Bilirubin from heme oxygenase-1 attenuates vascular endothelial activation and dysfunction. *Arterioscler Thromb Vasc Biol,* 25**,** 155-60.

KESHAVAN, P., DEEM, T. L., SCHWEMBERGER, S. J., BABCOCK, G. F., COOK-MILLS, J. M. & ZUCKER, S. D. 2005. Unconjugated bilirubin inhibits VCAM-1-mediated transendothelial leukocyte migration. *J Immunol,* 174**,** 3709-18.

KIKUCHI, A., PARK, S. Y., MIYATAKE, H., SUN, D., SATO, M., YOSHIDA, T. & SHIRO, Y. 2001. Crystal structure of rat biliverdin reductase. *Nat Struct Biol,* 8**,** 221-5.

KIM, H. S., LOUGHRAN, P. A., RAO, J., BILLIAR, T. R. & ZUCKERBRAUN, B. S. 2008. Carbon monoxide activates NF-kappaB via ROS generation and Akt pathways to protect against cell death of hepatocytes. *Am J Physiol Gastrointest Liver Physiol,* 295**,** G146-G152.

KINGSTON, R. L., SCOPES, R. K. & BAKER, E. N. 1996. The structure of glucose-fructose oxidoreductase from Zymomonas mobilis: an osmoprotective periplasmic enzyme containing non-dissociable NADP. *Structure,* 4**,** 1413-28.

KRAVETS, A., HU, Z., MIRALEM, T., TORNO, M. D. & MAINES, M. D. 2004. Biliverdin reductase, a novel regulator for induction of activating transcription factor-2 and heme oxygenase-1. *J Biol Chem,* 279**,** 19916-23.

KRONCKE, K. D., FEHSEL, K. & KOLB-BACHOFEN, V. 1998. Inducible nitric oxide synthase in human diseases. *Clin Exp Immunol,* 113**,** 147-56.

KUREISHI, Y., LUO, Z., SHIOJIMA, I., BIALIK, A., FULTON, D., LEFER, D. J., SESSA, W. C. & WALSH, K. 2000. The HMG-CoA reductase inhibitor simvastatin activates the protein kinase Akt and promotes angiogenesis in normocholesterolemic animals. *Nat Med,* 6**,** 1004-10.

KUTTY, R. K. & MAINES, M. D. 1981. Purification and characterization of biliverdin reductase from rat liver. *J Biol Chem,* 256**,** 3956-62.

KWAK, J. Y., TAKESHIGE, K., CHEUNG, B. S. & MINAKAMI, S. 1991. Bilirubin inhibits the activation of superoxide-producing NADPH oxidase in a neutrophil cell-free system. *Biochim Biophys Acta,* 1076**,** 369-73.

LANONE, S., BLOC, S., FORESTI, R., ALMOLKI, A., TAILLE, C., CALLEBERT, J., CONTI, M., GOVEN, D., AUBIER, M., DUREUIL, B., EL-BENNA, J., MOTTERLINI, R. & BOCZKOWSKI, J. 2005. Bilirubin decreases nos2 expression via inhibition of NAD(P)H oxidase: implications for protection against endotoxic shock in rats. *FASEB J,* 19**,** 1890-2.

LAWRENCE, T. & GILROY, D. W. 2007. Chronic inflammation: a failure of resolution? *Int J Exp Pathol,* 88**,** 85-94.

LAZZERINI, G., DEL TURCO, S., BASTA, G., O'LOGHLEN, A., ZAMPOLLI, A. & CATERINA, R. D. 2009. Prominent role of NF-kappaB in the induction of endothelial activation by endogenous nitric oxide inhibition. *Nitric Oxide,* 21**,** 184-91.

LEE, H. S., LEE, M. J., KIM, H., CHOI, S. K., KIM, J. E., MOON, H. I. & PARK, W. H. 2010. Curcumin inhibits TNFalpha-induced lectin-like oxidised LDL receptor-1 (LOX-1) expression and suppresses the inflammatory response in human umbilical vein endothelial cells (HUVECs) by an antioxidant mechanism. *J Enzyme Inhib Med Chem,* 25**,** 720-9.

LERNER-MARMAROSH, N., MIRALEM, T., GIBBS, P. E. & MAINES, M. D. 2007. Regulation of TNF-alpha-activated PKC-zeta signaling by the human biliverdin reductase: identification of activating and inhibitory domains of the reductase. *FASEB J,* 21**,** 3949-62.

LERNER-MARMAROSH, N., MIRALEM, T., GIBBS, P. E. & MAINES, M. D. 2008. Human biliverdin reductase is an ERK activator; hBVR is an ERK nuclear transporter and is required for MAPK signaling. *Proc Natl Acad Sci U S A,* 105**,** 6870-5.

LERNER-MARMAROSH, N., SHEN, J., TORNO, M. D., KRAVETS, A., HU, Z. & MAINES, M. D. 2005. Human biliverdin reductase: a member of the insulin receptor substrate family with serine/threonine/tyrosine kinase activity. *Proc Natl Acad Sci U S A,* 102**,** 7109-14.

LI, H. & FORSTERMANN, U. 2009. Prevention of atherosclerosis by interference with the vascular nitric oxide system. *Curr Pharm Des,* 15**,** 3133-45.

LIBBY, P., OKAMOTO, Y., ROCHA, V. Z. & FOLCO, E. 2010. Inflammation in atherosclerosis: transition from theory to practice. *Circ J,* 74**,** 213-20.

LIN, J. P., O'DONNELL, C. J., SCHWAIGER, J. P., CUPPLES, L. A., LINGENHEL, A., HUNT, S. C., YANG, S. & KRONENBERG, F. 2006. Association between the UGT1A1*28 allele,

bilirubin levels, and coronary heart disease in the Framingham Heart Study. *Circulation,* 114**,** 1476-81.

LIN, Z., KUMAR, A., SENBANERJEE, S., STANISZEWSKI, K., PARMAR, K., VAUGHAN, D. E., GIMBRONE, M. A., JR., BALASUBRAMANIAN, V., GARCIA-CARDENA, G. & JAIN, M. K. 2005. Kruppel-like factor 2 (KLF2) regulates endothelial thrombotic function. *Circ Res,* 96**,** e48-57.

LINGENHEL, A., KOLLERITS, B., SCHWAIGER, J. P., HUNT, S. C., GRESS, R., HOPKINS, P. N., SCHOENBORN, V., HEID, I. M. & KRONENBERG, F. 2008. Serum bilirubin levels, UGT1A1 polymorphisms and risk for coronary artery disease. *Exp Gerontol,* 43**,** 1102-7.

LIU, S., SHEN, H., XU, M., LIU, O., ZHAO, L., GUO, Z. & DU, J. 2010a. FRP inhibits ox-LDL-induced endothelial cell apoptosis through an Akt-NF-{kappa}B-Bcl-2 pathway and inhibits endothelial cell apoptosis in an apoE-knockout mouse model. *Am J Physiol Endocrinol Metab,* 299**,** E351-63.

LIU, S. H., MA, K., XU, B. & XU, X. R. 2010b. Protection of carbon monoxide intraperitoneal administration from rat intestine injury induced by lipopolysaccharide. *Chin Med J (Engl),* 123**,** 1039-46.

LIU, Y., LI, P., LU, J., XIONG, W., OGER, J., TETZLAFF, W. & CYNADER, M. 2008. Bilirubin possesses powerful immunomodulatory activity and suppresses experimental autoimmune encephalomyelitis. *J Immunol,* 181**,** 1887-97.

LOVREN, F., PAN, Y., SHUKLA, P. C., QUAN, A., TEOH, H., SZMITKO, P. E., PETERSON, M. D., GUPTA, M., AL-OMRAN, M. & VERMA, S. 2009. Visfatin activates eNOS via Akt and MAP kinases and improves endothelial cell function and angiogenesis in vitro and in vivo: translational implications for atherosclerosis. *Am J Physiol Endocrinol Metab,* 296**,** E1440-9.

MAGHZAL, G. J., LECK, M. C., COLLINSON, E., LI, C. & STOCKER, R. 2009. Limited role for the bilirubin-biliverdin redox amplification cycle in the cellular antioxidant protection by biliverdin reductase. *J Biol Chem,* 284**,** 29251-9.

MAINES, M. D. 2005. New insights into biliverdin reductase functions: linking heme metabolism to cell signaling. *Physiology (Bethesda),* 20**,** 382-9.

MAINES, M. D. 2007. Biliverdin reductase: PKC interaction at the cross-talk of MAPK and PI3K signaling pathways. *Antioxid Redox Signal,* 9**,** 2187-95.

MAINES, M. D., EWING, J. F., HUANG, T. J. & PANAHIAN, N. 2001. Nuclear localization of biliverdin reductase in the rat kidney: response to nephrotoxins that induce heme oxygenase-1. *J Pharmacol Exp Ther,* 296**,** 1091-7.

MAINES, M. D., MIRALEM, T., LERNER-MARMAROSH, N., SHEN, J. & GIBBS, P. E. 2007. Human biliverdin reductase, a previously unknown activator of protein kinase C betaII. *J Biol Chem,* 282**,** 8110-22.

MAINES, M. D. & TRAKSHEL, G. M. 1993. Purification and characterization of human biliverdin reductase. *Arch Biochem Biophys,* 300**,** 320-6.

MALIK, S. G., IRWANTO, K. A., OSTROW, J. D. & TIRIBELLI, C. 2010. Effect of bilirubin on cytochrome c oxidase activity of mitochondria from mouse brain and liver. *BMC Res Notes,* 3**,** 162.

MALLIKA, V., GOSWAMI, B. & RAJAPPA, M. 2007. Atherosclerosis pathophysiology and the role of novel risk factors: a clinicobiochemical perspective. *Angiology,* 58**,** 513-22.

MATSUURA, E., HUGHES, G. R. & KHAMASHTA, M. A. 2008. Oxidation of LDL and its clinical implication. *Autoimmun Rev,* 7**,** 558-66.

MAZZONE, G. L., RIGATO, I., OSTROW, J. D., BOSSI, F., BORTOLUZZI, A., SUKOWATI, C. H., TEDESCO, F. & TIRIBELLI, C. 2009a. Bilirubin inhibits the TNFalpha-related induction of three endothelial adhesion molecules. *Biochem Biophys Res Commun,* 386**,** 338-44.

MAZZONE, G. L., RIGATO, I., OSTROW, J. D. & TIRIBELLI, C. 2009b. Bilirubin effect on endothelial adhesion molecules expression is mediated by the NF-kappaB signaling pathway. *Biosci Trends,* 3**,** 151-7.

MCDONAGH, A. F., PALMA, L. A. & SCHMID, R. 1981. Reduction of biliverdin and placental transfer of bilirubin and biliverdin in the pregnant guinea pig. *Biochem J,* 194**,** 273-82.

MCEVER, R. P. 2002. Selectins: lectins that initiate cell adhesion under flow. *Curr Opin Cell Biol,* 14**,** 581-6.

MENG, F., LIU, L., CHIN, P. C. & D'MELLO, S. R. 2002. Akt is a downstream target of NF-kappa B. *J Biol Chem,* 277**,** 29674-80.

MESTAS, J. & LEY, K. 2008. Monocyte-endothelial cell interactions in the development of atherosclerosis. *Trends Cardiovasc Med,* 18**,** 228-32.

MIRALEM, T., HU, Z., TORNO, M. D., LELLI, K. M. & MAINES, M. D. 2005. Small interference RNA-mediated gene silencing of human biliverdin reductase, but not that of heme oxygenase-1, attenuates arsenite-mediated induction of the oxygenase and increases apoptosis in 293A kidney cells. *J Biol Chem,* 280**,** 17084-92.

MIYAUCHI, H., MINAMINO, T., TATENO, K., KUNIEDA, T., TOKO, H. & KOMURO, I. 2004. Akt negatively regulates the in vitro lifespan of human endothelial cells via a p53/p21-dependent pathway. *EMBO J,* 23**,** 212-20.

MORALES-RUIZ, M., FULTON, D., SOWA, G., LANGUINO, L. R., FUJIO, Y., WALSH, K. & SESSA, W. C. 2000. Vascular endothelial growth factor-stimulated actin reorganization and migration of endothelial cells is regulated via the serine/threonine kinase Akt. *Circ Res,* 86**,** 892-6.

MORI, H., OTAKE, T., MORIMOTO, M., UEBA, N., KUNITA, N., NAKAGAMI, T., YAMASAKI, N. & TAJI, S. 1991. In vitro anti-human immunodeficiency virus type 1 activity of biliverdin, a bile pigment. *Jpn J Cancer Res,* 82**,** 755-7.

MORITA, T. 2005. Heme oxygenase and atherosclerosis. *Arterioscler Thromb Vasc Biol,* 25**,** 1786-95.

MOSCAT, J., RENNERT, P. & DIAZ-MECO, M. T. 2006. PKCzeta at the crossroad of NF-kappaB and Jak1/Stat6 signaling pathways. *Cell Death Differ,* 13**,** 702-11.

MULLER, G. & MORAWIETZ, H. 2009. Nitric oxide, NAD(P)H oxidase, and atherosclerosis. *Antioxid Redox Signal,* 11**,** 1711-31.

MYERS, M. G., JR., ZHANG, Y., ALDAZ, G. A., GRAMMER, T., GLASHEEN, E. M., YENUSH, L., WANG, L. M., SUN, X. J., BLENIS, J., PIERCE, J. H. & WHITE, M. F. 1996. YMXM motifs and signaling by an insulin receptor substrate 1 molecule without tyrosine phosphorylation sites. *Mol Cell Biol,* 16**,** 4147-55.

NAGEH, M. F., SANDBERG, E. T., MAROTTI, K. R., LIN, A. H., MELCHIOR, E. P., BULLARD, D. C. & BEAUDET, A. L. 1997. Deficiency of inflammatory cell adhesion molecules protects against atherosclerosis in mice. *Arterioscler Thromb Vasc Biol,* 17**,** 1517-20.

NAKAGAMI, T., TOYOMURA, K., KINOSHITA, T. & MORISAWA, S. 1993. A beneficial role of bile pigments as an endogenous tissue protector: anti-complement effects of biliverdin and conjugated bilirubin. *Biochim Biophys Acta,* 1158**,** 189-93.

NAKAO, A., MURASE, N., HO, C., TOYOKAWA, H., BILLIAR, T. R. & KANNO, S. 2005. Biliverdin administration prevents the formation of intimal hyperplasia induced by vascular injury. *Circulation,* 112**,** 587-91.

NAKAO, A., OTTERBEIN, L. E., OVERHAUS, M., SARADY, J. K., TSUNG, A., KIMIZUKA, K., NALESNIK, M. A., KAIZU, T., UCHIYAMA, T., LIU, F., MURASE, N., BAUER, A. J. & BACH, F. H. 2004. Biliverdin protects the functional integrity of a transplanted syngeneic small bowel. *Gastroenterology,* 127**,** 595-606.

NAKAYAMA, M., TAKAHASHI, K., KOMARU, T., FUKUCHI, M., SHIOIRI, H., SATO, K., KITAMURO, T., SHIRATO, K., YAMAGUCHI, T., SUEMATSU, M. & SHIBAHARA, S. 2001. Increased expression of heme oxygenase-1 and bilirubin accumulation in foam cells of rabbit atherosclerotic lesions. *Arterioscler Thromb Vasc Biol,* 21**,** 1373-7.

NAPOLI, C., DE NIGRIS, F., WILLIAMS-IGNARRO, S., PIGNALOSA, O., SICA, V. & IGNARRO, L. J. 2006. Nitric oxide and atherosclerosis: an update. *Nitric Oxide,* 15**,** 265-79.

NEUZIL, J. & STOCKER, R. 1994. Free and albumin-bound bilirubin are efficient co-antioxidants for alpha-tocopherol, inhibiting plasma and low density lipoprotein lipid peroxidation. *J Biol Chem,* 269**,** 16712-9.

NEWTON, A. C. 2001. Protein kinase C: structural and spatial regulation by phosphorylation, cofactors, and macromolecular interactions. *Chem Rev,* 101**,** 2353-64.

NIGRO, P., ABE, J., WOO, C. H., SATOH, K., MCCLAIN, C., O'DELL, M. R., LEE, H., LIM, J. H., LI, J. D., HEO, K. S., FUJIWARA, K. & BERK, B. C. 2010. PKCzeta decreases eNOS protein stability via inhibitory phosphorylation of ERK5. *Blood,* 116**,** 1971-9.

NOGUCHI, M., YOSHIDA, T. & KIKUCHI, G. 1979. Purification and properties of biliverdin reductases from pig spleen and rat liver. *J Biochem,* 86**,** 833-48.

OKON, E. B., CHUNG, A. W., RAUNIYAR, P., PADILLA, E., TEJERINA, T., MCMANUS, B. M., LUO, H. & VAN BREEMEN, C. 2005. Compromised arterial function in human type 2 diabetic patients. *Diabetes,* 54**,** 2415-23.

OLLINGER, R., WANG, H., YAMASHITA, K., WEGIEL, B., THOMAS, M., MARGREITER, R. & BACH, F. H. 2007. Therapeutic applications of bilirubin and biliverdin in transplantation. *Antioxid Redox Signal,* 9**,** 2175-85.

OLSSON, R., BLIDING, A., JAGENBURG, R., LAPIDUS, L., LARSSON, B., SVARDSUDD, K. & WITTBOLDT, S. 1988. Gilbert's syndrome--does it exist? A study of the prevalence of symptoms in Gilbert's syndrome. *Acta Med Scand,* 224**,** 485-90.

OTTERBEIN, L., CHIN, B. Y., OTTERBEIN, S. L., LOWE, V. C., FESSLER, H. E. & CHOI, A. M. 1997. Mechanism of hemoglobin-induced protection against endotoxemia in rats: a ferritin-independent pathway. *Am J Physiol,* 272**,** L268-75.

OU, H. C., LEE, W. J., LEE, S. D., HUANG, C. Y., CHIU, T. H., TSAI, K. L., HSU, W. C. & SHEU, W. H. 2010. Ellagic acid protects endothelial cells from oxidized low-density lipoprotein-induced apoptosis by modulating the PI3K/Akt/eNOS pathway. *Toxicol Appl Pharmacol,* 248**,** 134-43.

PACHER, P. & SZABO, C. 2008. Role of the peroxynitrite-poly(ADP-ribose) polymerase pathway in human disease. *Am J Pathol,* 173**,** 2-13.

PACHORI, A. S., SMITH, A., MCDONALD, P., ZHANG, L., DZAU, V. J. & MELO, L. G. 2007. Heme-oxygenase-1-induced protection against hypoxia/reoxygenation is dependent on biliverdin reductase and its interaction with PI3K/Akt pathway. *J Mol Cell Cardiol,* 43**,** 580-92.

PAE, H. O., OH, G. S., LEE, B. S., RIM, J. S., KIM, Y. M. & CHUNG, H. T. 2006. 3-Hydroxyanthranilic acid, one of L-tryptophan metabolites, inhibits monocyte chemoattractant protein-1 secretion and vascular cell adhesion molecule-1

expression via heme oxygenase-1 induction in human umbilical vein endothelial cells. *Atherosclerosis,* 187**,** 274-84.

PARK, S. U., JUNG, W. S., MOON, S. K., KO, C. N., CHO, K. H., KIM, Y. S., BAE, H. S. & CHI, S. G. 2005. Chunghyuldan activates NOS mRNA expression and suppresses VCAM-1 mRNA expression in human endothelial cells. *Can J Physiol Pharmacol,* 83**,** 1101-8.

PAUL, A., WILSON, S., BELHAM, C. M., ROBINSON, C. J., SCOTT, P. H., GOULD, G. W. & PLEVIN, R. 1997. Stress-activated protein kinases: activation, regulation and function. *Cell Signal,* 9**,** 403-10.

PAZ, Y., FROLKIS, I., PEVNI, D., SHAPIRA, I., YUHAS, Y., IAINA, A., WOLLMAN, Y., CHERNICHOVSKI, T., NESHER, N., LOCKER, C., MOHR, R. & URETZKY, G. 2003. Effect of tumor necrosis factor-alpha on endothelial and inducible nitric oxide synthase messenger ribonucleic acid expression and nitric oxide synthesis in ischemic and nonischemic isolated rat heart. *J Am Coll Cardiol,* 42**,** 1299-305.

PIANTADOSI, C. A. 2008. Carbon monoxide, reactive oxygen signaling, and oxidative stress. *Free Radic Biol Med,* 45**,** 562-9.

QIN, X. F. 2002. Impaired inactivation of digestive proteases by deconjugated bilirubin: the possible mechanism for inflammatory bowel disease. *Med Hypotheses,* 59**,** 159-63.

RADU, P. & ATSMON, J. 2001. Gilbert's syndrome--clinical and pharmacological implications. *Isr Med Assoc J,* 3**,** 593-8.

RAHMAN, A., ANWAR, K. N. & MALIK, A. B. 2000. Protein kinase C-zeta mediates TNF-alpha-induced ICAM-1 gene transcription in endothelial cells. *Am J Physiol Cell Physiol,* 279**,** C906-14.

RAJAN, S., YE, J., BAI, S., HUANG, F. & GUO, Y. L. 2008. NF-kappaB, but not p38 MAP kinase, is required for TNF-alpha-induced expression of cell adhesion molecules in endothelial cells. *J Cell Biochem,* 105**,** 477-86.

RAY, R. & SHAH, A. M. 2005. NADPH oxidase and endothelial cell function. *Clin Sci (Lond),* 109**,** 217-26.

READ, M. A., WHITLEY, M. Z., GUPTA, S., PIERCE, J. W., BEST, J., DAVIS, R. J. & COLLINS, T. 1997. Tumor necrosis factor alpha-induced E-selectin expression is activated by the nuclear factor-kappaB and c-JUN N-terminal kinase/p38 mitogen-activated protein kinase pathways. *J Biol Chem,* 272**,** 2753-61.

ROSS, R. & GLOMSET, J. A. 1976. The pathogenesis of atherosclerosis (second of two parts). *N Engl J Med,* 295**,** 420-5.

SAKAMOTO, T., ISHIBASHI, T., SAKAMOTO, N., SUGIMOTO, K., EGASHIRA, K., OHKAWARA, H., NAGATA, K., YOKOYAMA, K., KAMIOKA, M., ICHIKI, T., SUGIMOTO, N., KURABAYASHI,

M., SUZUKI, K., TAKUWA, Y. & MARUYAMA, Y. 2005. Endogenous NO blockade enhances tissue factor expression via increased Ca2+ influx through MCP-1 in endothelial cells by monocyte adhesion. *Arterioscler Thromb Vasc Biol,* 25**,** 2005-11.

SANO, K., NAKAMURA, H. & MATSUO, T. 1985. Mode of inhibitory action of bilirubin on protein kinase C. *Pediatr Res,* 19**,** 587-90.

SAWAMURA, T., KUME, N., AOYAMA, T., MORIWAKI, H., HOSHIKAWA, H., AIBA, Y., TANAKA, T., MIWA, S., KATSURA, Y., KITA, T. & MASAKI, T. 1997. An endothelial receptor for oxidized low-density lipoprotein. *Nature,* 386**,** 73-7.

SCHLUCHTER, W. M. & GLAZER, A. N. 1997. Characterization of cyanobacterial biliverdin reductase. Conversion of biliverdin to bilirubin is important for normal phycobiliprotein biosynthesis. *J Biol Chem,* 272**,** 13562-9.

SCHMITZ, M. L., BACHER, S. & KRACHT, M. 2001. I kappa B-independent control of NF-kappa B activity by modulatory phosphorylations. *Trends Biochem Sci,* 26**,** 186-90.

SCHRECK, R., RIEBER, P. & BAEUERLE, P. A. 1991. Reactive oxygen intermediates as apparently widely used messengers in the activation of the NF-kappa B transcription factor and HIV-1. *EMBO J,* 10**,** 2247-58.

SCHWERTNER, H. A., JACKSON, W. G. & TOLAN, G. 1994. Association of low serum concentration of bilirubin with increased risk of coronary artery disease. *Clin Chem,* 40**,** 18-23.

SCHWERTNER, H. A. & VITEK, L. 2008. Gilbert syndrome, UGT1A1*28 allele, and cardiovascular disease risk: possible protective effects and therapeutic applications of bilirubin. *Atherosclerosis,* 198**,** 1-11.

SEDLAK, T. W., SALEH, M., HIGGINSON, D. S., PAUL, B. D., JULURI, K. R. & SNYDER, S. H. 2009. Bilirubin and glutathione have complementary antioxidant and cytoprotective roles. *Proc Natl Acad Sci U S A,* 106**,** 5171-6.

SEDLAK, T. W. & SNYDER, S. H. 2009. Cycling the wagons for biliverdin reductase. *J Biol Chem,* 284**,** le11; author reply le12.

SHEN, B., GAO, L., HSU, Y. T., BLEDSOE, G., HAGIWARA, M., CHAO, L. & CHAO, J. 2010. Kallistatin attenuates endothelial apoptosis through inhibition of oxidative stress and activation of Akt-eNOS signaling. *Am J Physiol Heart Circ Physiol,* 299**,** H1419-27.

SHIOJIMA, I. & WALSH, K. 2002. Role of Akt signaling in vascular homeostasis and angiogenesis. *Circ Res,* 90**,** 1243-50.

SINGLETON, J. W. & LASTER, L. 1965. Biliverdin reductase of guinea pig liver. *J Biol Chem,* 240**,** 4780-9.

SIOW, R. C., ISHII, T., SATO, H., TAKETANI, S., LEAKE, D. S., SWEIRY, J. H., PEARSON, J. D., BANNAI, S. & MANN, G. E. 1995. Induction of the antioxidant stress proteins heme oxygenase-1 and MSP23 by stress agents and oxidised LDL in cultured vascular smooth muscle cells. *FEBS Lett,* 368**,** 239-42.

SIOW, R. C., SATO, H. & MANN, G. E. 1999. Heme oxygenase-carbon monoxide signalling pathway in atherosclerosis: anti-atherogenic actions of bilirubin and carbon monoxide? *Cardiovasc Res,* 41**,** 385-94.

SMITH, A. R. & HAGEN, T. M. 2003. Vascular endothelial dysfunction in aging: loss of Akt-dependent endothelial nitric oxide synthase phosphorylation and partial restoration by (R)-alpha-lipoic acid. *Biochem Soc Trans,* 31**,** 1447-9.

STEINBERG, D. 1989. The cholesterol controversy is over. Why did it take so long? *Circulation,* 80**,** 1070-8.

STEINBERG, D. 2009. The LDL modification hypothesis of atherogenesis: an update. *J Lipid Res,* 50 Suppl**,** S376-81.

STOCKER, R. 2004. Antioxidant activities of bile pigments. *Antioxid Redox Signal,* 6**,** 841-9.

STOCKER, R., YAMAMOTO, Y., MCDONAGH, A. F., GLAZER, A. N. & AMES, B. N. 1987. Bilirubin is an antioxidant of possible physiological importance. *Science,* 235**,** 1043-6.

TANG, X. & EDENHARDER, R. 1997. Inhibition of the mutagenicity of 2-nitrofluorene, 3-nitrofluoranthene and 1-nitropyrene by vitamins, porphyrins and related compounds, and vegetable and fruit juices and solvent extracts. *Food Chem Toxicol,* 35**,** 373-8.

TELL, G. & GUSTINCICH, S. 2009. Redox state, oxidative stress, and molecular mechanisms of protective and toxic effects of bilirubin on cells. *Curr Pharm Des,* 15**,** 2908-14.

TERRY, C. M., CLIKEMAN, J. A., HOIDAL, J. R. & CALLAHAN, K. S. 1999. TNF-alpha and IL-1alpha induce heme oxygenase-1 via protein kinase C, Ca2+, and phospholipase A2 in endothelial cells. *Am J Physiol,* 276**,** H1493-501.

TICKNER, T. R. & GUTTERIDGE, J. M. 1978. A simple colorimetric method for the estimation of plasma biliverdin. *Clin Chim Acta,* 85**,** 125-9.

TOGANE, Y., MORITA, T., SUEMATSU, M., ISHIMURA, Y., YAMAZAKI, J. I. & KATAYAMA, S. 2000. Protective roles of endogenous carbon monoxide in neointimal development elicited by arterial injury. *Am J Physiol Heart Circ Physiol,* 278**,** H623-32.

TUDOR, C., LERNER-MARMAROSH, N., ENGELBORGHS, Y., GIBBS, P. E. & MAINES, M. D. 2008. Biliverdin reductase is a transporter of haem into the nucleus and is essential for regulation of HO-1 gene expression by haematin. *Biochem J,* 413**,** 405-16.

UJHELYI, L., BALLA, G., JENEY, V., VARGA, Z., NAGY, E., VERCELLOTTI, G. M., AGARWAL, A., EATON, J. W. & BALLA, J. 2006. Hemodialysis reduces inhibitory effect of plasma ultrafiltrate on LDL oxidation and subsequent endothelial reactions. *Kidney Int,* 69**,** 144-51.

URANO, T., ITO, Y., AKAO, M., SAWA, T., MIYATA, K., TABATA, M., MORISADA, T., HATO, T., YANO, M., KADOMATSU, T., YASUNAGA, K., SHIBATA, R., MUROHARA, T., AKAIKE, T., TANIHARA, H., SUDA, T. & OIKE, Y. 2008. Angiopoietin-related growth factor enhances blood flow via activation of the ERK1/2-eNOS-NO pathway in a mouse hind-limb ischemia model. *Arterioscler Thromb Vasc Biol,* 28**,** 827-34.

VAN LENTEN, B. J., PRIEVE, J., NAVAB, M., HAMA, S., LUSIS, A. J. & FOGELMAN, A. M. 1995. Lipid-induced changes in intracellular iron homeostasis in vitro and in vivo. *J Clin Invest,* 95**,** 2104-10.

VERBEUREN, T. J., COENE, M. C., JORDAENS, F. H., VAN HOVE, C. E., ZONNEKEYN, L. L. & HERMAN, A. G. 1986. Effect of hypercholesterolemia on vascular reactivity in the rabbit. II. Influence of treatment with dipyridamole on endothelium-dependent and endothelium-independent responses in isolated aortas of control and hypercholesterolemic rabbits. *Circ Res,* 59**,** 496-504.

VIOLI, F., BASILI, S., NIGRO, C. & PIGNATELLI, P. 2009. Role of NADPH oxidase in atherosclerosis. *Future Cardiol,* 5**,** 83-92.

VITEK, L., JIRSA, M., BRODANOVA, M., KALAB, M., MARECEK, Z., DANZIG, V., NOVOTNY, L. & KOTAL, P. 2002. Gilbert syndrome and ischemic heart disease: a protective effect of elevated bilirubin levels. *Atherosclerosis,* 160**,** 449-56.

WAGENER, F. A., DA SILVA, J. L., FARLEY, T., DE WITTE, T., KAPPAS, A. & ABRAHAM, N. G. 1999. Differential effects of heme oxygenase isoforms on heme mediation of endothelial intracellular adhesion molecule 1 expression. *J Pharmacol Exp Ther,* 291**,** 416-23.

WAGENER, F. A., FELDMAN, E., DE WITTE, T. & ABRAHAM, N. G. 1997. Heme induces the expression of adhesion molecules ICAM-1, VCAM-1, and E selectin in vascular endothelial cells. *Proc Soc Exp Biol Med,* 216**,** 456-63.

WANG, J., ZHOU, H. C., PAN, P., ZHANG, N. & LI, W. Z. 2010. Exogenous biliverdin improves the function of lung grafts from brain dead donors in rats. *Transplant Proc,* 42**,** 1602-9.

WEGIEL, B., BATY, C. J., GALLO, D., CSIZMADIA, E., SCOTT, J. R., AKHAVAN, A., CHIN, B. Y., KACZMAREK, E., ALAM, J., BACH, F. H., ZUCKERBRAUN, B. S. & OTTERBEIN, L. E. 2009. Cell surface biliverdin reductase mediates biliverdin-induced anti-inflammatory effects via phosphatidylinositol 3-kinase and Akt. *J Biol Chem,* 284**,** 21369-78.

WHITBY, F. G., PHILLIPS, J. D., HILL, C. P., MCCOUBREY, W. & MAINES, M. D. 2002. Crystal structure of a biliverdin IXalpha reductase enzyme-cofactor complex. *J Mol Biol,* 319**,** 1199-210.

WOOLLARD, K. J. & GEISSMANN, F. 2010. Monocytes in atherosclerosis: subsets and functions. *Nat Rev Cardiol,* 7**,** 77-86.

WU, T. W., FUNG, K. P. & YANG, C. C. 1994. Unconjugated bilirubin inhibits the oxidation of human low density lipoprotein better than Trolox. *Life Sci,* 54**,** P477-81.

WU, Y. & ZHOU, B. P. 2010. TNF-alpha/NF-kappaB/Snail pathway in cancer cell migration and invasion. *Br J Cancer,* 102**,** 639-44.

XIE, Z., PIMENTAL, D. R., LOHAN, S., VASERTRIGER, A., PLIGAVKO, C., COLUCCI, W. S. & SINGH, K. 2001. Regulation of angiotensin II-stimulated osteopontin expression in cardiac microvascular endothelial cells: role of p42/44 mitogen-activated protein kinase and reactive oxygen species. *J Cell Physiol,* 188**,** 132-8.

YAMAGUCHI, T., KOMODA, Y. & NAKAJIMA, H. 1994. Biliverdin-IX alpha reductase and biliverdin-IX beta reductase from human liver. Purification and characterization. *J Biol Chem,* 269**,** 24343-8.

YAMAGUCHI, T., SHIOJI, I., SUGIMOTO, A., KOMODA, Y. & NAKAJIMA, H. 1996. Epitope of 24G7 anti-bilirubin monoclonal antibody. *Biochim Biophys Acta,* 1289**,** 110-4.

YAMASHITA, K., MCDAID, J., OLLINGER, R., TSUI, T. Y., BERBERAT, P. O., USHEVA, A., CSIZMADIA, E., SMITH, R. N., SOARES, M. P. & BACH, F. H. 2004. Biliverdin, a natural product of heme catabolism, induces tolerance to cardiac allografts. *FASEB J,* 18**,** 765-7.

YESILOVA, Z., SERDAR, M., ERCIN, C. N., GUNAY, A., KILCILER, G., HASIMI, A., UYGUN, A., KURT, I., ERBIL, M. K. & DAGALP, K. 2008. Decreased oxidation susceptibility of plasma low density lipoproteins in patients with Gilbert's syndrome. *J Gastroenterol Hepatol,* 23**,** 1556-60.

ZEIHER, A. M., FISSLTHALER, B., SCHRAY-UTZ, B. & BUSSE, R. 1995. Nitric oxide modulates the expression of monocyte chemoattractant protein 1 in cultured human endothelial cells. *Circ Res,* 76**,** 980-6.

ZENG, R., YAO, Y., HAN, M., ZHAO, X., LIU, X. C., WEI, J., LUO, Y., ZHANG, J., ZHOU, J., WANG, S., MA, D. & XU, G. 2008. Biliverdin reductase mediates hypoxia-induced EMT via PI3-kinase and Akt. *J Am Soc Nephrol,* 19**,** 380-7.

ZHANG, C., ZHAO, Y. X., ZHANG, Y. H., ZHU, L., DENG, B. P., ZHOU, Z. L., LI, S. Y., LU, X. T., SONG, L. L., LEI, X. M., TANG, W. B., WANG, N., PAN, C. M., SONG, H. D., LIU, C. X., DONG, B., ZHANG, Y. & CAO, Y. 2010a. Angiotensin-converting enzyme 2 attenuates

atherosclerotic lesions by targeting vascular cells. *Proc Natl Acad Sci U S A,* 107**,** 15886-91.

ZHANG, H., PARK, Y., WU, J., CHEN, X., LEE, S., YANG, J., DELLSPERGER, K. C. & ZHANG, C. 2009. Role of TNF-alpha in vascular dysfunction. *Clin Sci (Lond),* 116**,** 219-30.

ZHANG, W., WANG, J., WANG, H., TANG, R., BELCHER, J. D., VIOLLET, B., GENG, J. G., ZHANG, C., WU, C., SLUNGAARD, A., ZHU, C. & HUO, Y. 2010b. Acadesine inhibits tissue factor induction and thrombus formation by activating the phosphoinositide 3-kinase/Akt signaling pathway. *Arterioscler Thromb Vasc Biol.* 2010/02/27 ed.